VOLUME 86 NO. ST5
MAY 1960
PART 1

JOURNAL of the

Structural Division

PROCEEDINGS OF THE

AMERICAN SOCIETY OF CIVIL ENGINEERS

BASIC REQUIREMENTS FOR MANUSCRIPTS

Original papers and discussions of current papers should be submitted to the Manager of Technical Publications, ASCE. Authors should indicate the technical division to which the paper should be referred. The final date on which a discussion should reach the Society is given as a footnote with each paper. Those who are planning to submit material will expedite the review and publication procedures by complying with the following basic requirements:

1. Titles must have a length not exceeding 50 characters and spaces.

2. A 50-word summary must accompany the paper.

3. The manuscript (a ribbon copy and two copies) should be double-spaced on one side of 8½-in. by 11-in. paper.

4. The author's full name, Society membership grade, and footnote reference stating present employment must appear on the first page of the paper.

5. Mathematics are recomposed from the copy that is submitted. Because of this, it is necessary that letters be drawn carefully, and that special symbols be properly identified.

6. Tables should be typed (ribbon copies) on one side of 8½-in. by 11-in. paper. Specific reference and explanation must be made in the text for each table.

7. Illustrations must be drawn in black ink on one side of 8½-in. by 11-in. paper. Because illustrations will be reproduced with a width of between 3-in. and 4½-in., the lettering must be large enough to be legible at this width. Photographs should be submitted as glossy prints. Explanations and descriptions must be made within the text for each illustration.

8. Papers should average about 12,000 words in length and must be no longer than 18,000 words. As an approximation, each full page of typed text, table, or illustration is the equivalent of 300 words.

9. Papers must be written in the third person.

Reprints from this Journal may be made on condition that the full title of the paper, name of author, page reference, and date of publication by the Society are given. The Society is not responsible for any statement made or opinion expressed in its publications.

This Journal is published monthly by the American Society of Civil Engineers. Publication office is at 2500 South State Street, Ann Arbor, Michigan. Editorial and General Offices are at 33 West 39 Street, New York 18, New York. $4.00 of a member's dues are applied as a subscription to this Journal. Second-class postage paid at Ann Arbor, Michigan.

The index for 1959 was published as ASCE Publication 1960-10 (list price $2.00); indexes for previous years are also available.

Journal of the

STRUCTURAL DIVISION

Proceedings of the American Society of Civil Engineers

STRUCTURAL DIVISION
EXECUTIVE COMMITTEE
Robert D. Dewell, Chairman; Emerson J. Ruble, Vice Chairman;
George S. Vincent; Nathan D. Whitman, Jr.; Charles T. G. Looney, Secretary

COMMITTEE ON PUBLICATIONS
Henry G. Schlitt, Chairman; Mace H. Bell; Gerald F. Borrmann;
Edwin S. Elcock; Kurt H. Gerstle; John E. Goldberg; Wayne C. Lewis;
Alfred L. Parme; Philip A. Upp; Halsted N. Wilcox

CONTENTS

May, 1960

Papers

	Page
Charts for Design of Reinforced Concrete Columns by W. H. Gardner, Jr. and Donald H. Kline	1
Design Considerations for Fatigue in Timber Structures by Wayne C. Lewis	15
Minimum Cost Design of Large Support Rings by Kenneth P. Buchert	25
Rationale for Determining Design Wind Velocities by A. G. Davenport	39
Bar-Chain Method for Analyzing Truss Deformation by S. L. Lee and P. C. Patel	69
Influence of Partial Base Fixity on Frame Stability by Theodore V. Galambos	85
Discussion	109

Copyright 1960 by the American Society of Civil Engineers.

Journal of the
STRUCTURAL DIVISION
Proceedings of the American Society of Civil Engineers

CHARTS FOR DESIGN OF REINFORCED CONCRETE COLUMNS

By W. H. Gardner, Jr.,[1] A. M. ASCE and Donald H. Kline,[2] A. M. ASCE

SYNOPSIS

Curves are presented which enable the designer to immediately determine the necessary size and reinforcing for a given thrust and moment. The curves are based on the ultimate strength of the column section and cover six column sizes for each of three concrete strengths. The curves are directly applicable to square tied columns with eccentricities about one axis.

INTRODUCTION

Ever since the ASCE - ACI Joint Committee on Ultimate Strength Design published their report in 1955,[3] much has been written regarding the implications of the report, both from the standpoint of design philosophy and member sizes resulting from ultimate strength design.[4,5] A recent paper[6] by Alfred L. Parme, M. ASCE, discusses thoroughly the comparison between member

Note.—Discussion open until October 1, 1960. To extend the closing date one month, a written request must be filed with the Executive Secretary, ASCE. This paper is part of the copyrighted Journal of the Structural Division, Proceedings of the American Society of Civil Engineers, Vol. 86, No. ST 5, May, 1960.

[1] Assoc. Prof. of Civ. Engrg., Duke University, and Partner, W. H. Gardner, Jr. and Assocs., Durham, N. C.

[2] Partner, W. H. Gardner, Jr. and Assocs., N. C.

[3] "Report, ASCE-ACI Joint Committee on Ultimate Strength Design," Proceedings, ASCE, Vol. 81, October, 1955.

[4] "Simplification of Design by Ultimate Strength Procedures," by Phil M. Ferguson, Proceedings, ASCE, Vol. 82, No. ST 4, July, 1956.

[5] "Guide for Ultimate Strength Design of Reinforced Concrete," by Charles S. Whitney and Edward Cohen, Proceedings, ACI, Vol. 53, November, 1956, pp. 455-490.

[6] "Practical Aspects of Ultimate Strength Design," by Alfred L. Parme, Proceedings, ASCE, Vol. 84, No. ST 5, September, 1958.

sizes as designed by the conventional "working load" method and by ultimate strength. The economy to be gained by using ultimate strength design for columns with eccentric loads is clearly demonstrated therein. The writers have noted these substantial savings in columns actually designed.

At present, the designer who wishes to take advantage of the smaller column sizes permitted by ultimate strength analysis must perform several more steps in his computations that he would perform if he were using the conventional approach to the problem.[7] Several ingenious graphical solutions for the cumbersome formulas of ACI 318 - 56 have been published, and these design aids considerably lessen the time required to choose a section.[4,8] The curves here presented (Figs. 1 through 18) are an adaptation of those devised by Charles S. Whitney.[9] Although not as general, these curves permit faster determination of reinforcing when designing, or ultimate load capacity when checking. Examples later show how easily these steps can be accomplished.

LIMITATIONS AND ASSUMPTIONS

The writers understand that column design tables, similar to those of I. E. Morris,[10] are being prepared for ultimate loads rather than working loads. The publication date of these data is still uncertain, however. The curves presented herein are an effort to make immediately available design aids that, while not covering all possible column sections, should prove useful in the design of most conventional type structures. For the sake of more immediate presentation, therefore, the curves have been drawn only for square columns eccentrically loaded about one axis and symmetrically reinforced, with the steel arranged parallel to the axis of bending and a fixed percentage of the section depth therefrom. The reinforcing has been placed at 0.2 of the depth from the tension and compressive faces; this arrangement suffices without undue loss of accuracy for the column sizes shown.

The conditions to which the curves apply are:

1. Columns are square.
2. Axial loads are eccentric about one axis by an amount up to 1.25 times the section depth.
3. Tensile and compressive reinforcement is symmetrical about the axis of bending, the centroid of the steel at each face being 0.3 of the section depth from the axis.
4. Concrete and reinforcing strengths are as shown on the charts.

Spot checking of the curves has indicated a maximum error of 1 $\frac{1}{2}$% with most errors being less than 1%.

Notation corresponds to that defined in the ACI Building Code.[11]

---

7 "Concrete Reinforcing Steel Institute Handbook-Revised," 1957 Edition, pp. 255-336.

8 "Ultimate Strength Design Charts for Columns Controlled by Tension," by Tung Au, Proceedings, ACI, Vol. 54, December, 1957.

9 "Application of Plastic Theory to the Design of Modern Reinforced Concrete Structures," by Charles S. Whitney, Journal, Boston Soc. of Civ. Engrg., Vol. XXXV, January, 1948, p. 29.

10 "Allowable Loads on Eccentrically Loaded Concrete Columns," by I. E. Morris, Atlanta, Ga.

11 "Building Code Requirements for Reinforced Concrete," ACI 318-56, Proceedings, ACI, Vol. 52, May, 1956, p. 981.

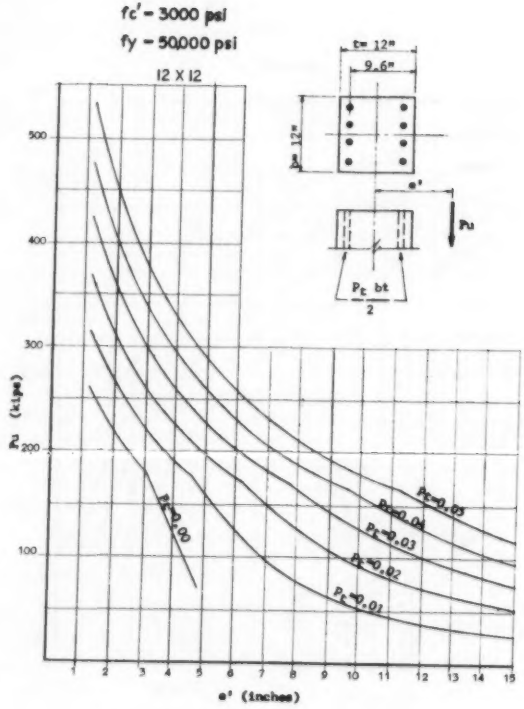
fc' = 3000 psi
fy = 50,000 psi
12 X 12
t= 12"
9.6"
12"
e'
Pu
Pt bt/2
Pu (kips)
e' (inches)
Pt=0.05
Pt=0.04
Pt=0.03
Pt=0.02
Pt=0.01
Pt=0.00

FIG. 1

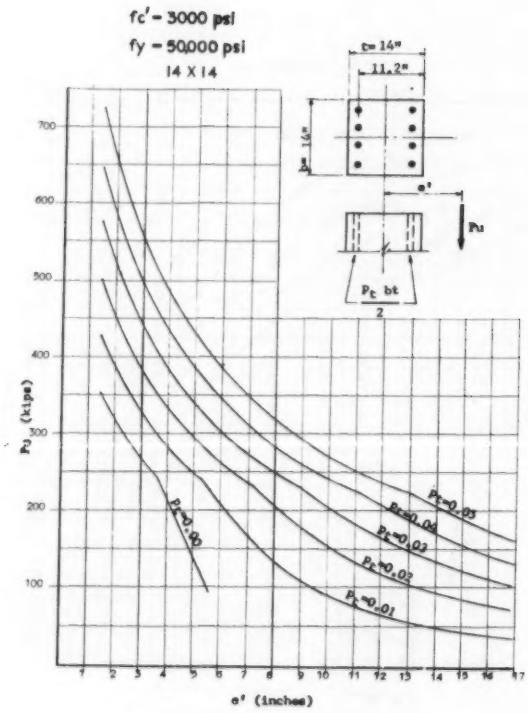
fc' = 3000 psi
fy = 50,000 psi
14 X 14
t= 14"
11.2"
14"
e'
Pu
Pt bt/2
Pu (kips)
e' (inches)
Pt=0.05
Pt=0.04
Pt=0.03
Pt=0.02
Pt=0.01
Pt=0.00

FIG. 2

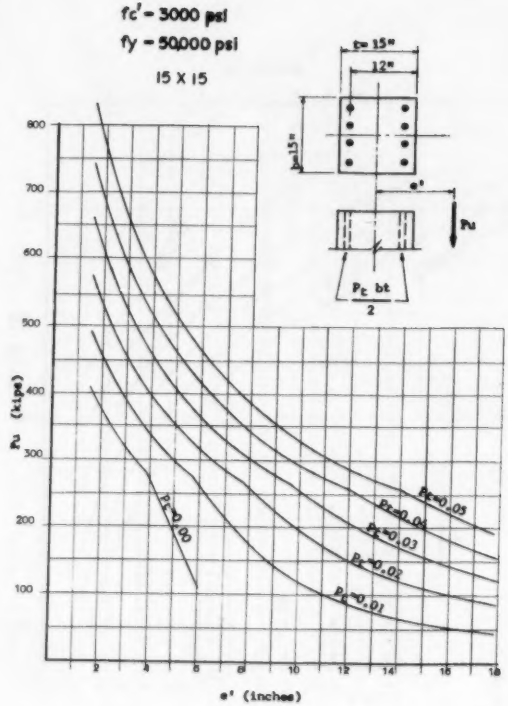
fc' = 3000 psi
fy = 50,000 psi
15 X 15
t= 15"
12"
15"
e'
Pu
Pt bt
2
Pu (kips)
e' (inches)
Pt=0.05
Pt=0.04
Pt=0.03
Pt=0.02
Pt=0.01
Pt=0.00

FIG. 3

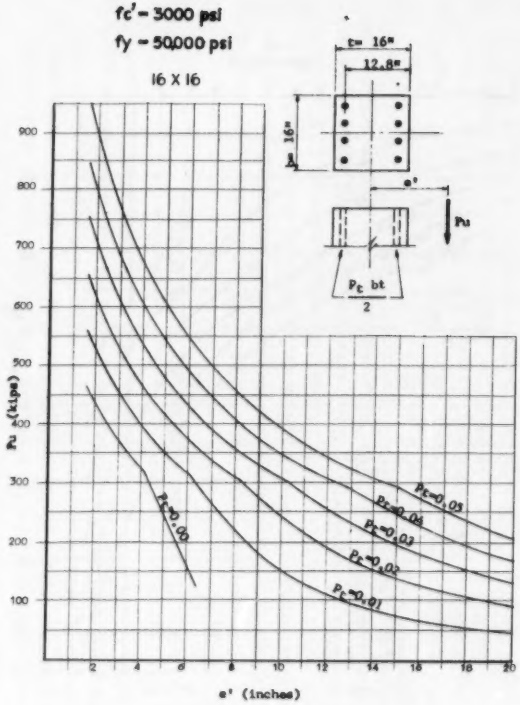
fc' = 3000 psi
fy = 50,000 psi
16 X 16
t= 16"
12.8"
16"
e'
Pu
Pt bt
2
Pu (kips)
e' (inches)
Pt=0.05
Pt=0.04
Pt=0.03
Pt=0.02
Pt=0.01
Pt=0.00

FIG. 4

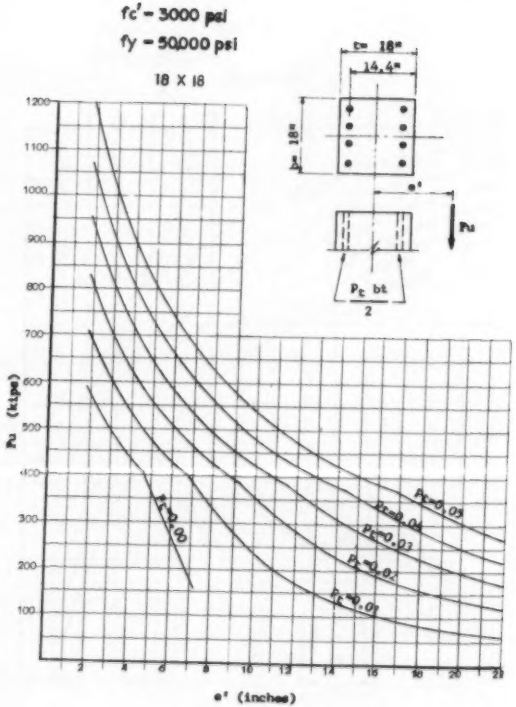
fc' = 3000 psi
fy = 50,000 psi
18 X 18
t= 18"
14.4"
18"
e'
Pu
Pc bt/2
Pu (kips)
e' (inches)
Pc=0.05
Pc=0.04
Pc=0.03
Pc=0.02
Pc=0.01
Pc=0.00

FIG. 5

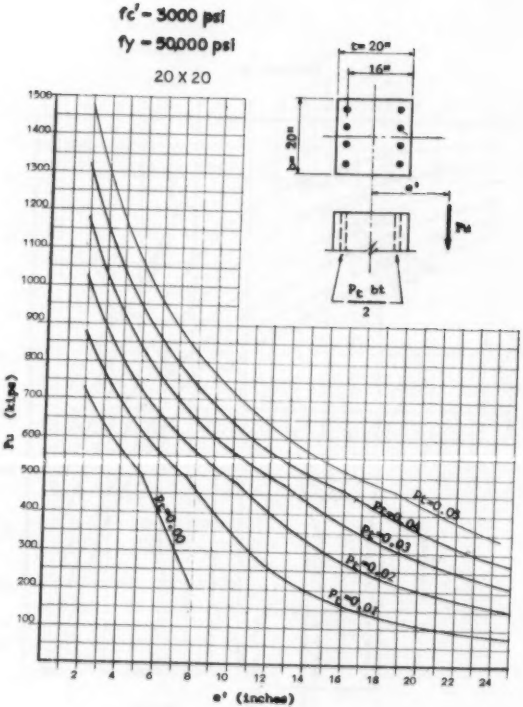
fc' = 3000 psi
fy = 50,000 psi
20 X 20
t= 20"
16"
20"
e'
Pu
Pc bt/2
Pu (kips)
e' (inches)
Pc=0.05
Pc=0.04
Pc=0.03
Pc=0.02
Pc=0.01
Pc=0.00

FIG. 6

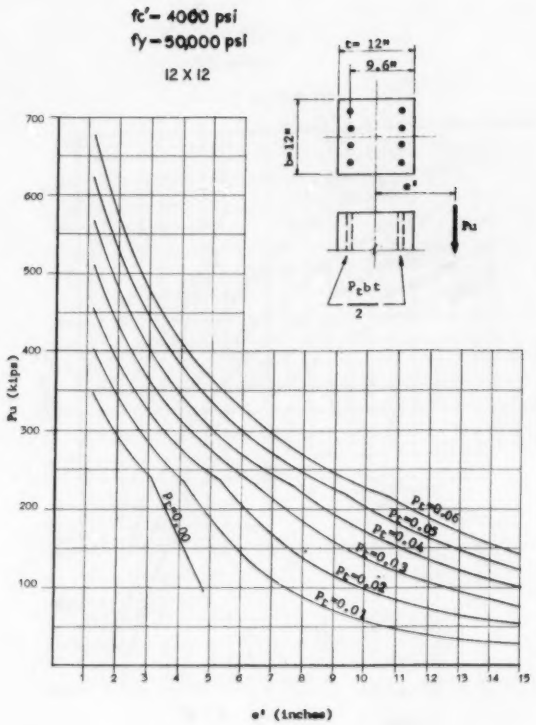
fc'= 4000 psi
fy = 50,000 psi
12 X 12
t= 12"
9.6"
b=12"
e'
Pu
Pu (kips)
e' (inches)
Pt=0.06
Pt=0.05
Pt=0.04
Pt=0.03
Pt=0.02
Pt=0.01

FIG. 7

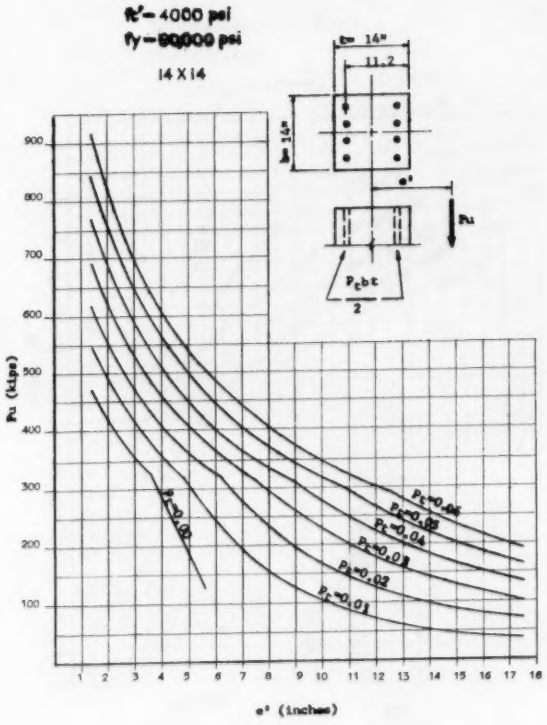
fc'= 4000 psi
fy = 50,000 psi
14 X 14
t= 14"
11.2
b=14"
e'
Pu
Pu (kips)
e' (inches)
Pt=0.06
Pt=0.05
Pt=0.04
Pt=0.03
Pt=0.02
Pt=0.01

FIG. 8

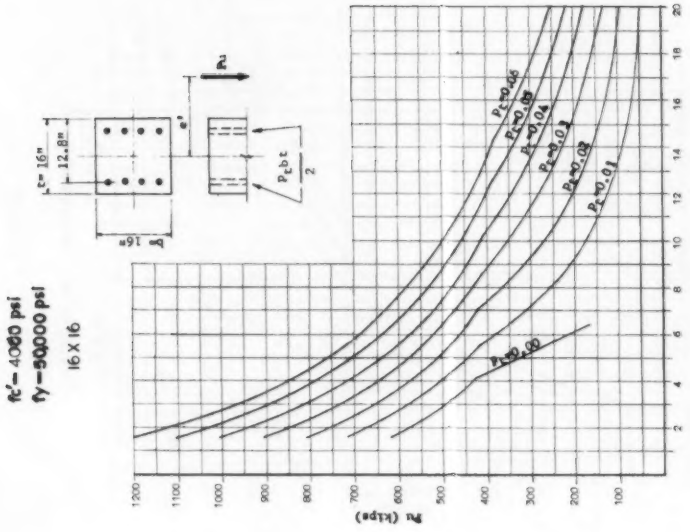
f'c = 4000 psi
fy = 50000 psi
16 X 16
t= 16"
12.8"
16"
e'
Pu
Pt b t / 2
Pt=0.06
Pt=0.05
Pt=0.04
Pt=0.03
Pt=0.02
Pt=0.01
Pt=0.00
Pu (kips)
e' (inches)

FIG. 10

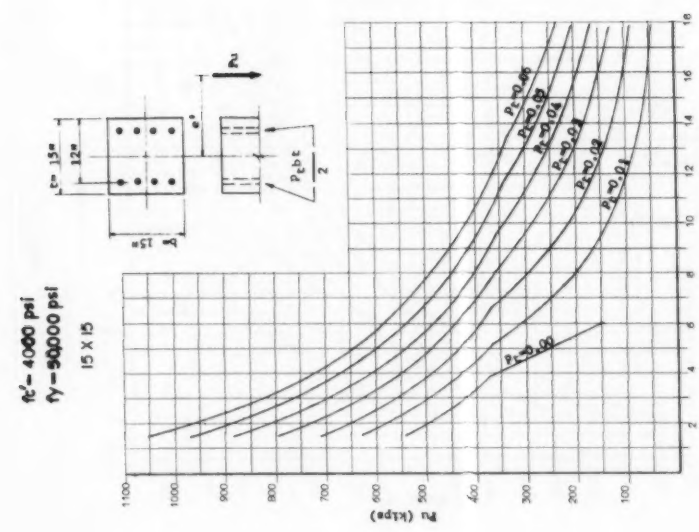
f'c = 4000 psi
fy = 50000 psi
15 X 15
t= 15"
12"
15"
e'
Pu
Pt b t / 2
Pt=0.06
Pt=0.05
Pt=0.04
Pt=0.03
Pt=0.02
Pt=0.01
Pt=0.00
Pu (kips)
e' (inches)

FIG. 9

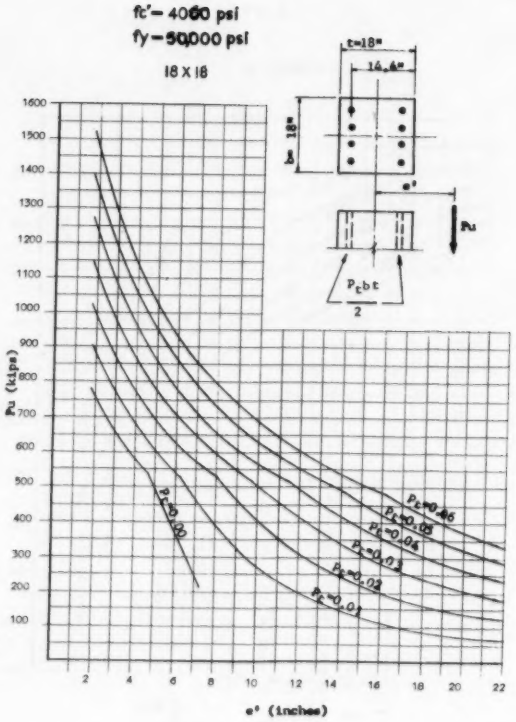
fc'= 4000 psi
fy= 50,000 psi
18 X 18
t=18"
16.6"
18"
b
e'
Pu
Pt b t
2
Pu (kips)
e' (inches)
Pt=0.06
Pt=0.05
Pt=0.04
Pt=0.03
Pt=0.02
Pt=0.01
Pt=0.00

FIG. 11

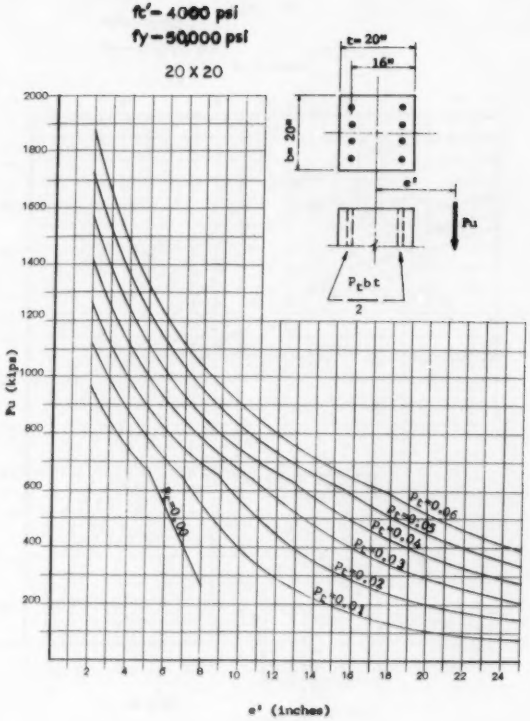
fc'= 4000 psi
fy= 50,000 psi
20 X 20
t= 20"
16"
20"
b
e'
Pu
Pt b t
2
Pu (kips)
e' (inches)
Pt=0.06
Pt=0.05
Pt=0.04
Pt=0.03
Pt=0.02
Pt=0.01
Pt=0.00

FIG. 12

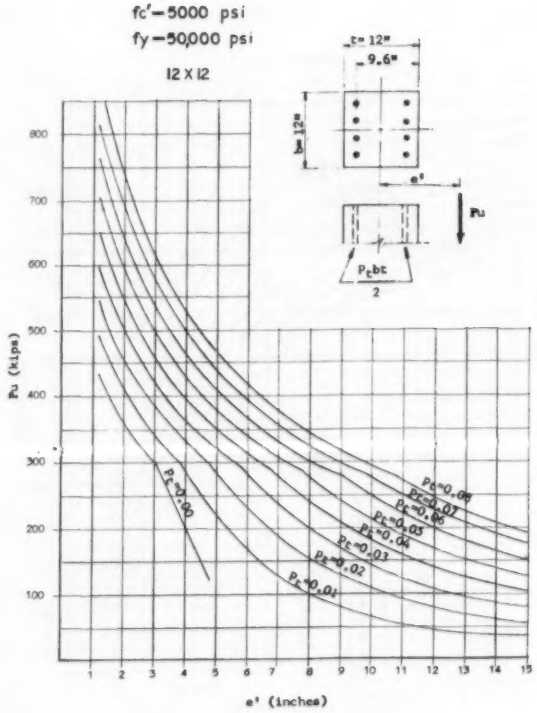
fc'=5000 psi
fy=50,000 psi
12 X 12
t= 12"
9.6"
h= 12"
e'
Pu
Pt bt
2
Pu (kips)
e' (inches)
Pt=0.00
Pt=0.01
Pt=0.02
Pt=0.03
Pt=0.04
Pt=0.05
Pt=0.06
Pt=0.07
Pt=0.08

FIG. 13

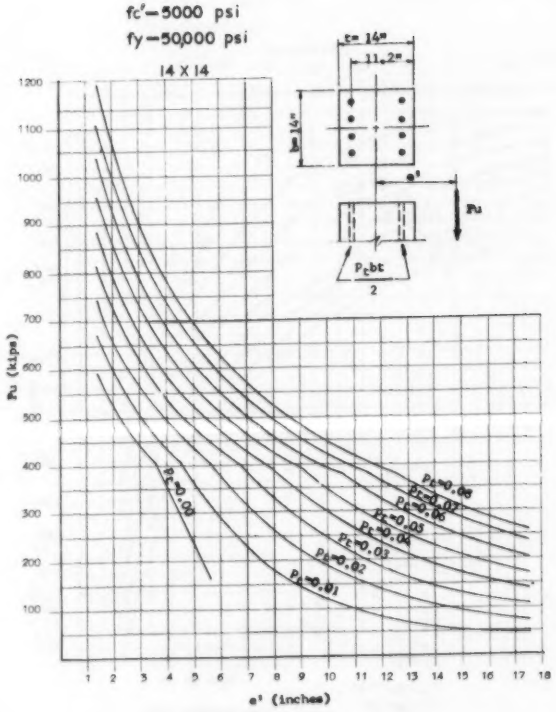
fc'=5000 psi
fy=50,000 psi
14 X 14
t= 14"
11.2"
h= 14"
e'
Pu
Pt bt
2
Pu (kips)
e' (inches)
Pt=0.00
Pt=0.01
Pt=0.02
Pt=0.03
Pt=0.04
Pt=0.05
Pt=0.06
Pt=0.07
Pt=0.08

FIG. 14

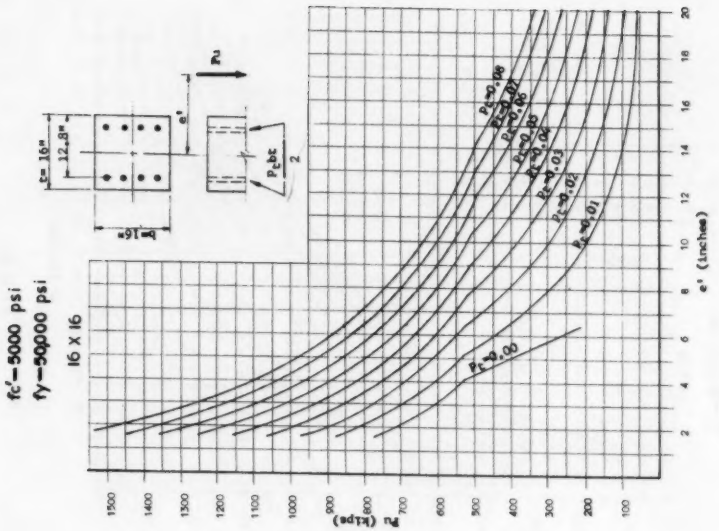
f'c=5000 psi
fy=50000 psi
16 X 16
t= 16"
12.8"
16"
e'
Pu
Pu (kips)
e' (inches)
Pt=0.08
Pt=0.07
Pt=0.06
Pt=0.05
Pt=0.04
Pt=0.03
Pt=0.02
Pt=0.01
Pt=0.00

FIG. 16

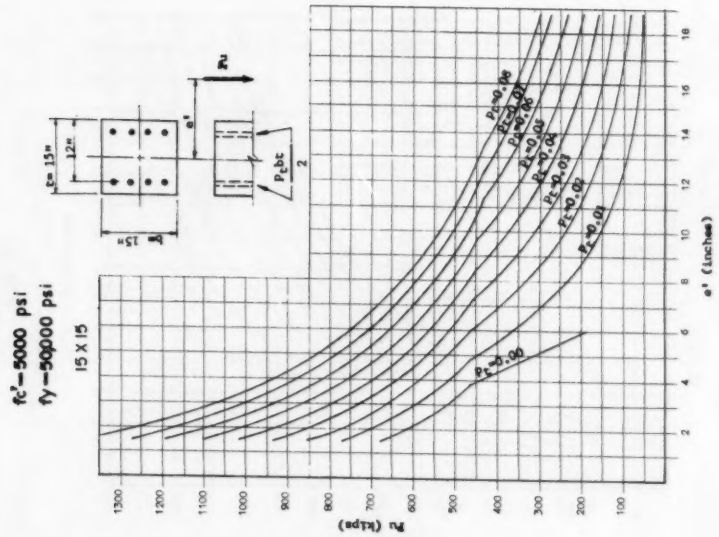
f'c=5000 psi
fy=50000 psi
15 X 15
t= 15"
12"
15"
e'
Pu
Pu (kips)
e' (inches)
Pt=0.08
Pt=0.07
Pt=0.06
Pt=0.05
Pt=0.04
Pt=0.03
Pt=0.02
Pt=0.01
Pt=0.00

FIG. 15

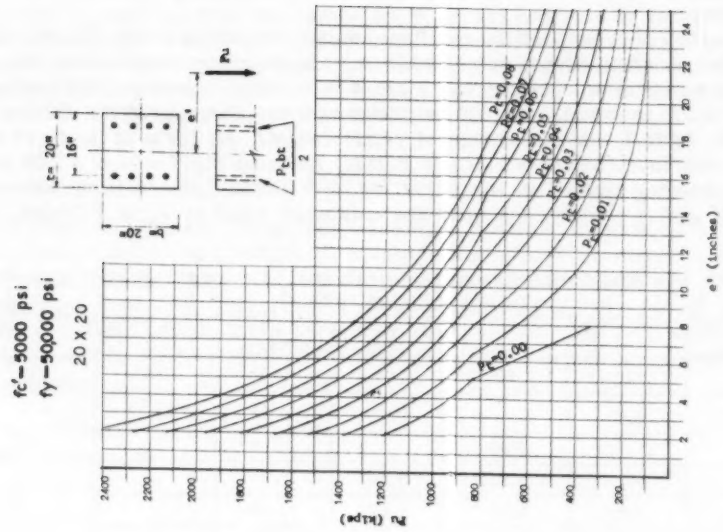
fc'=5000 psi
fy=50,000 psi
20 X 20
Pu (kips)
e' (inches)
Pt=0.08
Pt=0.07
Pt=0.06
Pt=0.05
Pt=0.04
Pt=0.03
Pt=0.02
Pt=0.01
Pt=0.00

FIG. 18

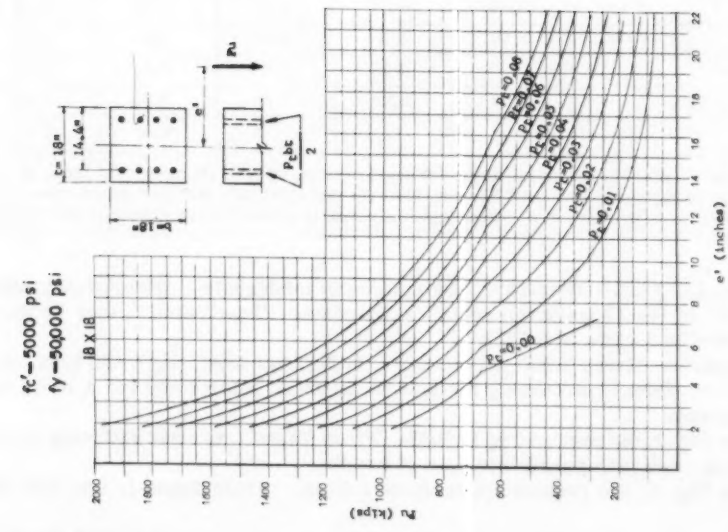
fc'=5000 psi
fy=50,000 psi
18 X 18
Pu (kips)
e' (inches)
Pt=0.08
Pt=0.07
Pt=0.06
Pt=0.05
Pt=0.04
Pt=0.03
Pt=0.02
Pt=0.01
Pt=0.00

FIG. 17

USE OF CHARTS

The use of the charts is largely self-evident and will be demonstrated by two examples.

Example 1.—Given a 12 in. by 12 in. column, reinforced with four #6 bars with 2 in. concrete cover, subjected to an ultimate compressive load, Pu, of 350 kips acting at an eccentricity, e', of 2.50 in. about one axis. With values of $f_c' = 4{,}000$ psi and $f_y = 50{,}000$ psi, determine the adequacy of the section.

From Table 1, the percentage of reinforcement, p_t, for a 12 in. by 12 in. column with four #6 bars is 1.22% or 0.0122. Entering Fig. 7 with $e' = 2.50$ in., and proceeding upward to the curve for $p_t = 0.0122$ (interpolating between $p_t = 0.01$ and $p_t = 0.021$, one finds the maximum value of P_u is 323 kips, or

TABLE 1.—REINFORCING FOR ONE-WAY BENDING. PERCENTAGES OF SQUARE COLUMN GROSS AREA, P_t

Reinforcement	Side, in Inches					
	12	14	15	16	18	20
Four #5	0.86					
Four #6	1.22	0.90				
Four #7	1.67	1.22	1.06			
Six #6	1.83	1.35	1.17	1.03		
Four #8	2.20	1.62	1.40	1.24	0.97	
Four #9	2.78	2.04	1.78	1.56	1.23	1.00
Four #10	3.55	2.58	2.26	1.98	1.57	1.27
Four #11	4.33	3.22	2.77	2.45	1.92	1.56
Six #10	5.29	3.90	3.39	2.97	2.35	1.90
Six #11	6.50	4.77	4.16	3.65	2.89	2.34
Eight #10			4.53	3.97	3.13	2.54
Eight #11			5.55	4.88	3.85	3.12
Ten #11					4.81	3.90

This table includes as many bars for each section as will fit along two faces of the column, in accordance with ACI 318-56, 1103 (b) and 1104 (a). Reinforcement placed in this manner is in agreement with assumptions made in constructing ultimate load charts.

less than 350 kips. Therefore, the section is inadequate. (Reinforcing such that $p_t = 0.02$ would make the section inadequate. From Table 1, four #8 bars would provide a ratio of 0.022).

Example 2.—Given 3,000 psi concrete, 50,000 psi steel, $P_u = 450$ kips, and $e' = 3.20$ in. Select reinforcing for a 14 in. by 14 in. column and for a 16 in. by 16 in. column.

From Fig. 2, the required p_t is 0.034. From Table 1, use six #10 (with three bars along each face parallel to axis of bending).

From Fig. 4, the required p_t is about 0.0115. From Table 1, use four #8 bars.

If the conditions for which the curves were drawn are not satisfied, the designer may be able to adapt them to his situation after studying the effects of

varying the parameters in the ACI 318 - 56 formulas or similar expressions. One common case to which the curves can be adapted arises with the use of concrete having a compressive strength of 3,750 psi. If one multiplies the values of P_u obtained from the curves for 4,000 psi concrete by 3,750/4,000 or 0.94, one obtains a value of P_u always on the conservative side with a maximum error of 4%. For instance, if fc' were 3,750 psi instead of 4,000 psi in Example 1, the maximum value of P_u with the given reinforcement would be 0.94 x 323 = 304 kips.

CONCLUSIONS

It is hoped that these design aids will help in breaking down resistance to the use of ultimate strength design. It should be borne in mind, however, that the curves presented are merely graphical solutions of Eqs. 9 and 13 of the Joint Committee Report (Eqs. A9 and A11 in the Appendix, ACI 318 - 56) for certain types of column sections. As such, they eliminate the need to do some arithmetic, but they do not reduce the requisite understanding of the provisions of the report.

Journal of the
STRUCTURAL DIVISION
Proceedings of the American Society of Civil Engineers

DESIGN CONSIDERATIONS FOR FATIGUE IN TIMBER STRUCTURES[a]

By Wayne C. Lewis,[1] M. ASCE

SYNOPSIS

Working stresses for timber are developed from average test values for clear wood by applying factors for normal variability, indeterminacy of stress analysis, natural strength-reducing characteristics present in structural timbers, and duration of loading. Normally, no allowance is made for fatigue—that is, to provide for the possibility that failure may result from an accumulation of cyclic stressing during the life of the structure. This paper summarizes information now available on fatigue of wood and investigates the adequacy of design based on present-day working stresses with respect to fatigue.

INTRODUCTION

Fatigue has been termed the "forgotten member of the design family." T. M. Barlow, in 1929, stated[2] that

> "Fokker's reasons for retaining wood-wing construction for monoplanes are summed up in the word 'fatigue.' Claims of new materials to lightness must be reviewed in association with their fatigue limits. Fatigue in properly seasoned wood is unknown."

Note.—Discussion open until October 1, 1960. To extend the closing date one month, a written request must be filed with the Executive Secretary, ASCE. This paper is part of the copyrighted Journal of the Structural Division, Proceedings of the American Society of Civil Engineers, Vol. 86, No. ST 5, May, 1960.

[a] Presented at the February 1959 ASCE Convention in Los Angeles, Calif.

[1] Engr., Forest Products Lab. Forest Service, U. S. Dept. of Agric., Madison, Wisc.

[2] "The Weight of Aircraft," by T. M. Barlow, Aircraft Engineering, Vol. 1, 1929, p. 29. (Abstracted in "Abstracts of Articles on the Fatigue of Metals under Repeated Stress Appearing in the Technical Press from July 1, 1928, to June 30, 1929," prepared by ASTM Research Committee on Fatigue of Metals.)

It is more likely that, with the approximate methods of design used in that day, actual stresses which were repeated in aircraft were so low that fatigue failures did not develop during the life of the aircraft. A more nearly accurate analysis of the aspects of fatigue failures in timber is contained in the report of the subcommittee on duration of load and fatigue, of the Committee on Timber Structures.[3] Pointing out that wood is subject to fatigue failures in the same way as other materials, the report states:

> "The fatigue strength of large numbers of repetitions of stress of fibrous materials, such as wood, is a higher proportion of the static strength than of crystalline materials like metals. As a consequence, actual stresses in a wood structure are usually lower than the repeated stresses that will produce failure during the normal service life of a structure."

Though there have been but few fully authenticated examples of fatigue failures in actual service, laboratory studies have clearly demonstrated that if a wood structural member or part is subjected to a sufficient number of repetitions of stress of sufficient magnitude, it will fail. Fatigue failures in wood have the same appearance as static failures. This points out the possibility that some service failures in fatigue have been classified as static structural failures.

In metals such as steel, where the ordinary static failure is accompanied by ductile flow, there is a noticeable difference between that kind of failure and failure from fatigue, which is characterized by its brittle appearance. Fatigue failures in steel show the crystalline character of the metal, and, in the vernacular, it is said that the component having the failure has "crystallized."

Much more is known about fatigue of metal, riveted joints, and the cold working and stress relieving of metal parts and structural components than is known of wood. This is largely because the science of fatigue behavior is an empirical one, and machine parts are more often stressed a sufficient number of times so that fatigue failures develop; although some moving parts of machines, such as Pitman arms, continue to be made from wood because of their superior fatigue resistance and their high strength-weight ratio.

As refinements are made in design methods, and with the growth of the glued laminating industry, more and more will there be a need to consider the possibility of failure from fatigue in engineered structures of wood. It is the purpose of this paper to assemble what information is available on the fatigue resistance of wood stressed in different ways and, on the basis of results of experimental programs completed to date (1960), to analyze existing data in light of the working stresses usually used in the design of civil engineering structures.

FATIGUE TERMS AND RESULTS DESCRIBED AND DEFINED

Before any good understanding of fatigue is possible, it is necessary to define and describe just what fatigue is. Fatigue in engineering materials is defined as the progressive damage and failure that occur when a structure or part is subjected to repeated loads of a magnitude smaller than the indicated

3 "Duration of Load and Fatigue in Wood Structures," Proceedings, by Committee on Timber, ASCE, Vol. 83, No. ST 5, 1957.

static strength. "Static strength," as used in the definition, means the one-time load strength and is the strength of a member as measured by a static-stress test of 5 min to 10 min duration.

Stresses in engineering members are of various types. If they come into the member slowly and stay for a length of time, they are said to be a static stress. If they come on quickly and stay for a short period, they are classified as an impact or shock loading. Actual stressing in any member may be a combination of static and dynamic loading, and in design the cumulative effects should be considered in two ways. One, that of duration of load, is handled by the factor for normal or long-time loading discussed[4] by L. W. Wood where a factor of 5/8 is applied to the average static-strength property for accumulations of about 10 yr in developing a working stress.

In fatigue, if the repetitions of design stress or near-design stress probable or possible during the normal life of the structure are more than 100,000 cycles, some such consideration for fatigue should be made. In design considerations, either duration or repetition of load will usually be a governing factor; and if repetition of load governs, then the design stress used should be less than that which would produce a fatigue failure under the number of repetitions possible or probable during the life of the structure.

How is fatigue resistance measured? In test, specimens are loaded repetitively to a predetermined level of stress and the number of cycles that produces failure is determined. For a number of different specimens loaded to different maximum stresses, several values of stress and numbers of cycles to failure will be obtained. When these values are plotted with the maximum repeated stresses as ordinates and the corresponding numbers of cycles of stress to failure (usually on a logarithmic scale) as abscissas, it is possible to connect the points into a curve of descending order. As the magnitude of repeated stress decreases, the number of cycles to failure increases. The curve is called the S-N diagram. Fig. 1 shows a typical S-N diagram for wood in shear.

In tests of steel and some other materials, the S-N diagram levels out on the lower portion, and it is possible to draw a horizontal line below which repeated stresses will not produce fatigue failure in an infinite number of cycles. The level of stress for the horizontal portion is called the endurance limit, and is defined as the maximum stress which can be repeated an infinite number of times without inducing failure. In wood, many metals other than steel, and plastics, the S-N curve continues to decrease even beyond 10,000,000 cycles, a common end point in test, so fatigue strength becomes the important term. Since fatigue strength is the maximum stress than can be repeated for a given number of cycles without causing failure, any value for fatigue strength must include the number of cycles—thus, "fatigue strength for 10 million cycles" or "fatigue strength for 100,000 cycles." For practical purposes, fatigue strenght for 10,000,000 cycles can be used for wood in civil engineering in the same way that the endurance limit is used for steel, because there is only a remote possibility that so many repetitions of stress will be encountered in actual use.

The fatigue behavior of materials is influenced by the amplitude of the stress cycle as well as by the amount of the maximum stress. The greater the difference between the minimum and the maximum stresses for each cycle, the

---

[4] "Safety Factor in Design of Timber Structures," by L. W. Wood, Proceedings, ASCE, Vol. 84, ST 7, 1958.

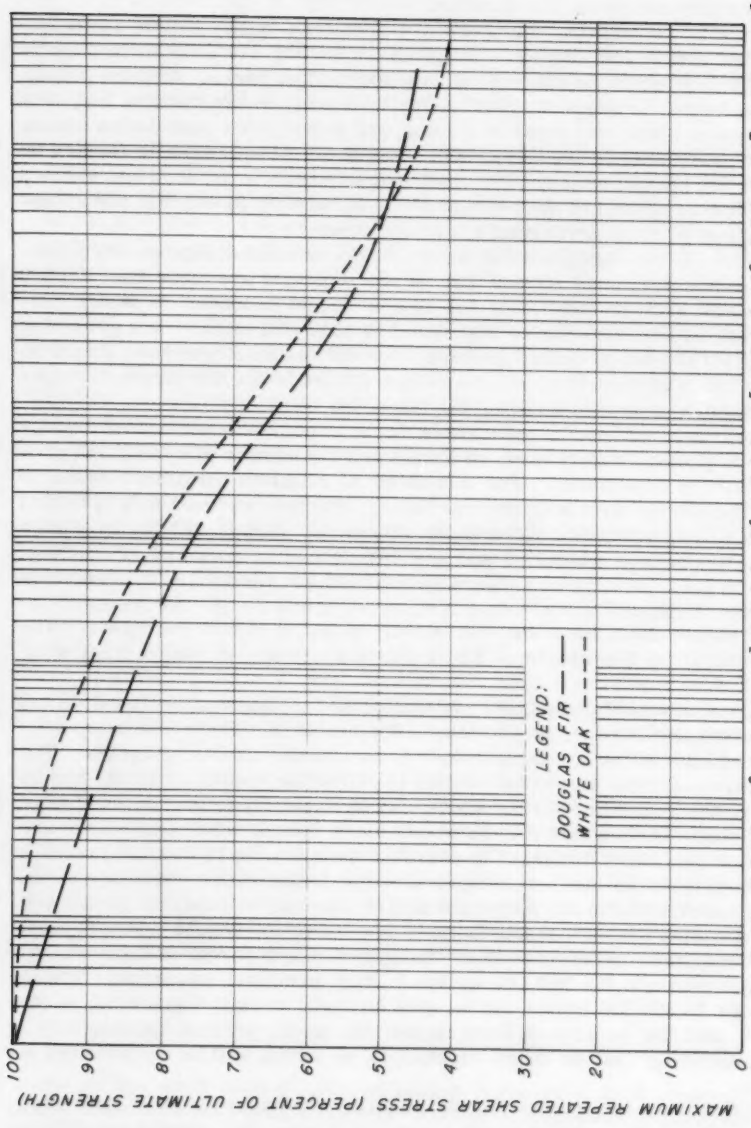

FIG. 1.—S-N CURVES FOR GLUE SHEAR IN LAMINATED DOUGLAS FIR AND WHITE OAK. RATIO OF MINIMUM REPEATED SHEAR STRESS TO MAXIMUM REPEATED SHEAR STRESS FOR EACH CYCLE WAS 0.10.

smaller will be the number of cycles before failure. The ratio of minimum to maximum repeated stress is called the stress ratio, R. It and other terms are defined by ASTM in its manual on fatigue testing.[5]

If groups of tests are made on the same material with the same kind of specimen at different stress ratios, the result will be a family of S-N curves, of which the curves with the greatest stress amplitude (lowest stress ratio) will be in the lowest position, relatively. This means that the fatigue life (number of cycles to failure) will be less at a given maximum stress when the minimum repeated stress is 10% of the maximum stress per cycle (stress ratio 0.10) than if it is 30% (stress ratio 0.30).

Stresses in a structure may be repeated, as from zero to some value, or from some value to another higher one in the same direction, or they may be partially or completely reversed. Partially reversed loading occurs where repeated stresses are not the same in either direction; fully reversed stresses are of equal magnitude, as in compression and tension or as in positive and negative shear. Fully reversed stressing is the most severe loading condition and will give S-N diagrams in the lowest position. Partially reversed stressing gives S-N diagrams higher in position than does fully reversed stressing, but lower in position than does repeated stressing. The stress ratio is expressed as -1 for fully reversed loading and as a negative deciman for partially reversed loading.

Nearly all fatigue tests on wood and wood construction have been made under repeated loading conditions, because this is the most common loading in such structures as timber-bridge stringers, other beams subjected to repeated loads, and components of arches and trusses. Because some dead load always remains on the members, and for practical reasons in testing, a stress ratio of 0.10 has been selected for most of the tests. In the following sections of this paper, the available information on fatigue-test results pertinent to timber and glued wood constructions is summarized.

FATIGUE OF WOOD IN BENDING

Much of the timber put into structures where repeated loading may be a factor is used for beams, such as stringers in bridges and girders in buildings, where vibratory stresses from heavy machines are transmitted through the floor system. A report has been made[6] on an investigation of the fatigue resistance of quarter-scale bridge stringers of green and dry southern pine. This research was jointly financed by the Association of American Railroads (AAR) and the U. S. Forest Products Laboratory.

Beams are subjected to a combination of forces, tension, and compression in opposite faces in areas of greatest bending moment and shear in areas of greatest total force as near supports. The span-depth ratio and location of loads determine the relative importance of the bending and shear stresses. In the study of quarter-scale stringers, specimens were loaded at the third points, and in the green and dry specimens with either straight of 1:12 sloping grain, failure in bending was critical under either static or fatigue (repeated) loading. In some of the dry specimens, artificial checks were cut in the shear

5 "Manual on Fatigue Testing," by Committee E-9 on Fatigue, ASTM, Special Tech. Publication No. 91, 1949.

6 "Fatigue Resistance of Quarter-Scale Bridge Stringers of Green and Dry Southern Pine," by W. C. Lewis, AREA Bulletin, No. 538, 1957, pp. 363-390.

portion to simulate the maximum checks that could occur from drying. In those specimens, shear was critical, and all of the fatigue specimens and most of the static specimens failed in shear.

The fatigue tests on green material indicated that, if the repeated maximum stresses were low enough so that compression failures did not develop, the specimen withstood 10,000,000 repetitions for a stress ratio of 0.10 without any failure. The fatigue strength for no failure at 10,000,000 cycles was indicated to be 50% of the static strength for straight-grained material, and 60% of the static strength for 1:12 slope of grain. The fatigue strength of the green material tested was indicated to be about 3,000 psi for both the straight-grained specimens and those with 1:12 slope of grain.

The fatigue tests of the dry specimens without the artificial checks indicated that the fatigue failures in the straight-grained specimens were in compression followed by tension and that, for a stress ratio of 0.10, the fatigue strength at 10,000,000 cycles was about 50% of the static strength, or about 7,000 psi for the material tested. Those with the 1:12 slope of grain usually failed in corss-grain tension with no visible compression, and the indicated fatigue strength for 10,000,000 cycles was about 45% of the static strength, or 4,500 psi for the material tested.

The air-dry specimens with the artificial checks, which reduced the width of the area in shear by one-half, indicated that fatigue strength for 10,000,000 cycles was 35% of the static strength for both the straight-grained specimens and those with a 1:12 slope. This amounted to 300 psi computed on the gross section for straight-grained material and 250 psi for material with a 1:12 slope.

FATIGUE OF WOOD IN COMPRESSION OR TENSION

Until a few years ago, the phenomenon of fatigue failure was associated only with tensile stressing. All fatigue failures observed in service were associated with a tension crack or failure. In most structures, members are sufficiently large so that nearly pure stresses occur in critical areas where fatigue failures could develop. The information already presented on compression introduced by bending is useful in appraising the possibility of fatigue failures in compression. If, as is borne out by those tests, stresses in compression are high enough so that failures can develop in green material after a very few cycles and those stresses are 50% or more of the modulus of rupture, there is little possibility of fatigue failure. In terms of compressive strength, there is little question about the resistance to fatigue. Compressive strength of green wood is 1/2 to 2/3 of the modulus of rupture, so the fatigue strength for 10,000,000 cycles in compression parallel to grain would be at least 75% of the static strength for green material.

The static compressive strength of air-dry wood ranges from about 45% to 60% of the modulus of rupture. The fatigue bending tests of air-dry wood with straight grain indicated that the fatigue strength for 10,000,000 cycles (stress ratio 0.10) was about 50% of the modulus of rupture. On that basis, the fatigue strength in compression can be estimated to be at least 80% of the compressive strength parallel to the grain. These analyses can be considered conservative, since, in members so stressed, the ability of the member to carry compressive loads is not lost entirely when compression failures develop in the fibers. Members with compression failures will be strong enough to carry practically the same loads as those that produced the failure.

This is not so in tension parallel to the grain. When a tension failure develops, either in service or during test, the breakage of fiber that results means that the portion that failed is incapable of carrying further load. If the failure is complete, it means the member can carry no load. It has been reported[7] that fatigue strength in tension parallel to grain for Douglas fir and white oak for 10,000,000 repetitions of stress (stress ratio 0.10) was 50% or more of the static strength. Static tensile strength values of the Douglas fir ranged from 9,000 psi to 20,900 psi for a range in specific gravity of 0.40 to 0.55, with an average of 14,370 psi for a specific gravity of 0.47 (based on weight and volume of ovendry wood). Corresponding values for white oak ranged from 9,000 psi to 24,300 psi for a range in specific gravity from 0.54 to 0.83, with an average of 16,620 psi for a specific gravity of 0.66.

FATIGUE OF BOLTED JOINTS

The Central Research Laboratory of the AAR has been engaged in a fatigue study of bolted joints corresponding to the joints used in trestles where sway bracing is bolted to piling. While quantitative values of fatigue strength are not available because the study has not been completed, important qualitative information on the mode of failure has been obtained. The failures in fatigue in the wood members of a bolted joint are indefinite, in that the end point in test is an arbitrary one based on an enlargement of the hole in which the bolt is fitted. Repetitions of load, by increasing the size of hole, produce a joint that has more slippage than can be tolerated. As a result, it becomes necessary to repair the joint. The fatigue damage requires a maintenance expenditure but does not cause a loss in strength, and the type of failure does not endanger the structure itself.

FATIGUE OF GLUED JOINTS USED IN LAMINATED MEMBERS

Because more glued-laminated members are now used in structures than formerly, the question of the fatigue resistance of the glue and the glued joints in wood is an important consideration for repetitions of loading. A series of tests was conducted[7] that involved (1) tension parallel to grain of Douglas fir and white oak specimens, with and without glued scarf joints; (2) tension perpendicular to the grain in specimens of Douglas fir; and (3) glue shear (corresponding to stresses that can be introduced in glue lines between lamina) in laminated Douglas fir and white oak. It was concluded that, as long as proper considerations are made for any reduction in static strength, there is no greater likelihood that fatigue failures will develop in the well-made glued joints than in the wood.

In the glued-laminated shear specimens, failures occurred both under static loading and from fatigue in the wood itself, rather than in the glue line, so values obtained are significant from the standpoint of fatigue of wood in shear. Fatigue strength at 10,000,000 cycles of stress (stress ratio 0.10) was about 45% of the static strength for both species. Static strength averaged about 750 psi for the Douglas fir and 1,300 psi for the white oak. On that basis, for material of the quality included in those tests, the fatigue strength for 10,000,000

[7] "Fatigue of Wood and Glued Joints Used in Laminated Construction," by W. C. Lewis, Proceedings, Forest Products Research Soc. Vol. 5, 1951, pp. 221-229.

repetitions of stress would be about 340 psi for Douglas fir and 580 psi for white oak.

THE RELATION OF FATIGUE STRENGTH TO WORKING STRESSES

While the data on fatigue of wood are admittedly incomplete, there is sufficient information available for some comparisons based on working stresses currently recommended. In any structure subjected to a large number of repetitions of stress, the engineer is interested in determining whether or not the design stresses he uses are below those that will cause either failure or excessive maintenance from fatigue produced by repetitions of stress. Wood points out[4] that, in arriving at working stresses for normal loading, factors for (1) variability, (2) duration of load, (3) a combination of other factors, and (4) the strength ratio based on the maximum defect allowed in a certain stress grade are applied to the strength of clear wood in arriving at a working stress. A working stress developed in this way gives a near minimum factor of safety of 1-1/4 to 1-1/2, with an average more nearly equal to 2 to 2-1/2.

If factor (2) and the near minimum of safety are combined, the minimum combined factor is 5/8 times 4/5, or 0.50, for normal loading; the 0.50 is equal to or less than the indicated fatigue strength for 10,000,000 cycles of stress in the following instances:

1. Bending of green, straight-grained material
2. Bending of green, 1:12 slope-of-grain material
3. Bending of air-dry, straight-grained material
4. Compression parallel to surface, green material
5. Compression parallel to surface, air-dry material
6. Tension parallel to grain, air-dry material

The values were less than the 0.5 obtained by combining the factor for duration of load and a near minimum factor of safety only in (1) bending of air-dry specimens with a 1:12 slope of grain, where the fatigue strength was indicated to be 45% of the modulus of rupture; (2) shear of artificially checked specimens with either straight grain or 1:12 slope with an indicated fatigue strength for 10,000,000 cycles of 35% of static strength; and (3) the laminated shear specimens of Douglas fir and white oak with an indicated fatigue strength for 10,000,000 cycles of 45%.

The question naturally arises: "Why was near minimum factor of safety used in the combination of factors?" Repeated loadings do not reduce the margin of safety from static loading. Tests at the Forest Products Laboratory, involving specimens loaded repeadedly in bending up to 1,000,000 times to 50% of static strength, have shown no measurable reduction in static strength. This finding is supported by tests of metal and other materials. Until actual fatigue failure starts, the strength of a material is not impaired.

All analyses in this paper are based on the fatigue strength for 10,000,000 cycles, and the results presented are based on tests wherein the minimum stress for each cycle was 10% of the maximum for that cycle. Indications are that in most civil engineering structures the number of repetitions probable in service is much less than that. Committee 7, Wood Bridges and Trestles of the American Railway Engineering Association, which cooperates with the

staff of the Central Research Laboratory of the AAR, estimates that the stringers in a short-span railroad bridge will have no more than 2,000,000 repetitions of stress during the normal life of the structure. At fewer cycles of stress than 10,000,000, the fatigue strength would be a higher percentage of the static strength. Because of this, it appears reasonable to assume that fatigue resistance of timber in most applications is adequate with present design allowables. Only in the case of more severe loading, such as fully or partially reversed loading, is there doubt.

The limited amount of data available on the phenomenon of fatigue of wood, and a corresponding lack of information on the number and nature of repetitions imposed in service, suggest further research.

Journal of the
STRUCTURAL DIVISION
Proceedings of the American Society of Civil Engineers

MINIMUM COST DESIGN OF LARGE SUPPORT RINGS

By Kenneth P. Buchert,[1] F. ASCE

SYNOPSIS

There is suggested a method of design for large support rings. The method proposes that the outer flange plate of the ring can be eliminated on various sections of the ring without materially affecting the ring stresses. Significant savings in the fabrication cost of the ring can thus be realized.

INTRODUCTION

Support rings of the type shown in Fig. 1 have been used extensively in recent years to support the weight of penstocks, tanks, large ducts, wind tunnels, and other structures.

Herman Schorer has presented[2] a method for the design of supports for large pipelines. The method proposed was to use a constant-moment-of-inertia support ring welded to the shell, which, in turn, was supported at the ends of its horizontal diameter to support the pipe. In recent years, larger and larger lines have been designed and built, many using support rings. These rings often consist of a web member welded to the shell and a flange member welded to the web. For relatively small pipes, sometimes the flange member has been eliminated and only a web member is used. For very large pipes or ducts, double, triple, and sometimes quadruple webs and multiple flanges have

Note.—Discussion open until October 1, 1960. To extend the closing date one month, a written request must be filed with the Executive Secretary, ASCE. This paper is part of the copyrighted Journal of the Structural Division, Proceedings of the American Society of Civil Engineers, Vol. 86, No. ST 5, May, 1960.

1 Genl. Supervisor, Design Engrg., Consol. Western Steel Div., U. S. Steel Corp., Los Angeles, Calif.

2 "Design of Large Pipe Lines," by Herman Schorer, Transactions, ASCE, Vol. 98, 1933, pp. 101-191.

SECTION A-A

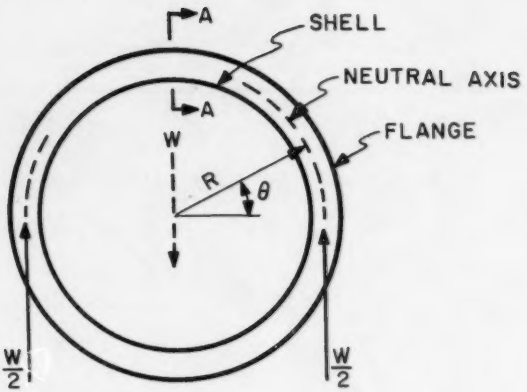

(a)

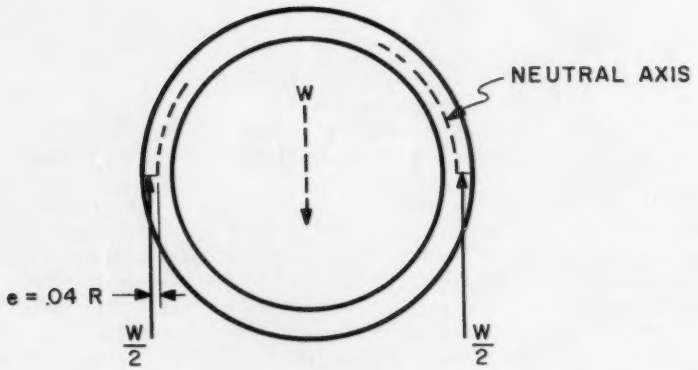

(b)

FIG. 1.—CIRCULAR SUPPORT RING

been used. Since the unit costs of these support rings are relatively high and since the stress in some parts of the ring is relatively low, it appears that a variable-moment-of-inertia ring in which fabrication costs are considered might result in a ring that could be produced at minimum cost with a given predetermined design factor of safety. Before a ring with a variable moment of inertia is used, however, it is necessary for the designer to evaluate the change in stresses due to the variable moment of inertia.

RING WITH CONSTANT MOMENT OF INERTIA

Fig. 1(a) shows a constant-moment-of-inertia support ring supported at the ends of the horizontal diameter. The support loads are applied at the neutral axis of the ring. The load W is applied to the ring by shear stresses in the shell that are zero at the ends of the vertical diameter and are maximum at the ends of the horizontal diameter. The statically indeterminate solutions for the bending moments, normal forces, and shears have been presented by Schorer and others. Fig. 2 gives moment, normal force and shear force in the ring as a function of θ.

In some instances a more economical support ring can be built by applying the support load at some distance e from the neutral axis of the ring. This eccentricity introduces a moment at the supports and reduces the maximum moments in the rings. In some cases this reduces the stresses in the ring. If e in Fig. 1(b) is made 0.04, the moment at the horizontal diameter of the ring is equal to the maximum moment in other parts of the ring. The moments, normal forces, and shears for an externally applied moment is given in Fig. 3. The moments, normal forces, and shears in a ring due to a vertical load W and a support eccentricity of e = 0.04 R is given in Fig. 4.

RING WITH VARIABLE MOMENT OF INERTIA

After a study of Figs. 2 and 4 it is apparent that the constant-moment-of-inertia ring is not stressed to its maximum allowable value in several locations. This would lead to the conclusion that for minimum weight a ring with a variable moment of inertia could be built that would result in maximum structural efficiency for the ring. The problem then becomes: How can a variable-moment-of-inertia ring be designed that will be more uniformly stressed and result in a minimum-cost design? An approach to the solution, for large-diameter rings where a web and flange are used, is to attempt to eliminate the flange plate of the ring where the stresses are small. With a proper choice of location, depending on size of the ring, etc., the cost of fabrication can be reduced by using less material, decreasing shop fitup time, reducing the amount of weld between the web and flange, and reducing or eliminating butt welds in the flange. If this approach is used, the question then arises: What is the effect on the moments, normal forces, and shears if a ring of this type is used? The following is a derivation of the forces and moments that will exist in the above type of ring.

Fig. 5 shows a ring with the shear loads applied that are a result of the vertical loads applied to the ring. Then,

$$M_\theta = \frac{W R}{4}\left(\text{vers } \theta\right) - \int_0^\theta \frac{W \cos x}{\pi R}\left[R \text{ vers}\left(\theta - x\right)\right] R\, dx - H_0 R \sin \theta \quad . . (1)$$

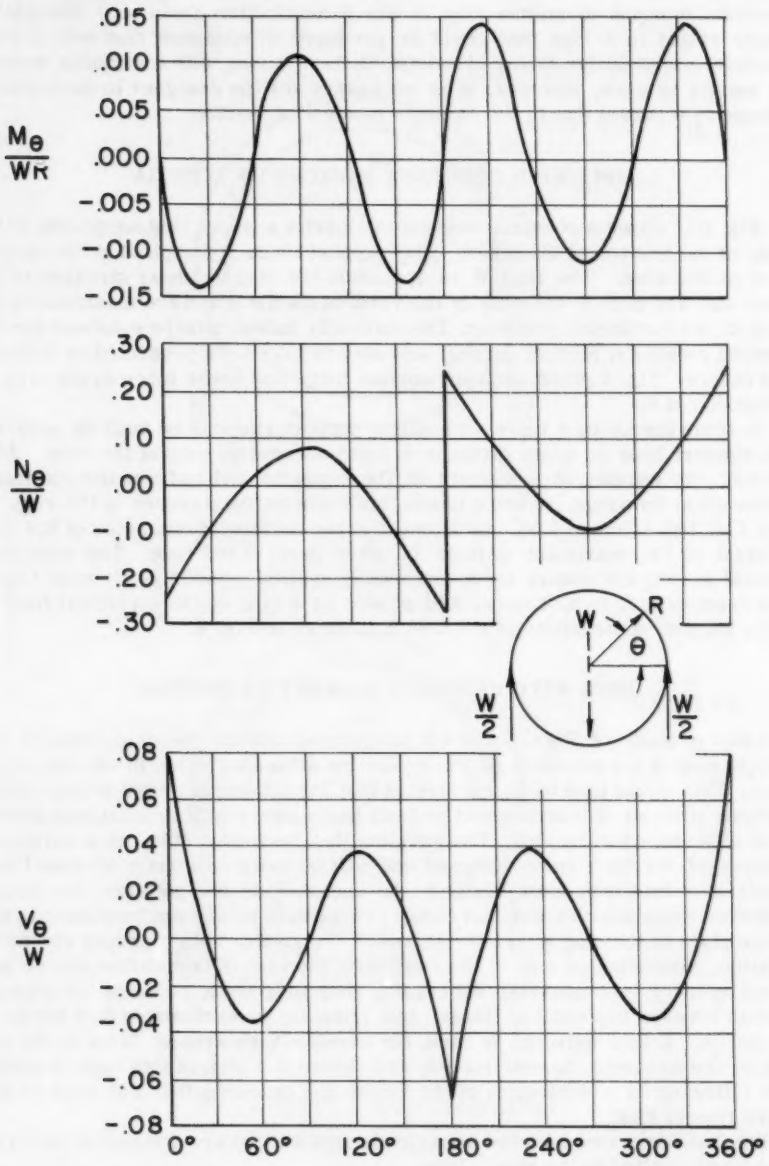

FIG. 2.—SUPPORT RING WITH SUPPORT LOAD APPLIED AT NEUTRAL AXIS

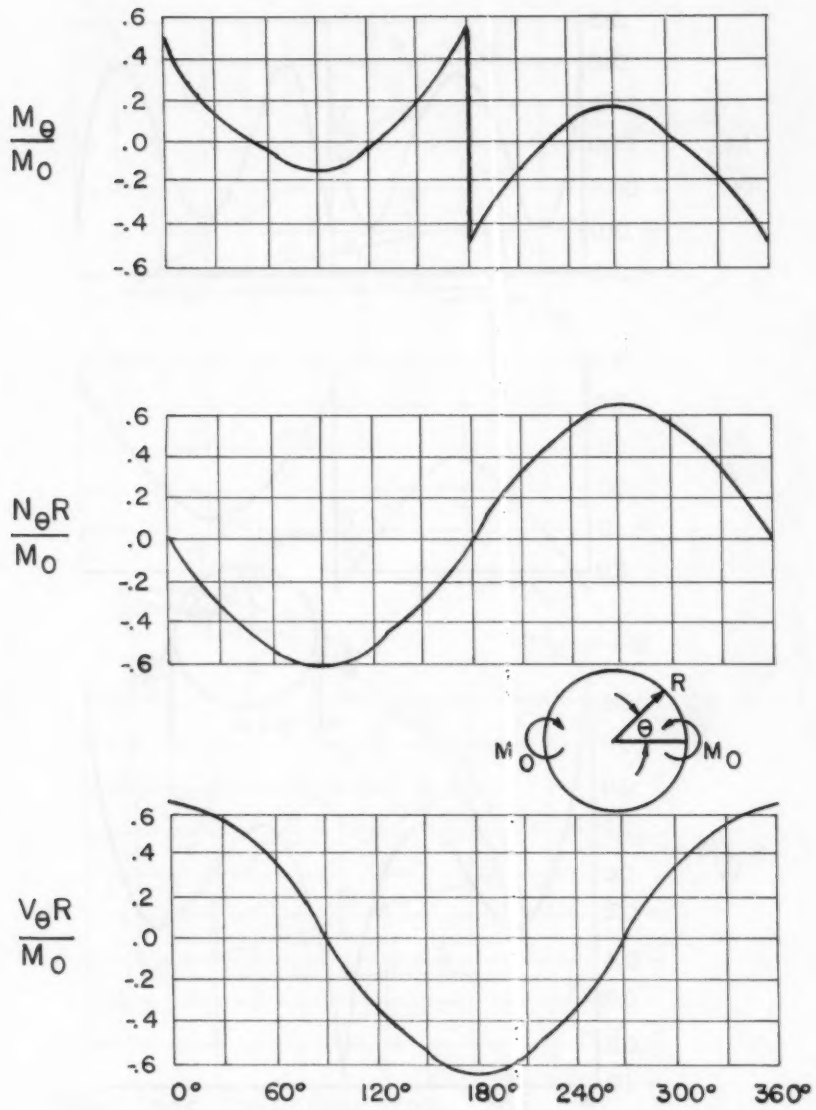

FIG. 3.—SUPPORT RING WITH APPLIED EXTERNAL MOMENT AT EXTREMETIES OF A HORIZONTAL DIAMETER.

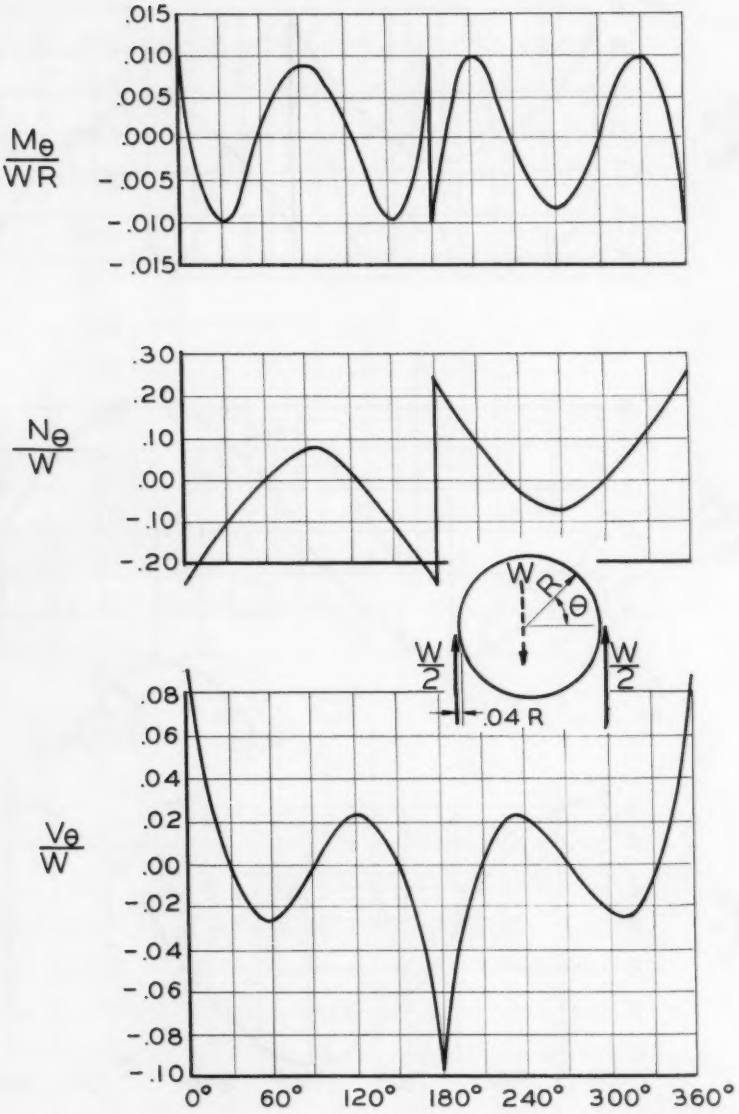

FIG. 4.—SUPPORT RING WITH SUPPORT LOAD APPLIED ECCENTRIC TO NEUTRAL AXIS

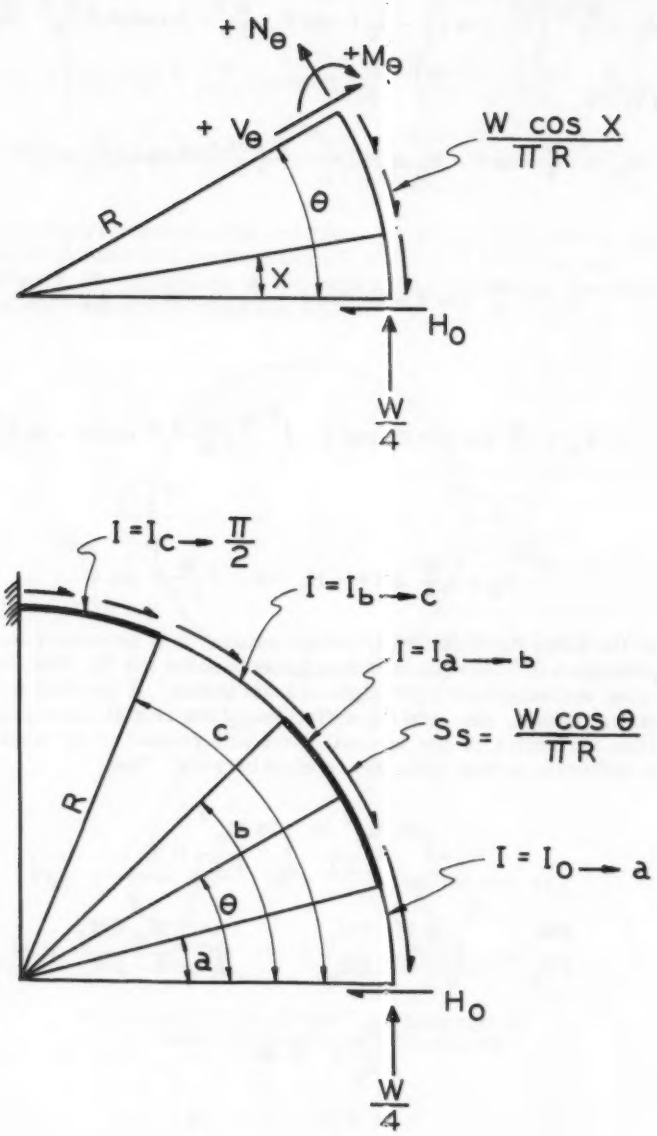

FIG. 5.—SUPPORT RING WITH APPLIED LOADS

or

$$M_\theta = \frac{W\,R}{4}\left(1 - \cos\theta\right) - H_0\,R\sin\theta + \frac{W\,R}{2\pi}\,\theta\cos\theta - \frac{W\,R}{\pi}\,\frac{\sin\theta}{2} \quad ..(2)$$

and

$$N_\theta = -\frac{W}{4}\cos\theta - H_0\sin\theta + \int_0^\theta \frac{W\cos x}{\pi R}\,R\cos(\theta - x)\,dx \quad .....(3)$$

or

$$N_\theta = -\frac{W}{4}\cos\theta - H_0\sin\theta + \frac{W}{2\pi}\,\theta\cos\theta + \frac{W}{2\pi}\sin\theta \quad .....(4)$$

and

$$V_\theta = -\frac{W}{4}\sin\theta + H_0\cos\theta + \int_0^\theta \frac{W\cos x}{\pi R}\,R\sin(\theta - x)\,dx \quad ....(5)$$

or

$$V_\theta = -\frac{W}{4}\sin\theta + H_0\cos\theta + \frac{W}{2\pi}\,\theta\sin\theta \quad .....(6)$$

Since the force H_0 is statically indeterminate, it is necessary to apply one of the principles of indeterminate structures to solve for H_0. One method that can be used is Cantigliano's principle of least action. If the ring is cut at the horizontal diameter, the relative deflection of the ring at the cut is zero, or the partial derivative of the internal work with respect to H_0 must equal the relative deflection at this point, hence must be zero. Then,

$$W_i = \int_0^{2\pi} \frac{M_\theta^{\,2}\,ds}{2\,E\,I} \int_0^{2\pi} \frac{M_\theta^{\,2}}{2\,E\,I}\,R\,d\theta \quad .....(7)$$

$$\frac{\partial W_i}{\partial H_0} = 0 = \int_0^{2\pi} \frac{M_\theta}{E\,I}\,\frac{\partial M_\theta}{\partial H_0}\,R\,d\theta = 4\int_0^{\pi/2} \frac{M_\theta}{E\,I}\,\frac{\partial M_\theta}{\partial H_0}\,R\,d\theta \quad ....(8)$$

$$\frac{\partial M_\theta}{\partial H_0} = -R\sin\theta \quad .....(9)$$

$$\frac{\partial W_i}{\partial H_0} = 0 = \int_{0,a,b,c}^{a,b,c,\pi/2} \left[\frac{W}{4I}(1 - \cos\theta) - \frac{H_0}{I} \sin\theta + \frac{W}{2\pi I}\theta\cos\theta - \frac{W}{2\pi I}\sin\theta \right] \sin\theta \, d\theta = \left\{ \frac{W}{4I}(-\cos\theta) - \frac{W}{4I}\left(\frac{\sin^2\theta}{2}\right) - \left(\frac{H_0}{I} + \frac{W}{2\pi I}\right)\left(\frac{\theta}{2} - \frac{\sin\theta\cos\theta}{2}\right) + \frac{W}{16\pi I}(\sin 2\theta - 2\theta\cos 2\theta) \right\}_{0,a,b,c}^{a,b,c,\pi/2} \quad \ldots\ldots\ldots\ldots (10)$$

in which I is considered to be different from $\theta = 0$ to a, θ = a to b, etc. For this particular solution I is constant from $\theta = 0$ to a, θ = a to b, etc.

If a moment M_0 is applied to the ends of the horizontal diameter of a variable-moment-of-inertia ring (Fig. 6),

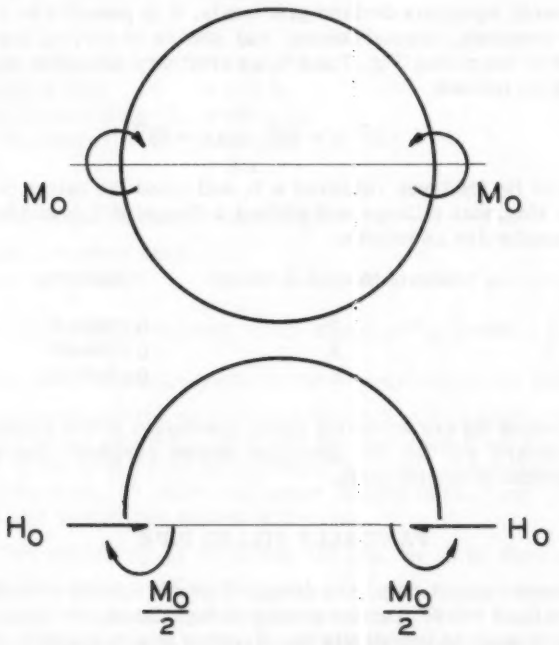

FIG. 6.—EXTERNALLY APPLIED MOMENT AT ENDS OF HORIZONTAL DIAMETER

$$M_\theta = \frac{M_0}{2} - H_0 R \sin\theta \quad \ldots\ldots\ldots\ldots\ldots\ldots (11)$$

$$\frac{\partial W_i}{\partial H_0} = 0 = \int_0^{2\pi} \frac{M_\theta^{\,2}\, ds}{2EI} = \int_0^{2\pi} \frac{M_\theta}{EI}\frac{\partial M_\theta}{\partial H_\theta} R \, d\theta \quad \ldots\ldots\ldots\ldots (12)$$

$$\frac{\partial M_\theta}{\partial H_0} = - R \sin \theta \quad \ldots\ldots\ldots\ldots\ldots\ldots (13)$$

$$\frac{\partial W_i}{\partial H_0} = 0 = 4\int_0^{\pi/2} \frac{1}{I}\left(\frac{M_0}{2} - H_0 R \sin\theta\right) R \sin\theta \, d\theta$$

$$= \left\{ \frac{1}{I}\left[\frac{M_0}{2}(-\cos\theta) - H_0 R \left(\frac{\theta}{2} - \frac{\sin\theta\cos\theta}{2}\right)\right]\right\}_{0,a,b,c}^{a,b,c,\pi/2} \quad \ldots (14)$$

in which I is a variable as before.

COMPARISON OF FORCES AND MOMENTS

With the basic equations derived previously, it is possible to determine the effect on the moments, normal forces, and shears of varying the geometry of the ring. After examining Fig. 2 and 4, an arbitrary selection of ring geometry was made as follows:

$$a = 5^0,\ b = 50^0, \text{ and } c = 65^0$$

The value of H_0 for these values of a, b, and c and for ratios of moments of inertia of the ring, with a flange and without a flange, of 1, 3, and 6 were calculated. The results are as follows:

Ratio of Moment of Inertia	Value of H_0
1	0.07958 W
3	0.07964 W
6	0.07967 W

Since the values of H_0 are so nearly alike, the values of the moments, normal forces, and shears will be, for practical design purposes, the same for the ratios of moments of inertia given.

PARTIALLY FILLED PIPE

In some cases support rings are designed relatively close together and the pipe carries a fluid whose specific gravity is significant. In such cases it is sometimes necessary to investigate the stresses in a ring under partially full conditions because the stresses for the partially full condition sometimes exceed those for the full or full and pressurized condition. The basic equations for this condition were summarized by Schorer.[2] It should be noted in the equations that follow that the stresses in a ring under the half-full condition are considerably less when the eccentricity of the supports is zero than when eccentricity exists. Therefore, the designer must carefully evaluate whether or not to build eccentricity into the ring. Schorer gave the following conservative formulas for the half-full condition (the notation used has been changed to conform to that of the writer):

$$M = \frac{W}{2}\frac{R}{\pi}\left[\frac{2\,r}{\pi\,R} - \frac{\pi}{4}\left(1 + \frac{e}{r}\right) + \left(\frac{5}{4} - \frac{r}{R} + \frac{e}{R}\right)\sin\theta\right] \quad \ldots\ldots\ldots (15)$$

for the upper quadrants of the ring where W is the load assuming a full pipe and

$$M = \frac{W}{2}\,\frac{R}{\pi}\left[\frac{2\,r}{\pi\,R} + \frac{\pi}{4}\left(1 + \frac{e}{R}\right) + \left(\frac{1}{4} + \frac{r}{R} + \frac{e}{R}\right)\sin\theta + \left(\frac{3\,\pi}{2} - \theta\right)\cos\theta\right] \quad \ldots (16)$$

for the lower quadrants. It should be pointed out that the foregoing results are conservative; the normal force in the ring is only one-half of that for a full pipe, and the direct stress due to pressure is zero.

EXAMPLE

The following will illustrate one method of how a variable-moment-of-inertia ring could result in cost savings:

Design Criteria

Diameter of Duct	= 18 ft
Thickness of Pipe	= 5/8 in.
Load on Support Ring	= 400 kips
Design Pressure	= 42 psig
Service	= Air
Allowable Stress in Ring	= 12,650 psi = $\frac{P}{A} + \frac{N_\theta}{A} + \frac{M_\theta\,C}{I}$
Allowable Length of Shell Acting with Ring	= 0.78 $\sqrt{r\,t}$ on each side of web of ring

Consider a ring similar in detail to that shown in Fig. 1 with a $\frac{1}{2}$ in. by 12 in. web and a $\frac{1}{2}$ in. by 10 in. flange and with the eccentricity of the supports zero. The section properties of the ring will be A = 19.3 in.^{2}, I = 579.in.^{4}, c_o = 7.33 in., and c_i = 5.80 in. where c_o and c_i are the distances from the neutral axis to the outside of the ring and to the inside of the ring, respectively. Fig. 7(a) gives the stresses on the outer and inner flanges of the ring. Note that the stresses are high in only two places in the ring.

Consider the possibility of removing the $\frac{1}{2}$ in. by 12 in. flange plate in the region of $\theta = 0^0$ to 5^0, $\theta = 50^0$ to 55^0, etc., around the ring. The properties of the ring where the flange is removed are A = 14.3 in.^{2}, I = 213 in.^{4}, c_o = 9.31 in., and c_i = 3.32 in. Since the stresses are relatively high in the region of $\theta = 0$ to -5^0 and $\theta = 180^0$ to 185^0, the flange should not be removed in this area or the details of the support connection should reinforce this portion of the ring. The resulting ring will not be symmetrical about the horizontal axis and, therefore, is not exactly the same as the ring that was analyzed previously. However, the same conclusions regarding the relatively constant value of H_0 will apply in this case. One method of qualitatively justifying this conclusion is that those portions of the ring that contribute very little to the total work done by the internal stresses in the ring can be changed considerably without a significant effect on the value of H_0. Using this reasoning, the value

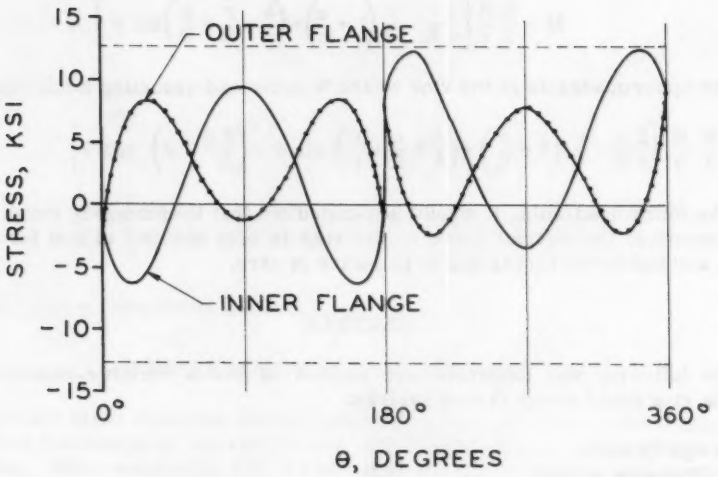

(*a*)

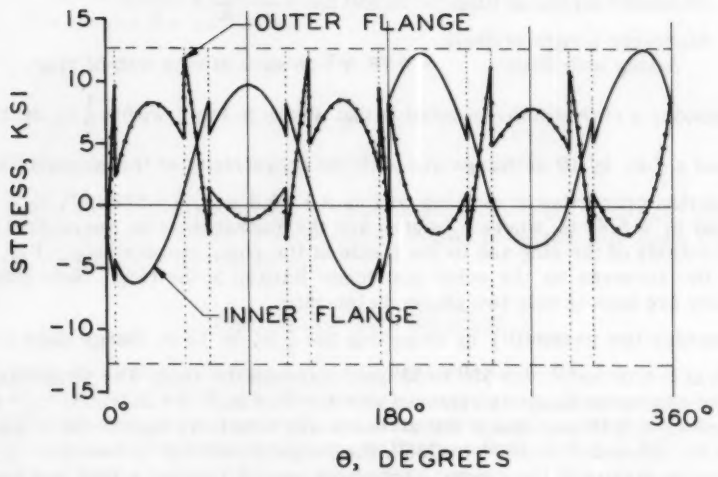

(*b*)

FIG. 7.—STRESSES IN SUPPORT RING

of H_0 in this example should be closer to the constant-moment-of-inertia value than those previously determined. By inspection, then, the change in the amount of ring flange removed will have a negligible effect on the moments and forces in the ring. The stresses in the resulting ring are shown in Fig. 7(b).

An estimate of the two rings indicates an order of magnitude savings of 10% in the cost of the ring. With further refinement in the design, and depending on loading conditions, it is felt that even greater savings in fabrication costs could be made.

FUTURE WORK

Although the analysis herein is rather straightforward, the time involved to obtain usable results may become lengthy. Fortunately, the problem can be readily adapted for solution on a digital computer. The computer, in addition to the speed factor, will allow the designer a wide latitude in the selection of moments of inertia and thus allow further economies that probably would not be attempted by hand methods. The computer will also probably reduce the design costs.

Many support rings are subjected to loads in addition to those presented herein. Horizontal loads, concentrated loads, and unsymmetrical loads are examples. Here again is a field where the variable ring and the computer can combine forces to save the client money.

CONCLUSIONS

A method has been presented which can be used to obtain more economical designs of support rings for large pipe or ducting. It is found that by eliminating the flange in large rings a significant savings will result in the cost of fabrication of the ring, and the stresses in the ring will be within predetermined allowable values. By a judicious choice of places where the flanges are eliminated, it is possible to use the same design moments, normal forces, and shears in the ring as would be used with a constant moment of inertia ring. It appears possible by the use of digital computers to obtain still further economies in the design of support rings and also to analyze many conditions or combinations of loading.

ACKNOWLEDGMENT

The writer wishes to acknowledge his indebtedness to John A. Dosier for checking the equations and calculations and to those people in the United States Steel Corporation who presented suggestions during the preparation of this paper.

NOTATION

The following notation has been used in this paper:

A = cross-sectional area of ring and effective portion of shell;

a, b, c = angles between horizontal axis of ring and point on ring where moment of inertia changes;

c_o or c_i = distance from neutral axis to extreme fiber of ring section;

E = modulus of elasticity of ring material;

e = eccentricity of supporting force from neutral axis of ring section;

H_0 = indeterminate shear force at each end of horizontal diameter (Fig. 5);

I = moment of inertia;

$I_{a \rightarrow b}$ = moment of inertia of ring between angles θ = a and θ = b;

M_θ = bending moment on ring section at angle θ;

M_0 = externally applied moment at each end of horizontal diameter;

N_θ = normal (hoop) force on section at angle θ;

P = normal force in ring due to pressure;

R = mean radius of ring;

r = mean radius of shell;

s = distance along circumference of ring;

S_s = unit shear loading from shell to ring = $\frac{W \cos x}{\pi R}$;

V_θ = shear force on section at angle θ;

W = total load to be supported;

W_i = internal strain energy of ring under load;

x = angle between horizontal diameter and point on ring; and

θ = angular location of section under analysis.

Journal of the
STRUCTURAL DIVISION
Proceedings of the American Society of Civil Engineers

RATIONALE FOR DETERMINING DESIGN WIND VELOCITIES

By A. G. Davenport[1]

SYNOPSIS

This paper first justifies the use of the "extreme wind velocity averaged over a mile or minute" as a "basic design wind velocity" in preference to absolute peak velocities which cannot be considered independently of the size of the structure, and of the dynamic response of anemometer, structure, and structural materials.

An attempt is, then, made to show from published records that reasonably systematic relationships exist between the ground roughness (as characterized by such general qualitative descriptions as "city," "treed countryside," and "open prairie") and both the magnitude of the extreme wind velocities near the ground and its rate of increase with height. This allows approximate estimates of the ratio of surface velocity to gradient velocity to be made. By these means, independent sets of anemometer records taken at locations differing in surface roughness can be compared.

By further introducing the extreme value theory a method is suggested whereby these sets of records may be numerically related taking into account the relative ground roughness, the number of years of record, the quality and consistency of the records, and the height of the anemometer. This process assists in minimizing the systematic errors which are often introduced into individual anemometer records.

Some published extreme-value data for the British Isles are analyzed according to the described procedure and an example is given illustrating how design wind velocities can be determined in a manner which takes into account

Note.—Discussion open until October 1, 1960. To extend the closing date one month, a written request must be filed with the Executive Secretary, ASCE. This paper is part of the copyrighted Journal of the Structural Division, Proceedings of the American Society of Civil Engineers, Vol. 86, No. ST 5, May, 1960.

[1] University of Bristol, England, formerly with the Div. of Bldg. Research, Natl. Research Council, Ottawa, Canada.

the important influence of surface roughness, the variability of useful life of different structures, and the risks involved if the wind velocity is exceeded.

INTRODUCTION

One of the principal loads acting on above-ground engineering structures is that due to the wind. Its accurate determination, therefore, is of fundamental importance in deciding what degree of safety and economy can be achieved in such a structure.

Formerly, it was common practice to design structures to resist the highest wind ever recorded by the instruments then in use. Although this did provide a sort of yardstick from which design wind loads could be estimated, it was unreliable and subject to the difficulty that most meteorological records will eventually be broken. A longer period of record increased the chances of recording a very high wind velocity. Another problem was that instruments which responded rapidly to fluctuations in wind speed tended to indicate higher velocities than those which were more sluggish. In other known instances, the highest wind had unfortunately blown away the instrument and the crucial information was lost.

All these difficulties tended to throw the problem of determining design wind velocities into the lap of the statistician who, from the records of several years, could estimate the probability of a given wind velocity recurring. Such are the vagaries of climate that the structural engineer can never hope for information much more certain than this.

Further problems emerge from other considerations. Because the velocity of the wind is continually fluctuating, recorded peak velocities will depend largely on the sensitivity of the anemometer. The pressures exerted on a structure will also fluctuate, leading to dynamic amplification of the actual stresses in the structure. This dynamic amplification, as well as being dependent on the intensity and power of the fluctuations, will also depend on the size and shape of the structure (as they will determine the rate of build-up of gust pressures) and on the response of the structure and its constituent materials to dynamically applied loads. The dynamic amplification will vary, therefore, with the size and flexibility of the structure.

For these reasons, wind loads are perhaps best considered in terms of a steady, applied force, independent of the structure's shape, size, and dynamic characteristics, together with a coefficient denoting the amplification which can arise through the interaction of the superimposed pressure fluctuations and the structure's dynamic response. The resolving of this coefficient, however, which is similar in many respects to the "earthquake problem," is not discussed herein.

This paper is confined to the determination of what will be termed the basic design wind velocity, which corresponds to the extreme sustained wind velocity giving rise to the steady component of the pressure. It is, therefore, an average velocity and the determination of a suitable averaging interval forms part of this discussion.

An attempt is made, also, to determine how records from a wide variety of anemometers of differing exposures and periods of record may be related to one another, thereby minimizing the systematic errors which may arise in the records due to anemometer siting and to the improvement of their overall re-

liability. This requires that cognizance be taken of the important influence of surface roughness both on the magnitude of the surface velocities and on the increase of velocity with height. Combining these results with the extreme-value theory leads to an exploratory method through which basic design wind velocities of given probability of occurrence may be predicted for locations of differing surface roughness.

STRUCTURE OF NATURAL WIND

The wind is caused by the atmospheric pressure differentials which rise over the surface of the earth. The acceleration produced by these pressure differentials is accompanied by other components of acceleration known as the geostrophic acceleration, due to the curvature and rotation of the earth, and the centripetal acceleration. The resultant of these accelerations produces a motion in the free air, unaffected by friction near the surface, which is parallel to the lines of equal barometric pressure (known as isobars). The velocity of the free air is known as the gradient velocity.

Under steady state conditions the gradient velocity can be determined directly if the latitude, the radius of curvature of the isobars, and the pressure gradient (or spacing of the isobars) are known (1).[2] For zones of cyclonic winds (associated with a low pressure system and with storms and high winds) the gradient velocity V_G is given by

$$V_G = r\,w\,\sin\lambda\left[\sqrt{\frac{\frac{dp}{dN}}{\rho\,r\,w^2\,\sin^2\lambda}+1}\;-\;1\right] \quad \ldots\ldots\ldots (1)$$

in which r is the radius of curvature of isobars, w denotes the rotational speed of the earth; λ is the latitude, dp/dN represents the pressure gradient, and ρ is the density of the air. Eq. 1 lends itself ideally to simple nomographic solution, as shown by W. J. Humphreys (1), and the gradient velocity may be estimated directly from isobar charts. Accurate estimates of gradient velocity, however, are difficult to obtain unless the grid of meteorological stations measuring surface pressures is close.

The velocity of the gradient wind is, however, attained only at heights around 1,000 ft to 2,000 ft above the ground. Closer to the ground, the wind is retarded by the frictional forces and obstructions at the surface and the virtual stresses produced by the vertical exchange of momentum by turbulence; its direction, then, is no longer parallel to the isobars. Turbulence also causes rapid fluctuations in the velocity of a wide range of frequencies and amplitudes. The velocity of the wind at lower levels, therefore, is usefully expressed in terms of its mean speed and the deviations from this velocity.

The time or distance interval over which the mean is averaged depends on the purpose for which the wind velocity is to be used.

Choice of a Suitable Averaging Interval.—In determining basic wind velocities for the design of structures certain fundamental considerations determine what averaging interval is most appropriate. These may be stated as follows:

1. The interval should coincide, as far as possible, with some natural periodicity of the wind.

---

2 Numerals in parentheses, thus (1), refer to corresponding items in the Bibliography.

2. The interval should be "long" compared to both (a) the natural frequency of the structure, and (b) the response time of the instrument; in this way there will be no dynamic interaction between the structure and fluctuations in the mean wind; measured wind velocities will be independent of the instruments response.

3. The interval should be short enough to record the "peaks" of severe storms.

4. The interval should correspond to a body of air of sufficient size to envelop completely a structure and its vortex regions.

The "mile of wind" or the "minute of wind" both represent suitable, if not optimum, intervals for measuring high-wind velocities for purposes of structural design. Both these intervals satisfy the foregoing conditions for reasons now discussed:

1. By means of auto-correlation coefficients, Durst (2) found that in storm winds a major group of eddies, thermal in origin, had a wavelength of about 4,000 ft to 6,000 ft, corresponding closely to the mile interval or the minute interval in winds of 60 mph.

2. a. The natural period of most structures is of the order of 0.1 sec to 3 sec (3), with that for the Empire State Building of 8.14 sec (4). With the damping present in most structures, fluctuations corresponding to one mile in extreme winds would have infinitesimal dynamic action.

b. R. H. Sherlock and M. B. Stout (5), referring to the response time of commercial anemometers, wrote in 1937, "that because of the inertia of moving parts of the instruments the records could only be accepted as accurate if they were averaged over 10 seconds or more." Thus, even at 150 mph, the mile of wind (or the minute of wind) satisfies the second requirement.

3. The mile of wind also represents a body of air far larger than most structures, so that static pressures at least equivalent to this average speed can be anticipated.

4. The mile of wind will be of sufficiently short duration to record the peak of a sudden severe local thunderstorm or squall.

These arguments, justifying the use of the extreme mile or minute of wind as basic design velocities, are endorsed further in that the mile of wind has been recommended for use in the United States (where records are available for many years) as the basis for design wind velocities and the minute of wind in the British Isles.[3]

Increase of Velocity with Height: Influence of Surface Roughness and Stability.—One of the most important factors to be considered is the increase of this mean wind velocity with height; a corollary to this is the retarding effect of the surface friction on the wind velocity nearer the surface.

---

[3] Since writing this, the existence of a gap in the energy spectrum of wind speed, centered at a frequency of about 1 cycle per hr, appears to have been established by Van der Hoven (Journal of Meteorology, Vol. 14, 1957, pp. 160-164). This, together with the results from a recent study at the University of Bristol, of over 100 spectra of strong winds now suggests that reliable predictions of the turbulence at higher frequencies (necessary in predicting maximum wind loads) can be made from the average wind speed taken over a longer period, such as one hour. In many countries climatological records of mean hourly wind velocities are more readily available. The discussion that follows applied equally to these mean hourly wind-speeds as well as to those averaged over a rather shorter period.

Various empirical, semi-empirical, and theoretical formulas have been derived to represent the variation of wind velocity with height. Three of the more familiar forms are the spiral, logarithmic, and exponential profiles. For structural purposes, the exponential or power law profile has been used most widely because of its simplicity. It can be stated as

$$V_z = k\, z^{1/\alpha} \quad \ldots\ldots\ldots\ldots\ldots\ldots \quad (2)$$

where V_z is the velocity at height z above ground, and k and α are constants.

By suitable choice of exponent, Eq. 2 can be made to correspond closely over a considerable range to the other forms of profile which are less empirical. The power law is applicable only in the layer extending from the ground up to the height at which the gradient velocity is first attained (usually in the range of 1,000 ft to 2,000 ft). Above this height, the wind velocity may be regarded as constant.

D. Brunt (6) has noted that "If the variation of wind with height be represented by a lower law z^p it is found that p is increased by an increase in either roughness or stability" (z being the height above ground). Here Brunt refers specifically to a range of heights above approximately 10 m (33 ft), the height being of interest to structural engineers.

An attempt is now made to evaluate these influences of stability and surface roughness on first, the rate of increase of mean velocity with height; and second, the magnitude of the mean surface velocity. Both of these values are of prime importance in estimating basic design wind velocities for structures.

Stability.—The stability of a storm is measured by the lapse rate or rate of temperature variation with height. In storm winds of long duration, in which turbulence causes thorough mixing, the lapse rate near the ground is invariably close to the adiabatic which corresponds to a state of natural stability (7,8). Rudolf Geiger (9) has stated that this condition is generally attained at velocities greater than 6 m per sec (13 mph). Observations of hurricanes Edna (1954) and Ione (1955) off the New England coast, reported by Edwin Kessler (10), apparently confirm the general assertion that the stability of mature and large-scale storms, whether of the tropical or extra-tropical variety, is close to being neutral.

Exceptions may be found, however, in severe local storms such as thunderstorms and frontal squalls (and perhaps in larger storms such as hurricanes in their early incipient stages, before full maturity is reached) which are notably unstable, where air near the ground is warmer than that aloft. As a consequence of this instability, extreme thermal interchange takes place between the air near the surface and the faster moving upper air which is unretarded by friction near the surface. Under circumstances of extreme instability, the value of the exponent $1/\alpha$ may attain the limiting value of zero, corresponding to zero increase in velocity with height. At Agra, Barkat Ali (11) measured an exponent of 0.02 (1/50) in very unstable conditions and O. G. Sutton (7) suggests a value of 1/100.

From these remarks the following general inferences may be drawn with regard to the effects of stability on the profile:

a. Severe local storms, such as thunderstorms or frontal squalls, are extremely unstable and so the increase of mean velocity with height is very small; the frictional characteristics of the ground surface may have almost negligible effects on the velocity profile.

b. Large-scale mature storms of either tropical or extra-tropical description exhibit nearly neutral stability with no marked tendency for violent thermal interchange; the dominating influence on the velocity profile in these storms is not the stability but the surface roughness.

Surface Roughness.—The important question now arises as to how great an effect surface roughness has on the wind velocity profile in large-scale mature storms which are probably the most important. In comparison with the vast amount written in engineering papers on this general subject, scant attention has been given to this particular question. It appears to be of paramount importance in the accurate evaluation of wind velocities.

It should first be emphasized that what is referred to by the term "surface roughness" is neither the shielding due to individual obstacles nor the orographic effects influencing the airflow in mountain regions, but the cumulative statistical drag effect of many obstructions on the wind. The surface roughness, therefore, is characterized by the density, size, and height of the buildings, trees, vegetation, rocks, etc., on the ground, around, and over which the wind must flow; it will be a minimum over the ocean and a maximum in a large city.

For years the measurement of wind-velocity profiles has been of interest in the fields of meteorology, aviation, agriculture, and wind power as well as in civil engineering. Information has now accumulated from which it is possible to evaluate the influence of the surface roughness on the wind velocity profile.

In Table 1, the exponents $1/\alpha$ corresponding to the accumulated experimental results of a number of observers are shown on a comparative basis and the corresponding power law profiles plotted in Fig. 1. The records from which these exponents and equivalent power-law curves are derived are given in the Appendix. Where the results were not explicitly stated as a power law, it was found that, in each case, a power law could be closely fitted to the records with only small deviations. It should be noted that the records refer specifically to mean velocity profiles prevailing above a height of 30 ft in strong winds, over flat ground surface at lapse rates which, if not explicitly stated, from the nature of the storms studied presumably could not have differed greatly from the adiabatic. The records, therefore, are homogeneous except that the nature of the ground roughness and the aggregate nature of obstructions vary widely, from the smooth surface of the sea to the rough obstructed surface of a large city.

The exponent of the power law increase is seen to vary between 1/10.5 and 1, depending only on the surface roughness characteristics. It is seen that Curves 1 to 9 have exponents lying between 1/10.5 and 1/5.9 and, in each case, the surrounding terrain was characteristically flat and open. The average for the observations taken on land lies close to 1/7 which is a familiar exponent found at the boundaries of pipes and wind tunnels in which mechanical turbulence predominates and the fluid is neutrally stable. The exponents of Curves 12 to 16 lie between 1/5 and 1/2.8 and average 1/3.5. For these curves the terrain corresponded to the rougher characteristics of treed and wooded farmland, towns, scrub trees, etc. Curves 17, 18 and 19 are derived from records obtained in large cities (Copenhagen, Paris and New York) which probably represent conditions of extreme surface roughness; the corresponding exponents are 1/2.1 and 1/1.6. For all the curves (except 10 and 11 which are probably not typical of level country) the value of the exponent is seen to increase in a

TABLE 1.—INFLUENCE OF SURFACE ROUGHNESS ON VALUES OF THE EXPONENT $1/\alpha$ IN THE POWER-LAW VARIATION OF MEAN WIND VELOCITY WITH HEIGHT UNDER CONDITIONS OF STRONG WIND OR ADIABATIC LAPSE RATE BETWEEN HEIGHTS OF 30 FT AND 1,000 FT

Curve No.	Source	Location	Upper Limit of Investigation, in feet	Description of Terrain in Site Locality	$\frac{1}{\alpha}$	Remarks
1	Goptarev	Caspian Sea (off Apsheron Penin.)	166	Coastal waters of inland sea	$\frac{1}{10.5}$	
2	Juul	Masnedsund, Denmark	182	Flat shore on "Ocean of Small Islands"	$\frac{1}{8.3}$	
3	Scrase	Salisbury Plain, England	43	Open grassland without hedgerows or trees	$\frac{1}{7.7}$	
4	Wing	Ballybunion, Ireland	492	Flat treeless grassland, Atlantic Ocean 1/2 mile distant	$\frac{1}{7.4}$	
5	Sherlock	Ann Arbor, Michigan, U.S.A.	250	Open slightly rolling farm land	$\frac{1}{7}$	
6	Taylor	Salisbury Plain, England	-	Open grassland without hedgerows or trees	$\frac{1}{7}$	
7a	Giblett	Cardington, Beds., England	150	Open level agricultural land with only isolated trees	$\frac{1}{7.8}$	
7b	Frost	Cardington, Beds., England	350	Same as above	$\frac{1}{5.9}$	
7c	Frost	Cardington, Beds., England	1,000	Same as above	$\frac{1}{6.7}$	
8	Deacon	Sale, Victoria, Australia	503	Gently rolling grazing land with few trees	$\frac{1}{6.25}$	
9	Heywood	Leafield, Oxfordshire, England	313	Open fields divided by low stone walls and hedges	$\frac{1}{5.9}$	
10	Kamei	Japan	-	Rough coast	$\frac{1}{5}$	Observations not necessarily typical of level country
11	Wax	Orkney Islands	118	Flat topped grass hill, 1/3 mile inland from high cliff overlooking the sea	$\frac{1}{4.6}$	
12	Huss and Portman	Akron, Ohio, U.S.A.	352	Gently rolling country with many bushes and small trees	$\frac{1}{4.55}$	
13	Franckenberger and Rudloff	Quickborn, Germany	230	Relatively level meadow land but with numerous hedges and trees around the small fields	$\frac{1}{4.35}$	
14a	Smith	Upton, Long Island, N.Y., U.S.A.	410	Level country uniformly covered with scrub oak and pine to a height of 30 ft	$\frac{1}{4}$	
14b	Panofsky	Upton, Long Island, N.Y., U.S.A.	410		$\frac{1}{3.85}$	Hurricanes Carol and Edna 1954: (fastest 1 min. mean speed)
14c	U.S. Weather Bureau	Upton, Long Island, N.Y., U.S.A.	410		$\frac{1}{3.3}$	
14d	U.S. Weather Bureau	Upton, Long Island, N.Y., U.S.A.	410		$\frac{1}{2.9}$	(fastest 6 min. mean speed)
15	Kamei	Japan	-	Three Japanese towns	$\frac{1}{3}$	
16	Dines	Farnborough, England	1,650	Wooded and treed farm land	$\frac{1}{2.8}$	
17	Jensen	Copenhagen, Denmark	242	Centre of a large city	$\frac{1}{2.3}$	
18	Taylor	Paris, (Eiffel Tower)	900	Centre of a large city	$\frac{1}{2}$	
19	Rathbun	New York (Empire State Building)	1,263	Centre of a large city	$\frac{1}{1.6}$	

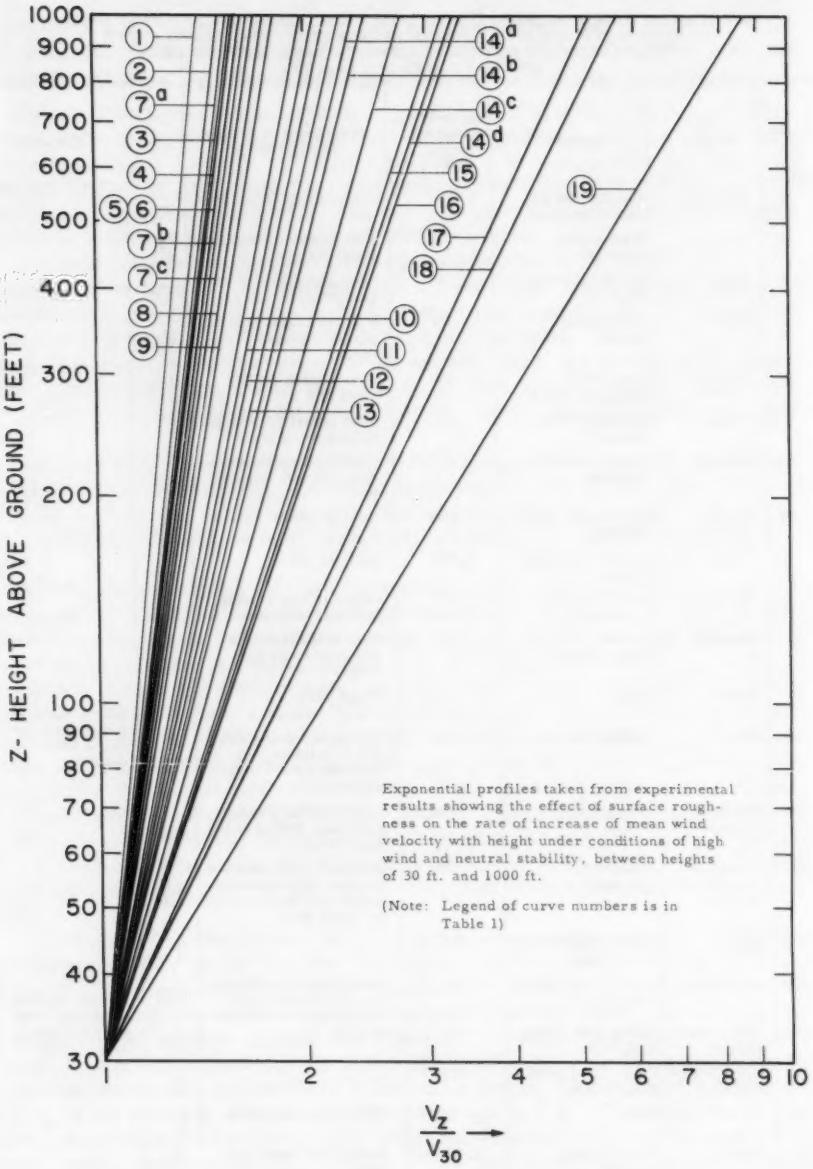

FIG. 1.—EFFECT OF SURFACE ROUGHNESS ON RATE OF INCREASE OF MEAN VELOCITY WITH HEIGHT

manner which is remarkably consistent with the increase in the roughness of the terrain and the number of obstructions.

Effect of Velocity.—It should be noted that velocity can be expected to have a slight secondary effect on the profile in that the value of the surface friction

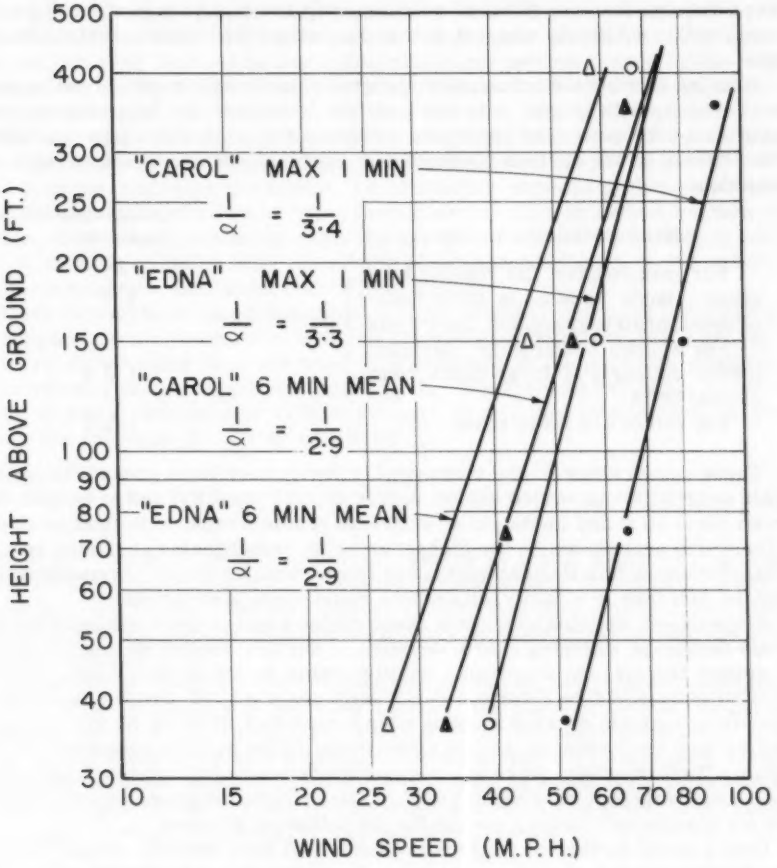

FIG. 2.—OBSERVATIONS OF HURRICANES "CAROL" AND "EDNA" (1954) AT BROOKHAVEN, LONG ISLAND. (TERRAIN: FLAT COUNTRY WITH SCRUB TREES)

increases slightly with wind velocity. As a result, the rate of increase of mean wind velocity with height increases slightly with velocity. This is familiar in wind-tunnel work.

Numerical evidence of the indirect influence of the velocity on the velocity-height relationship is furnished by G. F. Collins' investigations of nine storms (30), mainly at Brookhaven Laboratory, Long Island. He found (Fig. 2), by examining the 5-min mean velocities at different elevations up to 410 ft, that

the exponent of the power-law profile increased by approximately 0.02 for every 10-mph increase in surface wind velocity; at 50 mph the value being 0.27 (that is, 1/3.7) and the extrapolated value at 80 mph being 0.33 (1/3.0). These profiles, according to Collins, fitted the experimental records extremely well with the value of the standard deviation equalling 1.26 mph. These results, however, indicate that the effect of wind velocity (over the range of maxima encountered) is not nearly as great as that due to the differences in surface roughness.

Bearing in mind the influence of the wind velocity on the rate of increase of wind velocity with height, it is now possible to suggest the following approximate values for power law exponents corresponding to more or less qualitative descriptions of the surface roughness or aggregate nature of the surface obstructions:

Description of the Terrain	Power-Law Exponent
For open country, flat coastal belts, small islands situated in large bodies of water, prairie grassland, tundra, etc.	1/7
For wooded countryside, parkland, towns, outskirts of large cities rough coastal belts	1/3.5
For centers of large cities	1/2.5

These values refer to the mean wind velocity over level ground, to large-scale severe storms (which exhibit nearly neutral stability) and to heights between about 30 ft and the height at which the gradient velocity is first attained. If there are areas in which the highest probable velocities occur during severe local storms such as thunderstorms and frontal squalls (which seems improbable), no increase in velocity with height would seem appropriate.

Records.—If reliable long-term anemometer records were available for all areas exhibiting differing characteristics of surface roughness and incidence to severe storms, the discussion could perhaps be left at this point; a basic wind velocity could be determined for each geographical location based on a statistical analysis of wind records over a period of 40 yr or 50 yr, and then applied to a wind-velocity profile appropriate to the surface roughness of the vicinity. Unfortunately, there are serious obstacles to this approach (certainly, in a sparsely populated country such as Canada) since meteorological records are not always satisfactory enough for the following reasons:

Only a small number of stations in Canada will have records extending back a sufficient number of years. At some locations the anemometer will have been moved several times during the period of record, affecting the exposure and the homogeneity of the records. Severe storms may have blown the anemometer away or rendered it inoperative, thus losing crucial information. The anemometer may also give readings which are not representative of level country due to the siting of the anemometer on or near a building. Hugh L. Dryden and George C. Hill, for example, suggest that the well-exposed anemometer on top of the Empire State Building, situated more than 200 ft above the roof, reads 23% higher than the approaching flow, due to the presence of the building (31). If, at airports, anemometers were raised high enough to be free from the influence of the buildings they would present a hazard to aircraft. In winter, the period of worst storms, Dines anemometers sometimes clog with blow-

ing snow. Ice accretions sometimes form on cup anemometers. Anemometer readings taken in mountains, in valleys, and on coastal cliffs are subject to orographic effects sometimes resulting in noticeably higher velocities.

All of these considerations add emphasis to Sherlock's (32) recommendation, shared by many others, that design velocities should be based "on a statistical analysis of wind records over a period of 40 to 50 years." Also the results obtained from the records of one station should be related to those from other neighboring stations by a suitable statistical method. Only in this way can spurious and systematic errors arising in the records of an individual station be minimized.

The next step, therefore, is to explore a suitable method whereby the accumulated records of all meteorological wind records might be correlated. Since it is not desirable to restrict the admissible records to those obtained from anemometers situated in "open level country" (this, in certain regions of Canada, for example, would decimate the available records), it is first necessary to investigate more fully the effects of surface roughness on the velocities measured near the surface over level ground.

It has already been noted that there is some height at which the influence of the ground friction transmitted upwards through eddy viscosity, has a negligible effect on the velocity of the wind as it responds to the pressure gradient. If the velocity at this height is denoted by V_G (the gradient velocity), and the height at which this velocity is first attained by z_G, then by reference to the power-law increase of velocity with height

$$V_z = V_G \left(\frac{1}{z_G}\right)^{1/\alpha} z^{1/\alpha} \quad \ldots\ldots\ldots\ldots\ldots (3)$$

In order to determine the ratio of the velocity at height z above the ground to the gradient velocity, it is first necessary to determine values of z_G corresponding to the various surface roughness categories already discussed. An attempt is now made to do this on the basis of the pertinent experimental records that are available.

Examination of Sherlock's (16) investigations at Ann Arbor, Mich., indicates that for these conditions of flat open country, the value of z_G (the height at which the gradient velocity is first attained) is of the order of 900 ft. This value agrees reasonably well with that obtained by Taylor, at Salisbury Plain, (discussed by W. W. Pagon (17)) for similar terrain in which average values of z_G for strong winds were 1,250 ft in summer and 885 ft in winter. An approximate value of 900 ft, therefore, is chosen for the value of z_G in flat open country.

In large cities, Pagon (17), citing Taylor's studies at the Eiffel Tower in Paris, suggests a value of z_G for strong winds in a large city of 2,020 ft in summer and 1,420 ft in winter. An approximate average value of 1,700 ft is adopted for the present. The value of 1,300 ft is chosen for the intermediate conditions of rough wooded country. These values of z_G of 900 ft, 1,300 ft, and 1,700 ft (together with the appropriate exponents), corresponding to the three types of roughness conditions, give the three curves of Fig. 3.

It is not suggested at this stage that these curves are highly accurate. Indeed, the qualitative aspects of the problem do not permit great accuracy. It should be noted that in these curves the values of $1/\alpha$ are founded on a relatively greater amount of information than are the values of z_G; the errors involved in the latter, however, (which may differ by 200 ft) are of less consequence.

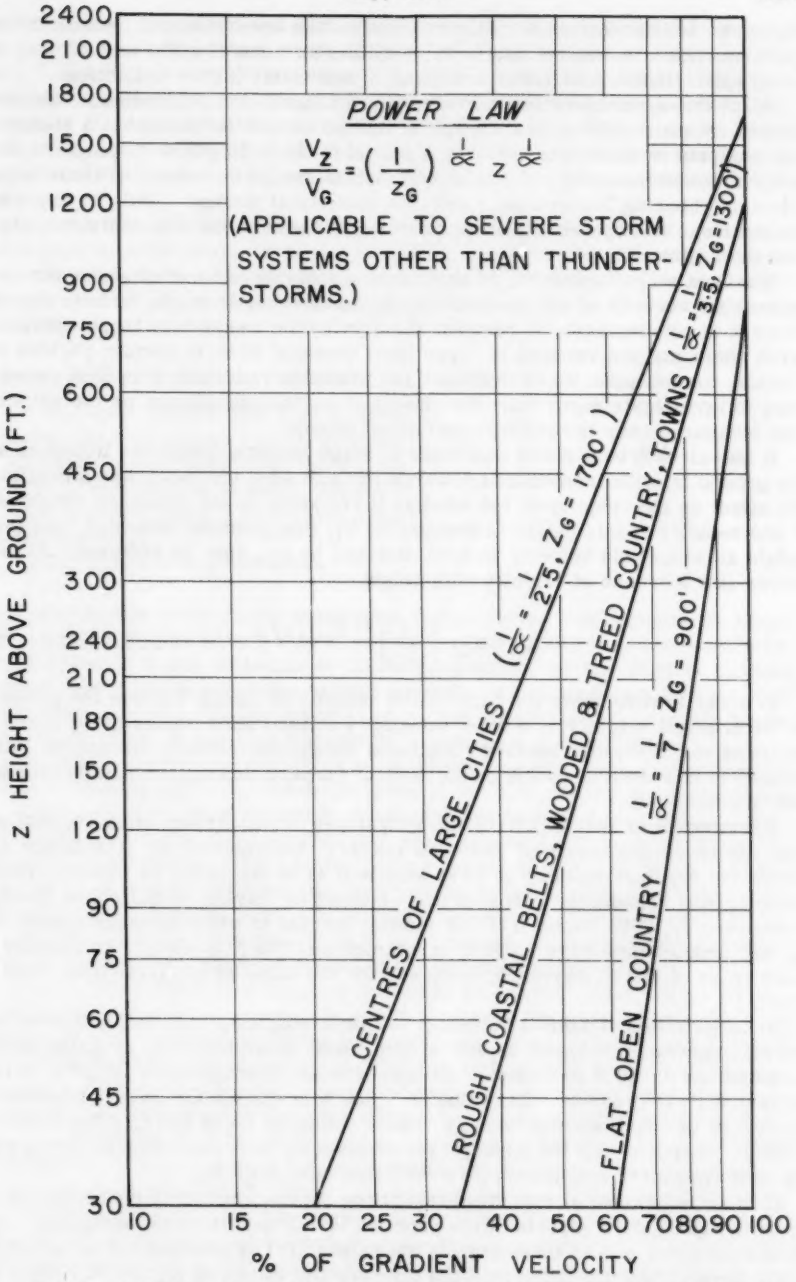

FIG. 3.—INCREASE OF VELOCITY WITH HEIGHT OVER LEVEL GROUND FOR THREE DIFFERENT TYPES OF SURFACE ROUGHNESS ACCORDING TO THE POWER LAW

Some confirmation of the rough accuracy of these curves is afforded by the comparison of the surface velocities over terrain of different surface roughnesses. In their study of the climate of Central Canada, W. G. Kendrew and D. Currie (33) observe that "the mean (annual wind speed in the prairies is between 12 and 16 mph. The speed is appreciably less in parklands with means of 9-12 mph and, again, less in forests 5-9 mph; the increased friction among the trees is the main cause." These reductions in wind velocity, compared to the archetypal flat open country of the prairies, are entirely compatible with those suggested by Fig. 3.

A comparison of mean wind speed in nine Canadian cities (34) and at airports on their outskirts indicates that the speed in the city is 65% of that near the outskirts (the value suggested by Fig. 3 is 59%). Elevation, shielding, and siting of the anemometers and periods of observation vary in every case, but the trend is obvious. A study of hurricane winds at Lake Okeechobee, Florida, by the U.S. Corps of Engineers (35), indicated that the wind off the land (everglades, covered with scrub cypress, etc.) averaged 60% of the wind over water when the latter was 50 mph, and 74% when the latter was 80 mph.

H. Ferrington (36), discussing the wind velocities found in Great Britain (in general terms, a terrain characterized by treed, rolling country and straggling urban areas), has made the following interesting note:

> "On one occasion when the whole of the British Isles was covered with parallel isobars running nearly west to east, all stations on the western side gave the wind as force 8 (42 mph) while those on the eastern side gave force 5 (21 mph) so that the velocity was reduced by one-half in consequence of the "friction" of the land. If the velocity at the exposed western stations be taken at two-thirds the velocity of the wind free from friction, we get the following interesting result which is probably correct enough for practical use; one-third of the velocity is lost by the sea friction on the western side, and one-third more by the land friction of the country between west and east."

In a series of measurements made at Valentia, N. Ireland, L. H. G. Dines (37) found that for this locality (flat open lowlands verging on the sea) the ratio of the surface wind to the gradient wind for 27 occasions on which the surface wind exceeded 15 m per sec, (34 mph) was 0.58. S. P. Wing (15) at a similar locality found an identical value for all directions taken together.

N. Carruthers (38), quoting an unpublished note by C. E. P. Brooks, gives the following values for the ratio of the wind velocity at 10 m (33 ft) above ground to the gradient wind W/G:

Exposure	W/G, in %
Open sea	60
Low islands	55
Windward coasts and neighboring lowland	50
Leeward coasts, neighboring lowland and sea	40
Open land, unsheltered	40
Sheltered land and townsites	30

All these values are again remarkably close to the values suggested by Fig. 3.

Design Velocities.—It is now possible to return to the problem of determining design velocities appropriate to different geographical regions. The prediction of probabilities and return periods of extreme wind velocities has been

suggested many times. In 1932, S. P. Wing (39) used the normal distribution curve to obtain the distribution curves for extreme wind velocities in several large American cities. More recently, Arne L. Johnson (40) has remarked that this type of distribution "gives a significant deviation from observed values." Since the date of Wing's correspondence, the extreme-value distribution (due largely to E. J. Gumbel (41)) has been developed. Johnson, who analyzed the anemometer records for both extreme indicated gusts and hourly mileages at thirteen stations in Sweden and six in the British Isles, states that "the results obtained do not contradict the assumption that the distribution of extreme values of type No. 1 is in close agreement with the distribution of the actual wind velocities," (p. 119 (40)). Arnold Court (42) analyzed the records of twenty five weather stations in the United States, having 37 yr of satisfactory records, according to the same theory and states "all of the wind data seems to follow the theory."

This distribution function takes the form (41)

$$\phi(x) = e^{-e^{-y}} \quad \ldots\ldots\ldots\ldots\ldots\ldots \quad (4)$$

The reduced variate

$$y = a(x - u) \quad \ldots\ldots\ldots\ldots\ldots\ldots \quad (5)$$

where a is the scale factor and u the mode of the extreme value data.

Suppose that all anemometer records are analyzed to obtain the parameters a and u (in terms of which the return period of extreme surface velocities can be completely determined according to the extreme value theory). Then, an estimate of the distribution of extreme gradient velocities at this location is given by the parameters $1/k$, a, and k_u where k is a "roughness coefficient" defined by

$$k = \left(\frac{z_G}{z_A}\right)^{1/\alpha} \quad \ldots\ldots\ldots\ldots\ldots\ldots \quad (6)$$

z_A being the height of the anemometer and z_G and $1/\alpha$ being given approximately by Fig. 3.

The object now is to try to correlate these estimates of the gradient velocities in order to reduce the systematic errors which may have occurred in the anemometer records, to improve the estimate of extreme-wind velocities occurring at stations with shorter periods of records, and to minimize the subjective elements involved in the determination of design-wind velocities.

Suppose that anemometer n situated at latitude ϕ_n and longitude λ_n possesses records extending back a period of N_n yr which, by extreme-value analysis, yields values for the scale factor and mode of a_n and u_n. Suppose that the best estimate of the "roughness factor" is k_n, then the corresponding values of scale factor and modal value referring to the gradient velocity at this point are $1/k_n$; $a_n = a'_n$ and $k_n u_n = u'_n$.

It is now assumed that these parameters follow some m^{th} degree contour surface (where m is less than the total number of records being analyzed) of the forms

$$a' = \sum_{j=0}^{m} \sum_{i=0}^{j} A_{ij} \lambda^i \phi^{j-i} \quad \ldots\ldots\ldots\ldots\ldots \quad (7)$$

and

$$u' = \sum_{j=0}^{m} \sum_{i=0}^{j} B_{ij} \lambda^i \phi^{j-i} \quad \ldots\ldots\ldots\ldots\ldots (8)$$

The values of the coefficients A_{ij} and B_{ij} are now obtained by fitting the observed values to these surfaces by the method of least squares. This problem is one well suited to electronic computation. In fitting the values, it would be appropriate to weight them first, by the factor $\sqrt{N_n}$ which puts more reliance on the records of longer period and, second, by a factor Q determined unavoidably, by a subjective evaluation of the quality of the records, with regard to the siting of the anemometer, the number of times it has been moved, and the possible amplification effects of mountains, valleys, etc. For example, a first-class weather station, where the anemometer is situated on level ground away from shielding and has not been moved, might be given a weighting of 9 or 10 (out of a possible 10), whereas an anemometer situated close to the roof of a building, in a shielded area or in a valley, might be weighted by a factor of only 1 or 2. The least-squares process minimizes the errors in a' and u' due to the many causes cited, on the assumption that the weighted errors are normally distributed.

This process leads directly to the contours of a' and u' for the territory considered. If it is now desired to erect a structure at a certain location to last a period of T yr (T >10) with a risk of q that the basic design wind velocity V will be exceeded within this time, the return period R of this wind velocity V is given by

$$R = \frac{-T}{\log_e (1 - q)} \approx \frac{T}{q} \quad \text{if q is small} \quad \ldots\ldots\ldots\ldots (9)$$

This represents a probability of 1/R. By extreme value theory, the value of the required gradient velocity

$$V_G = \frac{1}{a'} \left\{ - \log_e \left[- \log_e \left(1 - \frac{1}{R} \right) \right] \right\} + u' \quad \ldots\ldots\ldots (10)$$

where a' and u' are determined from the contours.

The values of the velocity nearer the surface corresponding to this gradient velocity are determined from Fig. 3 according to the appropriate roughness conditions.

If the structure is to be erected on a hill or in a valley, a suitable amplification factor should be used. Examples of these are given by Pagon (17) and P. C. Putnam (43). The only way to determine this will often be by actual observation of wind velocities at the site for a short period and then comparing their value with those at a nearby anemometer on level terrain.

In this way, it becomes possible to relate the "basic design wind velocity" for each structure to the roughness characteristics of the ground surrounding it, the anticipated span of the structures useful life, and the risks consequent on the design wind velocity being exceeded. Any system which does not take into account the wide variation in those factors which are to be encountered obviously does not permit either a full measure of safety or economy to be effected.

Extreme Wind Speeds Over the British Isles.—To study their practicality, the method and procedures described were applied to some extreme value data

obtained by H. C. Shellard (Table 3). Of the forty eight stations whose anemograph records have been analyzed by Shellard, only those described in "The Gazetteer of British Meteorological Stations," (H.M.S.O., London, 1931), are referred to here since the essential site descriptions of the other stations are not available in published form and, in any case, consist largely of those stations with only short periods of record.

Values of U and 1/a were calculated from Shellard's values for the 'once in ten years' and 'once in a hundred years' extreme wind speeds and these are

TABLE 2.—TYPES OF TERRAIN GROUPED ACCORDING TO THEIR AERODYNAMIC ROUGHNESS

Category	Description	$\frac{1}{\alpha}$	z_G
1	Very smooth surfaces: e.g. large expanses of open water; low unsheltered islands; tidal flats; low-lands verging on the sea	$\frac{1}{8.5}$	800
2	Level surfaces with only low, surface obstructions: e.g. prairie grassland; desert; arctic tundra	$\frac{1}{7.5}$	900
3	Level, or slightly rolling surfaces, with slightly larger surface obstructions: e.g. farmland with very scattered trees and buildings, without hedgerows or other barriers; wasteland with low brush or surface vegetation; moorland	$\frac{1}{6.5}$	1,000
4	Gently rolling, or level country with low obstructions and barriers: e.g. open fields with walls and hedges scattered trees and buildings	$\frac{1}{5.5}$	1,100
5	Rolling or level surface broken by more numerous obstructions of various sizes: e.g. farmland, with small fields and dense hedges or barriers; scattered windbreaks of trees, scattered two-story buildings	$\frac{1}{4.5}$	1,200
6	Rolling or level surface, uniformly covered with numerous large obstructions: e.g. forest, scrub trees, parkland	$\frac{1}{3.5}$	1,350
7	Very broken surface with large obstructions: e.g. towns; suburbs; outskirts of large cities; farmland with numerous woods and copses and large windbreaks of tall trees	$\frac{1}{3}$	1,500
8	Surface broken by extremely large obstructions: e.g. center of large city	$\frac{1}{2.5} - \frac{1}{1.5}$	1,800

recorded in Table 3. These values were also checked against Shellard's original computation sheets, with his kind permission.

The roughness category of each station was assessed by comparing the photographs and descriptions of the anemometer stations given in the "Gazetteer" (op. cit.) with the descriptions given in Table 2. (These roughness categories for each station are given in Table 3). Knowing the roughness category and the height of the anemometer (z_A) the roughness factor (k_A) was found from Fig. 4, and recorded in Table 3. The anemometer height given in Table 3

TABLE 3.—ANALYSIS OF EXTREME MEAN HOURLY WIND SPEEDS OVER THE BRITISH ISLES[a]

Stations[b]	Lat. °N	Long. ° ′	Category	z_A (ft)	k_A	$\frac{1}{a}$	U (mph)	Established gradient with $k_A \times \frac{1}{a}$	Established gradient with $k_A \times U$ (mph)	Q	N	Wt. $\propto Q\sqrt{N}$
Larwick	60 09	1 08W	2	39	1.65	5.30	56.4	8.75	93.1	7	24	3
Stornoway	58 11	6 21W	2	40	1.60	6.00	54.2	9.60	86.4	9	18	4
Tiree	56 32	6 55W	2	42	1.60	6.52	50.1	10.40	80.2	12	28	6
Aberdeen	57 10	2 06W	6	41	2.75	4.69	32.9	12.90	91.0	9	15	3
Eskdalemuir	55 19	3 12W	4	35	1.88	3.97	45.5	7.50	85.6	9	32	5
Aldergrove	54 39	6 13W	4	42	2.05	3.79	38.5	7.77	78.9	10	25	5
Pt. of Ayre	54 25	4 22W	1	40	1.50	5.21	47.7	7.82	71.6	11	19	5
Holyhead	53 19	4 37W	2	38	1.60	5.28	49.4	8.45	79.0	8	19	4
Southport	53 38	3 00W	2	33	1.65	5.02	48.3	8.28	79.7	12	42	8
Sealand	53 13	3 00W	4	42	1.80	4.41	40.8	7.94	73.4	10	19	4
Catterick	54 22	1 37W	4	33	1.90	6.80	35.4	12.92	67.3	10	10	3
Spurnhead	53 35	0 07E	1	34	1.55	3.58	48.5	5.24	75.2	13	29	7
Cranwell	53 02	0 30W	3	33	1.68	4.78	38.5	8.05	64.7	12	23	6
Birmingham	52 29	1 56W	7	118	2.40	4.06	34.2	9.75	82.0	10	31	6
Cardington	52 07	0 25W	3	135	1.40	6.06	42.9	8.48	60.1	12	23	6
Gorleston	52 35	1 43E	3	34	1.60	3.77	42.1	6.03	67.4	9	36	5
Felixstowe	51 37	1 20E	4	40	1.70	4.10	41.9	6.97	71.2	9	17	3
Shoeburyness	51 32	0 49E	4	89	1.57	4.49	44.9	7.05	70.5	10	29	5
Manston	51 21	1 21E	5	46	2.00	3.70	39.9	7.40	79.8	13	12	5
Kew Obs'vty	51 28	0 19W	8	75	2.75	2.42	29.7	6.65	81.7	7	24	3
Croydon	51 21	0 07W	7	105	2.15	4.26	37.4	9.16	80.5	9	23	4
Lympne	51 05	1 01E	4	48	1.75	3.72	42.7	6.51	74.7	10	27	5
Boscombe Down	51 10	1 45W	4	33	1.90	3.74	39.4	7.10	74.9	10	22	5
Calshot	50 49	1 18W	2	42	1.60	4.55	42.3	7.28	67.7	10	24	5
St. Ann's Hd.	51 41	5 11W	1	70	1.40	9.51	57.8	13.31	80.9	8	14	3
Scilly	49 56	6 18W	1	57	1.45	5.92	55.2	8.58	80.0	12	28	7
Lizard	49 57	5 12W	2	60	1.50	5.13	53.0	7.70	79.5	8	17	4
Pendennis	50 09	5 03W	3	42	1.65	4.30	58.2	7.10	96.0	7	20	3
Plymouth	50 22	4 08W	2	65	1.55	5.22	48.4	8.09	75.0	7	30	4

[a] Shellard, H. C., "Extreme Wind Speeds over Great Britain and Northern Ireland." Meteorological Magazine, vol. 87, Sept. 1958, pp. 257-265. [b] Stations are grouped according to general geographic locality.

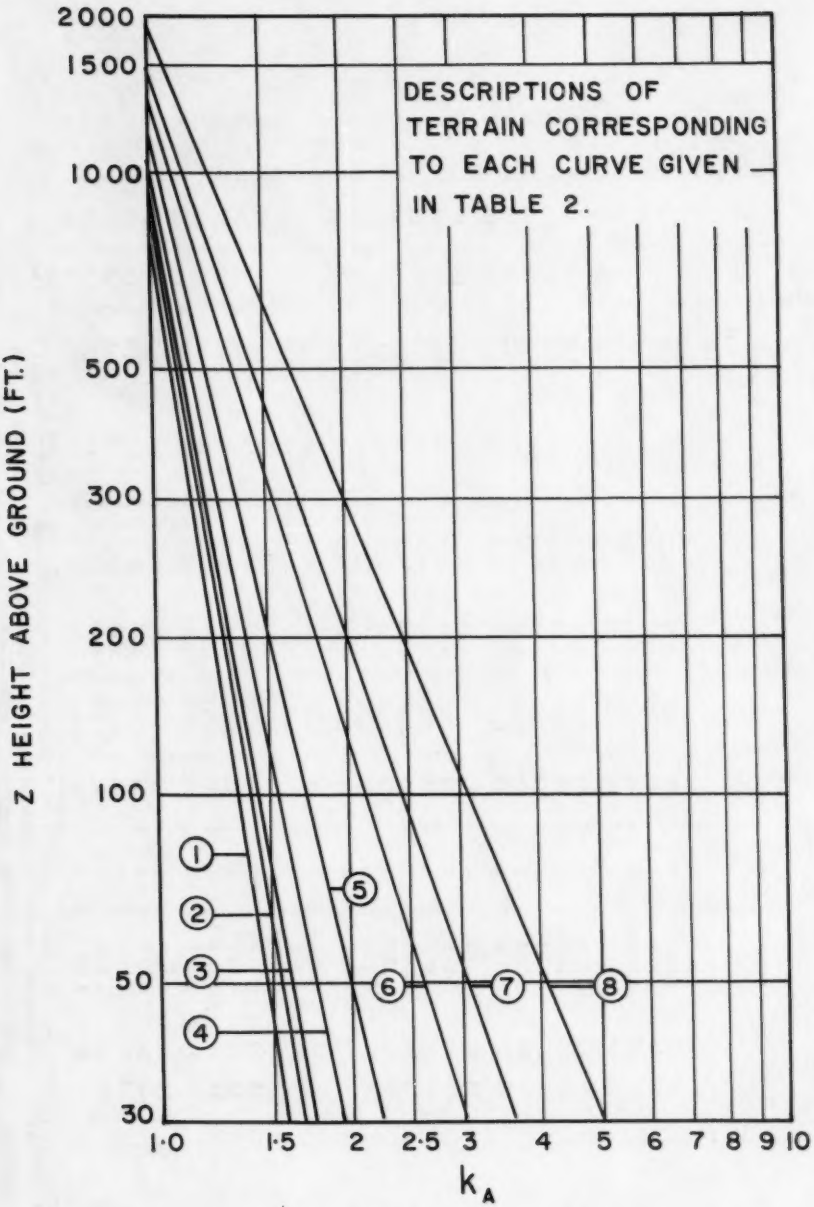

FIG. 4.—ROUGHNESS FACTORS (k_A) FOR DETERMINING THE RATIO OF GRADIENT TO SURFACE WIND SPEEDS OVER DIFFERENT TYPES OF TERRAIN

is either the so-called 'effective height' of the anemometer or the actual height given in the "Gazetteer;" in some cases, owing to poor exposure, neither height is entirely satisfactory.

From the same descriptions given in the Gazetteer, a Q-factor was determined for the anemometer site, based upon an assessment of the absence (or presence) of (a) possible orographic influences, (b) buildings and other local shielding and amplifying influences, and (c) the uniformity of the roughness for different wind fetches (particularly in a generally westerly direction, the direction of prevailing winds). Unfortunately, it was not possible to assess another important influence on the records, namely, the number of times the anometer had been moved during the period of record.

These values of Q (assessed out of a possible total of fifteen) were multiplied by the square root of the number of years of record ($\sqrt{N}$), and a 'weight' proportional to this product (in round numbers) is recorded in Table 3. On this basis, stations with higher weights were judged to be more reliable than those with relatively lower weights. It was found that estimates of U and 1/a deviating substantially from the average can always be associated with unsatisfactory anemometer exposures (such as cliff or hill-top sites), partially shielded sites, or stations with only short period records; consequently, weights are low. The large proportion of coastal and urban sites indicates that, in many cases, the exposure leaves much to be desired.

In order not to bias the results, assessments of the roughness category and Q-factor were made, as far as possible, without reference to the already determined values of 1/a and U. In a more detailed analysis, reference to mean annual wind speeds and direction rosettes would, perhaps, assist in assessing roughness categories and in revealing any anomalous directional properties of the surface winds.

The estimated values of 1/a and U for the gradient wind, obtained from the roughness factor and the surface values of these parameters are recorded in Table 3 and are summarized graphically in Fig. 5.

Also shown in Fig. 5 are contours of U and 1/a; these are drawn by eye and are based on the assumption that the average properties of the gradient wind field are not subject to wide variation over an area the size of the British Isles.

The map shown in Fig. 5 might form the basis for determining design wind velocities.

Illustrative Example.—If, for example, it is desired to erect a structure at some locality on the (U = 80 mph; 1/a = 8.0 mph) contour to have an anticipated lifetime T = 10 yr with a risk q = 10% that the design wind velocity is exceeded during this period, then the required return period for this design wind speed is $R = \frac{T}{q} = \frac{10}{0.1} = 100$ yr. The 'design gradient wind velocity' (V_G) is then given by

$$V_G = U + \frac{1}{a}\left\{ - \log_e \left[- \log_e \left(1 - \frac{1}{R} \right) \right] \right\} \quad \ldots\ldots\ldots (11)$$

$$= 80 + 8.0 \times 4.6$$
$$= 117 \text{ mph}$$

This, in fact, gives the extreme mean hourly velocity for the gradient wind. Recent unpublished information indicates that the mean minute wind velocity

LEGEND: 90:9·0 (6) LOCATION OF STATION SHOWN BY CIRCLE.
U : 1/σ WEIGHT UNITS – MILES PER HOUR.

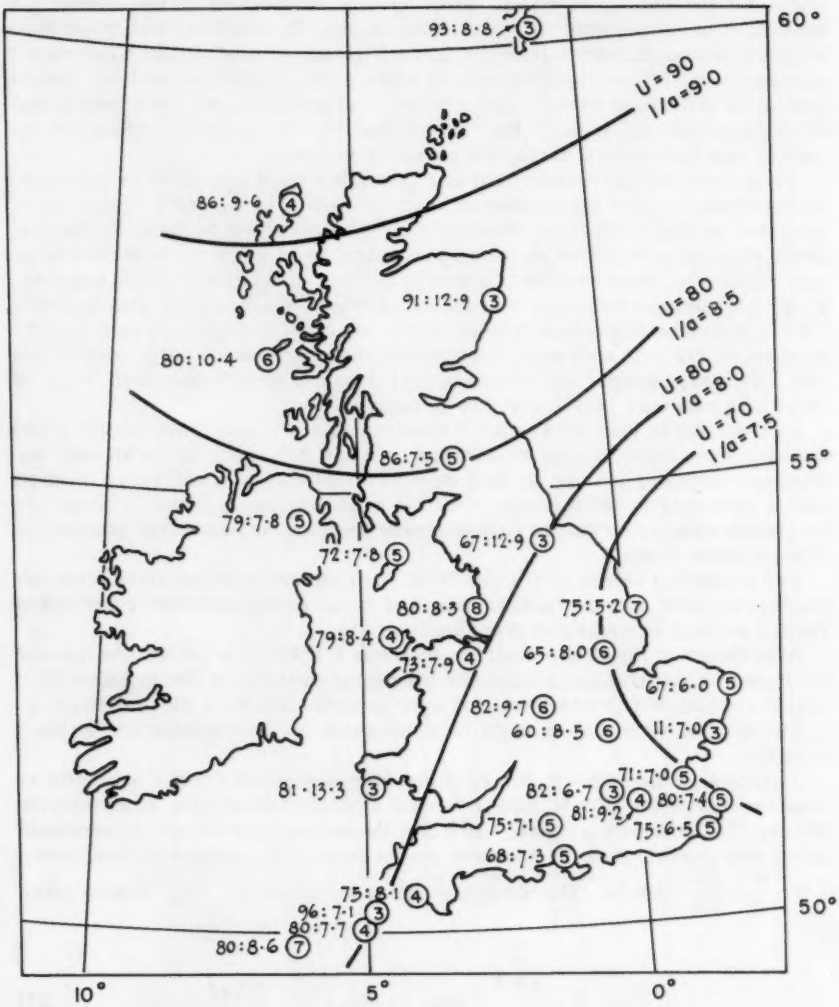

FIG. 5.—PARAMETERS OF EXTREME MEAN HOURLY GRADIENT WIND SPEED OVER THE BRITISH ISLES

(advocated in this report) is on the average 25% greater than this and so the extreme 'mean minute' speed is 117 x 1.25 = 146 mph.

If, now, the structure is to be erected in a town, for which (from Table 3) z_G is 1,500 ft and $1/\alpha = 1/3$, the design wind velocity at height z (ft) is given by

$$V_z = 146 \left[\frac{z}{1{,}500} \right]^{1/3} \quad \ldots\ldots\ldots\ldots \quad (12)$$

and V_{100} = 59 mph.

For open country without obstructions the expression would be

$$V_z = 146 \left(\frac{z}{900} \right)^{\frac{1}{7}} \quad \ldots\ldots\ldots\ldots \quad (13)$$

and V_{100} = 106 mph.

Finally, if the structure is to be erected in the center of a large city, the design wind velocity would be given by

$$V_z = 146 \left(\frac{z}{1{,}800} \right)^{1/2.5} \quad \ldots\ldots\ldots\ldots \quad (14)$$

and V_{100} = 46 mph.

The further difficult and largely unresolved problems of assessing the marked influence of the wind velocity profile on the pressure distribution, and of determining what dynamic amplification may arise due to the unsteady flow of gusts, lie outside the province of this paper which has attempted merely to discuss the derivation of a basic design mean velocity to which, it is felt, these other factors can then be related.

ACKNOWLEDGMENTS

The writer wishes to express his thanks to H. C. Shellard, Head of the Climatological Services Division of the Meteorological Office, London, England, for allowing the writer to examine his calculation sheets. The writer also expresses his appreciation to W. R. Schriever and D. W. Boyd of the Division of Building Research, National Research Council, Ottawa, Canada, for helpful criticism and assistance in the preparation of the paper.

This is a contribution from the Division of Building Research, National Research Council of Canada, and is published with the approval of the Director of the Division.

APPENDIX I.—BIBLIOGRAPHY

1. "Physics of the Air," by W. J. Humphreys, McGraw-Hill Book Co., Inc., New York, 3rd edition, 1940, pp. 129-136.
2. "Structure of Wind over Level Country," by M. A. Giblett, et al., Geophys. Mem. No. 54, Met. Office, London, 1932.
3. "Vibrations of Structures," by Franklin P. Ulrich and Dean S. Carder, Proceedings of Symposium on Earthquake and Blast, Los Angeles, Calif., June, 1952, p. 130.

4. "Wind Forces on a Tall Building," by J. Charles Rathbun, Transactions, ASCE, Vol. 105, 1940, pp. 1-41.

5. "Wind Structure in Winter Storms," by R. H. Sherlock and M. B. Stout, Journal of Aeronautical Sciences, Vol. 5, No. 2, December, 1937, pp. 53-61.

6. "Physical and Dynamical Meteorology," by D. Brunt, Cambridge Univ. Press, 2nd edition, 1952, p. 114.

7. "Atmospheric Turbulence," by O. G. Sutton, Methuen and Co., Ltd., 1949, p. 20.

8. "Relation of Gustiness to Other Meteorological Parameters," by I. I. Singer and M. E. Smith, Journal of Meteorology, Vol. 10, April, 1953, pp. 121-124.

9. "The Climate Near the Ground," by Rudolf Geiger, Harvard Univ. Press, 1950.

10. "Outer Precipitation Bands of Hurricane Edna and Ione," by Edwin Kessler, Bulletin of the Amer. Meteorological Soc., Vol. 38, No. 6, June, 1957, p. 335.

11. "Variation of Wind with Height," by Barkat Ali, Quarterly Journal, Royal Meteorological Soc., London, Vol. 58, 1932, pp. 285-288.

12. "Some Results of the Investigation of Gradients in the Vicinity of Oil-drilling Derricks," by N. P. Goptarev, Trudy Gosudarst venny. okeanografichesky institut, Moscow, Vypusk 36, 1957, p. 128.

13. "Measuring Wind Velocities at Varying Heights Above Ground," by J. Juul, Organization for European Economic Co-operation, Final Report of working group No. 2, "Wind Power," 1954.

14. "Some Characteristics of Eddy Motion in the Atmosphere," by F. J. Scrase, Geophys. Mem. No. 52, Met. Office, London, 1930.

15. "Wind Pressures and the Design of Radio and High Transmission Towers," by S. P. Wing, Electrician, Vol. 87, No. 2250, July 1, 1921, pp. 6-10.

16. "Variation of Wind Velocity and Gusts With Height," by R. H. Sherlock, Transactions, ASCE, Paper 2553, 1953.

17. "Wind Velocity in Relation to Height Above Ground," by W. W. Pagon, Engineering News-Record, Vol. 114, No. 21, May 23, 1935, pp. 742-51.

18. "The Velocity Profile in the Lowest 400 Ft," by R. Frost, Meteorological Magazine, Vol. 76, 1947, p. 14.

19. "Micrometeorology, A Study of Physical Processes in the Lowest Layers of the Earth's Atmosphere," by O. G. Sutton, McGraw-Hill Book Co., Inc., New York, 1953, p. 238.

20. "Gust Variation with Height up to 150 Metres," by E. L. Deacon, Quarterly Journal, Royal Meteorological Soc., Vol. 81, London, 1955, p. 562.

21. "Wind Structure Near the Ground and its Relation to Temperature Gradient," by G. S. P. Heywood, Quarterly Journal, Royal Meteorological Soc., Vol. 57, London, 1931, p. 433.

22. "Studies on Natural Wind Pressure on Buildings and Other Structures," by I. Kamei, Building Research Inst. of Japan, Vol. 1, No. 16, March, 1955.

23. "An Experimental Study of Wind Structure with Reference to the Design and Operation of Wind Driven Generators," by M. P. Wax, British Electrical and Allied Ind. Res. Assoc., Tech. Report C/T114, 1956.

24. Daniel Guggenheim Airship Inst. Report No. 156, by P. O. Huss and D. J. Portman, Akron Univ., Ohio, 1949.

25. "Wind messungen an den Quickborner Funkmasten 1947-8," by E. Franckenberger and W. Rudloff, Met. Amt. für N. W. Deutsch, Hamburg, 1949.

26. Discussion of R. H. Sherlock's "Variation of Wind Velocity and Gusts with Height," by I. I. Singer and M. E. Smith, Transactions, ASCE, Vol. 118, 1953, p. 493.

27. "Survey of Meteorological Factors Pertinent to Reduction of Loss of Life and Property in Hurricane Situations," by U. S. Weather Bur., Nat. Hurricane Research Proj., Washington, D. C., Report no. 5, March, 1957.

28. "Statistical Properties of the Vertical Flux and Kinetic Energy at 100 Metres," by H. A. Panofsky, Pennsylvania State College, Mineral Industries Exp. Station, Div. of Meteorology, Scientific Report No. 2, 1953. (AFCRC Contract No. AF 19(604) -166).

29. "4th Report on Wind Structure," by J. S. Dines, Aeronautical Research Council, Reports and Memoranda, Report 1912-1913, London, pp. 310-330.

30. "Determining Basic Wind Loads," by G. F. Collins, Proceedings, ASCE, Vol. 81, November, 1955.

31. "Wind Pressure on a Model of the Empire State Building," by Hugh L. Dryden and George C. Hill, Journal of Research of the Natl. Bur. of Standards, Vol. 10, 1933, pp. 493-523.

32. "The Nature of the Wind," by R. H. Sherlock, Proceedings, ASCE, Vol. 84, No. ST4, July, 1958.

33. "Climate of Central Canada," by W. G. Kendrew and D. Currie, Edmond Cloutier, Queen's Printer, Ottawa, 1955, p. 150.

34. "Climatic Summaries for Selected Meteorological Stations in Canada," by C. C. Boughner and M. K. Thomas, Vol. II, Dept. of Transport, Meteorological Division, Toronto, May, 1948, pp. 1-88.

35. "Characteristics of United States Hurricanes Pertinent to Levee Design for Lake Okeechobee, Fla.," by U. S. Weather Bur., Hydrometeorological Report, No. 32, 1954.

36. "Wind Loads on Buildings," by H. Ferrington, Structural Engineer, Vol. 21, No. 12, December, 1943, pp. 497-526; Vol. 22, No. 1, January, 1944, pp. 15-40.

37. "Comparison of Surface and Upper Winds at Valentia," by L. H. G. Dines, Professional Notes, Meteorological Office, Vol. 6, No. 83, London, 1938.

38. "Variations in Wind Velocity Near the Ground," by N. Carruthers, Quarterly Journal, Royal Meteorological Soc., Vol. 69, London, 1943, p. 291.

39. Discussion of "Wind Bracing in Steel Buildings," by S. P. Wing, Proceedings, ASCE, August, 1932, p. 1103.

40. "Strength Safety and Economical Dimensions of Structures," by Arne I. Johnson, Stockholm, Institutionem For Fyggnadsstatik Kunge Tekniska Hogskolan, No. 12, 1953.

41. "Statistical Theory of Extreme Values and Some Practical Applications," by E. J. Gumbel, Natl. Bur. of Standards, App. Maths. Series No. 33., Washington, D. C., 1954.

42. "Wind Extremes as a Design Factor," by Arnold Court, Journal of the Franklin Inst., Vol. 256, No. 1, July, 1953.

43. "Power From the Wind," by P. C. Putnam, Van Nostrand, 1948.

44. "The Model-Law for Phenomena in Natural Wind," by M. Jensen, Ingenioren, Internatl. Edition, Vol. 2, No. 4, Copenhagen, November, 1958, pp. 121-128.

APPENDIX II.—RECORDS OF WIND VELOCITY PROFILES

*1. GOPTAREV'S OBSERVATIONS

Location: Caspian Sea off Apsheron Peninsula
Terrain: Coastal waters of inland sea
Reference: 12

These observations taken at the site of offshore oil wells include many measurements of very strong winds. The average values for twenty seven occasions when the mean wind velocity (for 10 min) at 5.7 m (19 ft) above the sea exceeded 15 m per sec (approximately 34 mph) were as follows:

Height		Velocity	
meters	feet	m per sec	mph
5.7	19	16.80	37.8
15	50	19.30	43.3
27.3	91	20.07	45.2
50.6	168	20.57	46.5

2. JUUL'S OBSERVATIONS

Location: Masnedsund, Denmark
Terrain: Flat level coast of "ocean of small islands" (off sea wind)
Reference: 13

Height		Velocity	
meters	feet	m per sec	mph
5	16.5	14.2	32
15	49.5	16.5	37
35	115.5	17.2	39
55	182.0	18.8	42

* Numbers refer to those given in Fig. 1 and Table 1.

3. SCRASE'S OBSERVATIONS

Location: Salisbury Plain
Terrain: Open grass-covered plain
Reference: 14

Reported profile in adiabatic conditions given by power law with exponent of 0.13 (1/7.7). Wind measurements were made between heights of 3 m and 13 m (approximately 10 ft and 43 ft).

4. WING'S OBSERVATIONS

Location: Ballybunion, Ireland

Terrain: Low level plain. Atlantic Ocean $\frac{1}{2}$-mile beyond low level sand dunes.

Reference: 15

Height		Velocity	
meters	feet	m per sec	mph
4.5	15	10.7	24
92	300	14.3	32
149	492	15.6	35

(These records refer to curve '1' of Fig. 8 of Wing's paper "which is a curve which most of the high winds there very nearly approach," (p. 9, (15)).

5. SHERLOCK'S OBSERVATIONS

Location: Ann Arbor, Mich.
Terrain: Open farmland
Reference: 16

Fastest 1 min mean velocities

Height		Velocity	
meters	feet	m per sec	mph
15	50	19.9	44.5*
23	75	20.1	45 *
30	100	20.3	45.5*
38	125	21.0	47
46	150	21.2	47.5
53	175	21.7	48.5
61	200	21.7	48.5
76	250	24.1	54

6,18 TAYLOR'S OBSERVATIONS

These records were taken from Pagon's paper (17) in which Taylor's records are summarized in terms of the following Ekman spiral parameters.

---

* These values may be slightly higher than would otherwise be obtained because measurements were made near the brow of a slight rise.

	Cities	Open Country
θ	45°	20°
z_G (ft) summer	2020	1250
winter	1420	885

where θ = angle between directions of surface and gradient winds
z_G = height at which gradient velocity is first attained.

Taylor's experiments were conducted at Salisbury Plain and at the Eiffel Tower.

The Ekman spirals specified by the above parameters correspond closely with power laws with exponents of $\frac{1}{2}$ and 1/7 (for "cities" and "open country" respectively).

7a. GIBLETT'S OBSERVATIONS

Location: Cardington, England
Terrain: Large flat open airfield
Reference: 2

The ratio of wind velocities recorded by an anemometer at 150 ft to those at 50 ft under neutrally stable conditions and wind velocities in excess of 20 mph, was found to be 1.14 which corresponds to a power law increase with an exponent of 1/7.8.

N. B. Frost (18) has drawn attention to possible differences in exposure of the two anemometers used in this investigation which may account for the slight discrepancy between Giblett's results and Frost's.

7b, c. FROST'S OBSERVATIONS

Location: Cardington, England
Terrain: Flat open airfield

These were obtained from Sutton (19) (see also 18) who states:

"Layers 5 - 400 ft and 4 - 1,000 ft have been investigated by R. Frost using instruments suspended from a captive balloon over the airfield at Cardington, Southern England. His results indicate that in these layers the profile can be represented by power laws in all conditions of temperature gradient. From a further examination of extended profiles from 4 - 1,000 ft, Frost concludes that the value of $\frac{1}{\alpha}$ (the power law exponent) in conditions of adiabatic lapse rate is .149 (1/6.7) which is very close to the value 1/7 (.142) occurring in the generally accepted power-law profile for the turbulent boundary layer of a flat plate in a wind tunnel."

In the experiments between the heights 4 ft and 400 ft (18), the average wind velocities from fifty seven separate observations for which the lapse rate was approximately adiabatic were as follows:

Height		Velocity	
meters	feet	m per sec	mph
1	4	3.57	7.98
9	30	5.02	11.26
24	80	6.04	13.51
46	150	6.60	14.79
107	350	7.70	17.23

(Corresponding exponent = 0.17 = $\frac{1}{5.9}$)

8. DEACON'S OBSERVATIONS

Location: Sale, Victoria, Australia
Terrain: Gently rolling grazing land with very few trees
Reference: 20

Thirty-one successful observations were made of wind velocities greater than 20 mph at 40 ft and averaging 27.6 mph and the ratio of the velocities at different heights found to average at the following values:

Height		
meters	feet	$U_z/\overline{U}_{40}$
12	40	1
64	210	1.272
153	503	1.540

9. HEYWOOD'S OBSERVATIONS

Location: Leafield, Oxfordshire
Terrain: Open fields divided by low stone walls and hedges
Reference: 21 (and 20)

Deacon (20) states "In Heywood's Table 7 there are 38 observations with approximately adiabatic lapse rate and wind speed at 95 m (312 ft) greater than 8.5 m/sec (279 ft/sec) and these give a mean ratio $\overline{U}_{95}/\overline{U}_{12.7} = 1.40$."

10, 15. KAMEI'S OBSERVATIONS

These were obtained from the study of wind velocity profiles in three Japanese towns and, also, along the coast and represent summarized results (22). The power law exponents suggested by these studies were

1/3 in towns and
1/5 at the coast.

11. WAX'S OBSERVATIONS

Location: Costa Hill, Orkney Islands
Terrain: Rough coast, flat-topped hill, 1/3 mile inland from high cliff overlooking sea
Reference: 23

Height		Velocity	
meters	feet	m per sec	mph (100-sec mean)
17.7	58	19.5	43.7
26.8	88	20.9	46.8*
36.0	118	22.6	50.7

12. HUSS AND PORTMAN'S OBSERVATIONS

Location: Akron, Ohio, U. S. A.
Terrain: Gently rolling country with many bushes and small trees
Reference: 24 (and 20)

Deacon (20) states that "These authors evaluated $1/\alpha$ by least squares from 5 min mean velocities at 6 heights between 12 m and 107 m (39 ft and 350 ft). The 40 values for wind speeds greater than 9 m per sec (29.5 fps) at 50 m (164 ft) give a mean α = .219 with a standard deviation of the individual values of 0.042."

13. FRANCKENBERGER AND RUDLOFF'S OBSERVATIONS

Location: Quickborn (near Hamburg), Germany
Terrain: Level meadowland with numerous hedges and trees around the small fields
Reference: 25 (and 20)

Deacon (20) states that the mean of twenty one observations of mean wind speeds at 70 m (230 ft) greater than 15 m per sec (49.2 fps) gives the following

Height		
meters	feet	$\overline{U}_z/\overline{U}_{10}$
10	33	1
30	99	1.285
70	230	1.508

14a. SMITH'S OBSERVATIONS

Location: Brookhaven, Upton, Long Island, U. S. A.
Terrain: Level country uniformly covered with scrub oak and pine
Reference: 26

Reported average exponent for thirteen winter storms was 0.25.

14b. PANOFSKY'S OBSERVATIONS

Location: Brookhaven, Upton, Long Island, U. S. A.
Terrain: Level country uniformly covered with scrub oak and pine
Reference: 28 (and 20)

Deacon (20) gives the following velocity ratios for conditions of wind at 91 m (298 ft) greater than 9 m per sec (29.5 fps).

* Average of two simultaneous readings of 46.1 and 47.5 mph.

Height		
meters	feet	$\bar{U}_z/\bar{U}_{10m}$
11	36	1.02
45	147	1.47
91	298	1.81
125	410	1.91

14c, d. U. S. WEATHER BUREAU OBSERVATIONS

Location: Brookhaven, Upton, Long Island, U. S. A.
Terrain: Level country uniformly covered with scrub oak and pine
Reference: 27

Records taken during hurricanes Edna and Carol (1954) are shown in Fig. 2.

16. DINES' OBSERVATIONS

Location: Royal Aircraft Establishment, Farnborough, England
Terrain: Treed and wooded farmland and fields
Reference: 29

Height		Velocity*	
meters	feet	m per sec	mph
50	165	7.2	16.2
100	330	8.9	20.0
150	495	10.4	23.4
200	660	11.4	25.6
250	825	12.2	27.4
300	990	12.9	29.0
400	1320	14.5	32.6
500	1650	15.6	35.1

17. JENSEN'S OBSERVATIONS

Location: Copenhagen, Denmark
Terrain: Center of a large city
Reference: 44

In Jensen's Fig. 1, the following observations are recorded.

Height z		$\frac{\text{Velocity at height z m}}{\text{Velocity at 100 m}}$
meters	feet	
34	111	.68
50	164	.75
74	242	.91

* Measured by balloons and theodolites: average of 25 experiments in which velocities > 10 m per sec.

19. RATHBUN'S OBSERVATIONS

Location: Center of New York City
Terrain: Heavily built up city
Reference: 4

Velocities for the storm of March 22, 1936 (the most severe recorded) were as follows:

	Height		Velocity	
	meters	feet	m per sec	mph
N. Y. City Met. Obs.	18.9	62	12.5	28
U. S. Weather Bureau	138	454	25.9	58
Empire State Building	385	1263	40.2	90

Journal of the
STRUCTURAL DIVISION
Proceedings of the American Society of Civil Engineers

BAR-CHAIN METHOD FOR ANALYZING TRUSS DEFORMATION

By S. L. Lee,[1] M.ASCE and P.C. Patel[2]

SYNOPSIS

An attempt is made to extend the application of the bar-chain method in the analysis of statically determinate and indeterminate trusses. The relationships between the angles of inclination and the unit strains of the members to the actual rotations of the members, and the equivalent end rotations are established. The application of the method is illustrated by means of numerical examples.

INTRODUCTION

When a continuous frame is subjected to the action of applied loads or a change in temperature, its elastic line consists of smooth curves. In an articulated structure, however, the members in the deformed state remain straight and the elastic line is composed of a series of straight lines which change slope only at the joints. This series of straight lines may be likened to a bar chain from which the method gets its name.

The bar-chain method for analyzing truss deformation was first suggested by Mueller-Breslau.[3] The procedure for calculating the vertical component of the joint deflection in simple trusses was discussed in many textbooks on

Note.—Discussion open until October 1, 1960. To extend the closing date one month, a written request must be filed with the Executive Secretary, ASCE. This paper is part of the copyrighted Journal of the Structural Division, Proceedings of the American Society of Civil Engineers, Vol. 86, No. ST 5, May 1960.

[1] Assoc. Prof. of Civ. Engrg., Northwestern Univ., Evanston, Ill.

[2] Graduate Student, Civ. Engrg. Dept., Northwestern Univ., Evanston, Ill.

[3] "Die Neueren methoden der Festigkeitslehre und der Statik der Baukonstruktionen," by H. F. B. Mueller-Breslau, Baumgartner's Buchhandlung, Leipzig, 1904, p. 36.

theory of structures.[4-8] The determination of the horizontal as well as the vertical components of the joint deflections, the treatment of statically indeterminate trusses, and the construction of influence lines by this method will be discussed in the following.

The bar-chain method is analogous to the conjugate frame method[9] for analyzing the deformation of continuous frames; the conjugate frame method is an extension of the conjugate beam method[10,11] for calculating beam deflection. The deformation of a truss due to the changes in length of the members involves the distortion of the truss triangles, the rotation of the members, and the deflection of the joints. The joint deflection may be thought of as the combined consequence of the changes in the internal angles of the triangles and the rotation of the members. The effect of the latter may be conveniently represented by equivalent angular changes applied as elastic weights at the joints of a conjugate bar chain from which the deflection of a joint is determined simply by calculating the bending moment at this joint produced by the elastic weights.

The relationship between the different quantities will be derived in the following.

DISTORTION OF TRUSS TRIANGLES

Consider the internal angle α_n of triangle brs in the truss shown in Fig. 1. It can be shown[6] that the change in α_n may be expressed in terms of the unit strains of the members of the triangle in the form

$$\delta\ \alpha_n = \left(e_n - e'_n\right) \cot\ \alpha''_n + \left(e_n - e''_n\right) \cot\ \alpha'_n \quad \ldots\ldots\ldots (1)$$

in which α_n, α'_n, and α''_n are the internal angles and e_n, e'_n and e''_n are the unit strains of the members of the triangle (Fig. 1), positive if the member is in tension. The change in the internal angles at joint b, α_b, is given, therefore, by the expression

$$\delta\ \alpha_b = \sum_n \delta\ \alpha_n = \sum_n \left[\left(e_n - e'_n\right) \cot\ \alpha''_n + \left(e_n - e''_n\right) \cot\ \alpha'_n\right] \quad \ldots\ldots (2)$$

and the corresponding change in the external angle θ_b is

$$\delta\ \theta_b = \delta\left(2\pi - \alpha_b\right) = -\sum_n \left[\left(e_n - e'_n\right) \cot\ \alpha''_n + \left(e_n - e''_n\right) \cot\ \alpha'_n\right] \quad \ldots (3)$$

---

4 "The Theory and Practice of Modern Framed Structures," by J. B. Johnson, C. W. Bryan and F. E. Turneaure, Part II, Wiley, New York, 1929, p. 383.

5 "Elementary Structural Analysis," by J. B. Wilbur and C. H. Norris, McGraw-Hill Book Co., Inc., New York, 1948, p. 337.

6 "Structural Theory," by H. Sutherland and H. L. Bowman, 4th Edison, Wiley, New York, 1950, p. 202.

7 "Statically Indeterminate Structures," by C. K. Wang, McGraw-Hill Book Co., Inc., New York, 1953, p. 55.

8 "Indeterminate Structural Analysis," by J. S. Kinney, Addison-Wesley, Reading, Mass., 1957, p. 179.

9 "The Conjugate Frame Method and its Application in the Elastic and Plastic Theories of Structures," by S. L. Lee, J. Franklin Inst., Vol. 266, No. 3, September, 1958, p. 207.

10 "Beitrag Zur Theorie des Fachwerks," by H. F. B. Mueller-Breslau, Z. Architekt. u. Ing., Hannover, Vol. 31, 1885, p. 418.

11 "Deflection of Beams by the Conjugate Beam Method," by H. M. Westergard, J. Western Soc. Engrs., November, 1921.

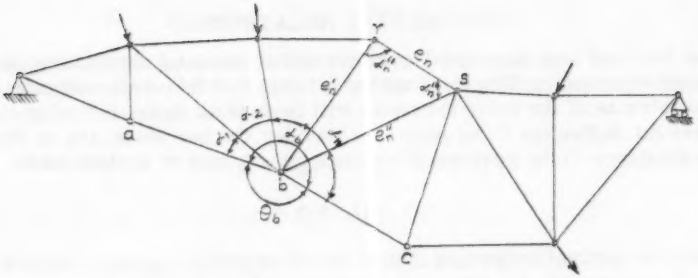

FIG. 1.—INTERNAL AND EXTERNAL ANGLES OF TRUSS TRIANGLES

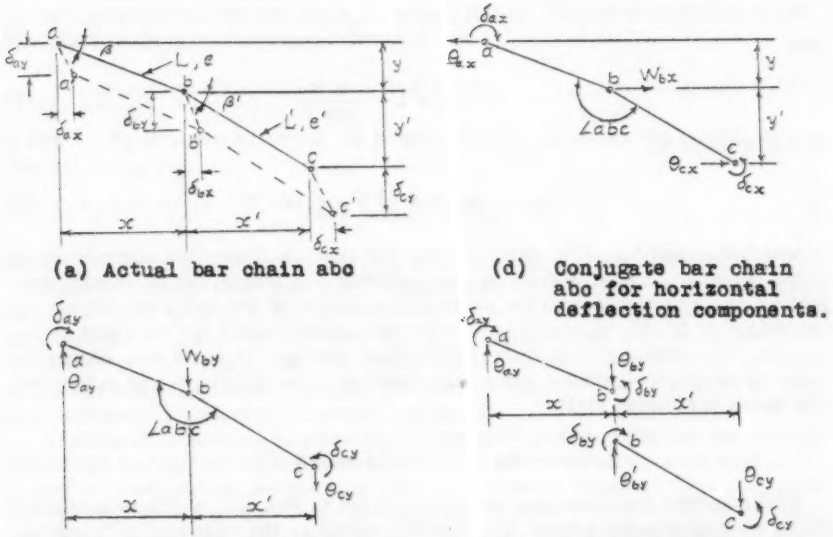
(a) Actual bar chain abc
(b) Conjugate bar chain abc for vertical deflection components.
(c) Conjugate bar chains ab and bc for vertical deflection components.
(d) Conjugate bar chain abc for horizontal deflection components.

FIG. 2.—ACTUAL AND CONJUGATE BAR CHAINS

The terms $\delta \alpha_b$ and $\delta \theta_b$ are positive if the angles are increasing in magnitude.

FUNDAMENTAL RELATIONSHIP

The vertical and horizontal components of the joint deflections are determined separately. The relationship between the deflection components and the unit strains of the truss members will be derived in the following.

Vertical Deflection Components.—Consider the bar chain abc in Fig. 2(a) which displaces to the position a'b'c' under the action of applied loads. Since

$$y = L \sin \beta \quad \ldots\ldots\ldots\ldots\ldots\ldots (4)$$

the relative vertical deflection of joint b with respect to joint a, due to the rotation of member ab, $\delta \beta$, and its deformation δL is given by

$$\delta_{by} - \delta_{ay} = \delta y = L \cos \beta \, (\delta \beta) + \sin \beta \, (\delta L) \quad \ldots\ldots\ldots (5)$$

Substituting

$$x = L \cos \beta \quad \ldots\ldots\ldots\ldots\ldots\ldots (6)$$

and

$$\delta L = e L = \frac{e x}{\cos \beta} \quad \ldots\ldots\ldots\ldots\ldots (7)$$

in Eq. 5 leads to

$$\delta_{by} - \delta_{ay} = x \, (\delta \beta + e \tan \beta) \quad \ldots\ldots\ldots\ldots (8)$$

in which δ_{ay} and δ_{by} are, respectively, the vertical deflection components of joints a and b; L, x, e, and β are, respectively, the length, the horizontal projection, the unit strain, and the angle of inclination of the left member ab. In the following, L', x', e', and β' are the corresponding items for the right member bc. The terms β and β' are considered positive if measured clockwise from the horizontal while e and e' are positive if the members are in tension. The same derivation yields

$$\delta_{cy} - \delta_{by} = x' \, (\delta \beta' + e' \tan \beta') \quad \ldots\ldots\ldots\ldots (9)$$

Next consider the conjugate bar chain shown in Fig. 2(b) which is subjected to the vertical elastic weight W_{by} and supported at the ends by the "shearing forces" θ_{ay} and θ_{cy} and the "bending moments" δ_{ay} and δ_{cy}. The relationship between the actual bar chain and the conjugate bar chain is similar to that which exists between an actual frame and the conjugate frames.[9] In the actual bar chain, δ_{ay} and δ_{cy} are considered positive if the joints move downward and clockwise end rotation are positive. In the conjugate bar chain, downward W_{by} is positive, δ_{ay} and δ_{cy} are positive if acting clockwise and counterclockwise, respectively, on the conjugate bar chain and θ_{ay} and θ_{cy} are positive, as shown in Fig. 2(b). Thus, the sign convention is the same as that used in beam analysis. It should be noted here that θ_{ay} and θ_{cy} are the equivalent rotations of members ab and bc at joints a and c, respectively. They represent the total effect of the rotations and the axial deformations of the members on the vertical deflections of joint b.

Equating the summation of the vertical forces to zero (Fig. 2(b)) yields

$$\theta_{ay} - \theta_{cy} - W_{by} = 0 \quad \ldots\ldots\ldots\ldots\ldots\ldots (10)$$

The conjugate bar chain, shown in Fig. 2(b), may be broken down into two separate free bodies, shown in Fig. 2(c). In the latter, equating the summations of moments about b to zero leads to

$$\delta_{by} - \delta_{ay} - \theta_{ay}\ x = 0 \quad \ldots\ldots\ldots\ldots\ldots\ldots (11)$$

and

$$\delta_{cy} - \delta_{by} - \theta_{cy}\ x' = 0 \quad \ldots\ldots\ldots\ldots\ldots\ldots (12)$$

Eliminating δ_{ay}, δ_{by}, δ_{cy}, θ_{ay} and θ_{cy} in Eq. 8 to Eq. 12 yields

$$W_{by} = \delta\beta - \delta\beta' + e \tan\beta - e' \tan\beta' \quad \ldots\ldots\ldots\ldots (13)$$

Since $\tan\beta = \tan\beta' = \infty$ when $\beta = \beta' = \pi/2$, vertical members must be excluded from a conjugate bar chain for the vertical deflection components. If angle abc measured below the bar chain, as shown in Fig. 2(b), is an external angle, which is true in this discussion, then

$$\delta\beta - \delta\beta' = \delta\theta_b \quad \ldots\ldots\ldots\ldots\ldots\ldots (14)$$

in which $\delta\theta_b$ is given by Eq. 3. If, however, angle abc, thus measured, is an internal angle, then

$$\delta\beta - \delta\beta' = \delta\alpha_b \quad \ldots\ldots\ldots\ldots\ldots\ldots (15)$$

in which $\delta\alpha_b$ is given by Eq. 2. This point will be further discussed later.

It has just been shown that if the elastic weight W_{by}, applied on the conjugate bar chain in Fig. 2 (b), is computed in terms of the unit strains of the members by means of Eq. 13 with the aid of either Eqs. 2 or 3, the vertical deflection components of the joints may readily be determined from the conjugate bar chain by simply applying the law of statics. The procedure is best demonstrated by means of numerical examples.

Horizontal Deflection Components.—The relationship between the elastic weight and the unit strains of the members for the calculation of the horizontal deflection components is readily derived in a similar manner. The conjugate bar chain is shown in Fig. 2(d). In this case, however, the elastic weight W_{bx} and the equivalent end rotations θ_{ax} and θ_{cx} are acting in the horizontal direction, positive as shown. In the actual bar chain, δ_{ax} and δ_{cx} are positive if the joints move to the right; their corresponding positive directions in the conjugate bar chain are as shown in Fig. 2(d). It can be shown that

$$W_{bx} = \delta\beta - \delta\beta' - e \cot\beta + e' \cot\beta' \quad \ldots\ldots\ldots\ldots (16)$$

The value of $\delta\beta - \delta\beta'$ is still governed by Eqs. 14 or 15. Since $\cot\beta = \cot\beta' = \infty$ when $\beta = \beta' = 0$, horizontal members must be excluded from a conjugate bar chain for the horizontal deflection components.

It will be shown later that, before proceeding to determine the horizontal deflection components, it is necessary to establish the relationship between θ_{ax} and θ_{ay} and/or between θ_{cx} and θ_{cy}.

Eliminating $\delta_{by} - \delta_{ay}$ in Eqs. 8 and 11 yields

$$\delta\beta = \theta_{ay} - e \tan \beta \quad \ldots\ldots\ldots\ldots\ldots\ldots (17)$$

Similarly, it can be shown that

$$\delta\beta = \theta_{ax} + e \cot \beta \quad \ldots\ldots\ldots\ldots\ldots\ldots (18)$$

Equating Eqs. 17 and 18 leads to

$$\theta_{ax} = \theta_{ay} - e (\tan \beta + \cot \beta) \quad \ldots\ldots\ldots\ldots\ldots\ldots (19)$$

In a similar manner, it can be shown that

$$\theta_{cx} = \theta_{cy} - e' (\tan \beta' + \cot \beta') \quad \ldots\ldots\ldots\ldots\ldots\ldots (20)$$

Sign Convention for Bar Chains.—The sign convention is summarized for convenient reference in the following.

In the actual bar chain, the vertical and horizontal components of joint deflection are positive if the joint moves downward and to the right, respectively; clockwise equivalent end rotations are positive.

In the conjugate bar chain for the vertical deflection components, positive elastic weights act downward; δ_{ay} is positive if acting clockwise on the bar at the left end and θ_{cy} is positive if acting counterclockwise on the bar at the right end; θ_{ay} is positive if acting upward and θ_{cy} is positive if acting downward.

In the conjugate bar chain for the horizontal deflection components, positive elastic weights act to the right; δ_{ax} and δ_{cx} are positive if acting clockwise and counterclockwise respectively on the ends of the conjugate bar chain; θ_{ax} is positive if acting to the left and θ_{cx} is positive if acting to the right.

Example 1.—Consider the truss[12] shown in Fig. 3(a), in which the numbers indicated on the members are the unit strains caused by the applied loads shown. As an illustration, take the bar chain $L_0U_1L_2U_3L_4$ shown in Figs. 3(b) and (c). The computation of the elastic weights for the vertical deflection components, W_y, and those for the horizontal deflection components, W_x, for joints U_1, L_2, and U_3 is shown in Table 1. Observe that $\delta\beta - \delta\beta'$, is equal to $\delta\alpha_n$ or $\delta\theta_b = -\delta\alpha_n$, depending on whether the angles marked in Fig. 3(b) are internal or external angles, respectively. The values of W_y and W_x are then indicated in Fig. 3(b) and (c), respectively.

In Fig. 3(b), equating the summation of moment about L_4 to zero yields

$$\theta_{L_0y} = 1.173 \times 10^{-3}$$

Setting the summation of forces equal to zero leads to

$$\theta_{L_4y} = -1.300 \times 10^{-3}$$

---

[12] "Statically Indeterminate Structures," by C. K. Wang, McGraw-Hill Book Co., Inc., New York, 1953, p. 55.

The vertical deflection components of joints U_1, L_2, and U_3 are then determined simply by calculating the moments about the respective joints. Thus,

$$\delta_{U_1y} = 1.173 \times 10^{-3} \times 15 \times 12 = 0.212 \text{ in.}$$

$$\delta_{L_2y} = \left[(1.173 \times 2) - 0.353\right] \times 10^{-3} \times 15 \times 12$$

$$= 0.360 \text{ in.}$$

and

$$\delta_{U_3y} = 1.300 \times 10^{-3} \times 15 \times 12 = 0.234 \text{ in.}$$

The positive signs indicate that the deflections are all downward.

Before proceeding to calculate the horizontal deflection components, observe that there are three unknowns in the conjugate bar chain shown in Fig. 3(c),

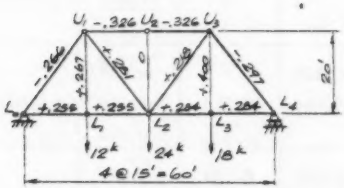

(a) Figures on members are unit strains, $\epsilon \times 10^3$

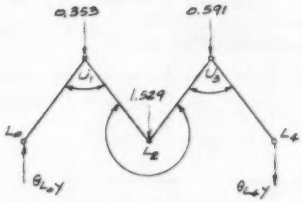

(b) Conjugate bar chain for vertical deflection components. All figures to be mutiplied by 10^{-3}

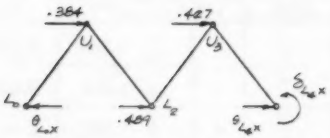

(c) Conjugate bar chain for horizontal deflection components. All figures to be multiplied by 10^{-3}.

FIG. 3.—EXAMPLE 1

namely θ_{L0x}, θ_{L4x}, and δ_{L4x}. Since only two conjugate frame equilibrium conditions are available, the third unknown θ_{L0x} is first determined from the value of θ_{L0y} just obtained by means of Eq. 19. Thus,

$$\theta_{L_0x} = [1.173 - (-0.266)(-1.333 - 0.750)] \times 10^{-3} = 0.620 \times 10^{-3}$$

Applying the conditions of static equilibrium yields

$$\theta_{L_4x} = -0.680 \times 10^{-3}$$

and

$$\delta_{L_4x} = 0.195 \text{ in.}$$

The latter can be determined irrespective of the values of θ_{L0x} and θ_{L4x}. The horizontal deflection of joints U_1, L_2, and U_3 are then found to be, respectively,

$$\delta_{U_1x} = 0.620 \times 10^{-3} \times 20 \times 12 = 0.149 \text{ in.}$$

$$\delta_{L_2x} = 0.384 \times 10^{-3} \times 20 \times 12 = 0.0927 \text{ in.}$$

$$\delta_{U_3x} = 0.1946 - \left(0.680 \times 10^{-3} \times 20 \times 12\right)$$
$$= 0.0314 \text{ in.}$$

The positive signs indicate that the deflections are to the right.

TABLE 1.—COMPUTATION OF ELASTIC WEIGHTS. (EXAMPLE 1)

Joint	Angle	$e_n - e'^{*}_n$	$\cot \alpha''_n$	$e_n - e''^{*}_n$	$\cot \alpha'_n$	$\delta\alpha_n^{*}$	$\delta\beta - \delta\beta'^{*}$
	$L_0U_1L_1$	-0.012	0	+0.521	0.750	0.391	
U_1	$L_1U_1L_2$	-0.026	0.750	-0.012	0	-0.020	+0.371
						+0.371	
	$U_1L_2U_2$	-0.607	0.750	-0.326	0	-0.455	
L_2	$U_2L_2U_3$	-0.326	0	-0.544	0.750	-0.408	+0.863
						-0.863	
	$L_2U_3L_3$	-0.116	0	+0.066	0.750	+0.050	
U_3	$L_3U_3L_4$	+0.581	0.750	-0.116	0	+0.436	+0.486
						+0.486	

Joint	e^{*}	e'^{*}	$\tan \beta$	$\tan \beta'$	$\cot \beta$	$\cot \beta'$	Wy^{*}	Wx^{*}
U_1	-0.266	0.281	$-\frac{4}{3}$	$+\frac{4}{3}$	$-\frac{3}{4}$	$+\frac{3}{4}$	0.353	0.384
L_2	+0.281	0.218	$+\frac{4}{3}$	$-\frac{4}{3}$	$+\frac{3}{4}$	$-\frac{3}{4}$	1.529	0.489
U_3	+0.218	-0.297	$-\frac{4}{3}$	$+\frac{4}{3}$	$-\frac{3}{4}$	$+\frac{3}{4}$	0.591	0.427

* All figures to be multiplied by 10^{-3}

The vertical deflection component of joint U_2 is equal to that of L_2, since the strain in member U_2L_2 is zero. The horizontal deflection component of member U_1U_2. Thus,

$$\delta_{U_2x} = 0.1488 + \left[(-0.326) \times 15 \times 12 \times 10^{-3}\right]$$
$$= 0.0901 \text{ in.}$$

The deflection components of L_1 and L_2 can be determined in similar manner by taking the bar chain $L_0L_1L_2L_3$ and L_4.

Example 2.—As a second illustration, consider the truss[13] shown in Fig. 4 (a), in which the unit strains are indicated on the respective members. The vertical deflection component of joint b is first determined by means of the

13 "Elementary Structural Analysis," by J. B. Wilbur and C. H. Norris, McGraw-Hill Book Co., Inc., New York, 1948, p. 337.

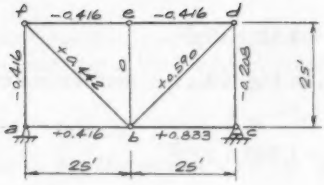

(a) Figures are unit strains multiplied by 10^3.

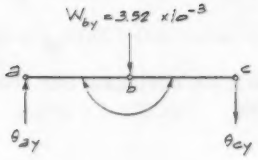

(b) Conjugate bar chain abc for vertical deflection components.

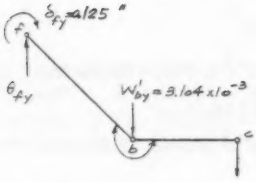

(c) Conjugate bar chain fbc for vertical deflection components.

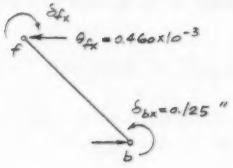

(d) Conjugate bar fd for horizontal deflection components.

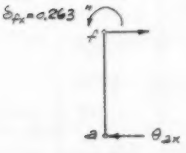

(e) Conjugate bar af for horizontal deflection components.

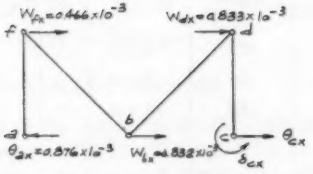

(f) Conjugate bar chain for horizontal deflection components.

FIG. 4.—EXAMPLE 2

conjugate bar chain abc, shown in Fig. 4(b), in which the elastic weight, W_{by}, is computed in Table 2. It should be noted that since angle abc indicated in Fig. 4(b) is an external angle, $\delta\beta - \delta\beta' = -\Sigma\,\delta\alpha_n$ given by Eq. 14. Since $\beta = \beta' = 0$, in this case, Eq. 13 gives

$$W_{by} = \delta\beta - \delta\beta' = 3.52 \times 10^{-3}$$

Considering the conjugate bar chain shown in Fig. 4(b), the equilibrium conditions yields

$$\theta_{ay} = -\theta_{cy} = 1.760 \times 10^{-3}$$

and taking moment about b leads to

$$\delta_{by} = 1.760 \times 10^{-3} \times 300 = 0.528 \text{ in.}$$

The vertical deflection components at f, e, and d can be readily calculated from those of a, b, and c, respectively.
Thus,

$$\delta_{fy} = 0 + (0.416 \times 10^{-3} \times 300) = 0.125 \text{ in.}$$

and

$$\delta_{ey} = 0.528 + 0 = 0.528 \text{ in.}$$

$$\delta_{dy} = 0 + (0.208 \times 10^{-3} \times 300) = 0.624 \text{ in.}$$

In order to determine the horizontal components of the joint deflections by means of the conjugate bar chain shown in Fig. 4(f), θ_{ax} must first be calculated.

TABLE 2.—COMPUTATION OF ELASTIC WEIGHT W_{by} (EXAMPLE 2).

Joint	Angle	$e_n - e'_n$ *	$\cot\alpha''_n$	$e_n - e''_n$ *	$\cot\alpha'_n$	$\delta\alpha_n$ *	$\delta\beta - \delta\beta'$
	abf	-0.832	0	-0.858	1	-0.858	
	fde	-0.858	1	-0.416	0	-0.858	
b	ebd	-0.416	0	-1.006	1	-1.006	+3.520
	dbc	-0.798	1	-1.041	0	-0.798	
						-3.520	

*All Figures to be multiplied by 10-3

Considering the conjugate bar chain fbc shown in Fig. 4(c), the elastic weight W'_{by} may be computed from the values of the angle changes given in the Table 2 by Eq. 13. Thus,

$$W'_{by} = [(0.858 + 1.006 + 0.798) + (0.442)\,(1) - (0.833)\,(0)] \times 10^{-3} = 3.104 \times 10^{-3}$$

The value of δ_{fy} was determined previously and equating the summation of moments about c yields

$$\theta_{fy} = 1.344 \times 10^{-3}$$

Consider next the conjugate bar fb shown in Fig. 2(d). The value of δ_{bx} is readily found from the strain of member ab to be

$$\delta_{bx} = 0.416 \times 10^{-3} \times 300 = 0.125 \text{ in.}$$

and that of θ_{fx} is calculated by Eq. 19 to be

$$\theta_{fx} = [1.344 - (0.442)(1 + 1)] \times 10^{-3}$$
$$= 0.460 \times 10^{-3}$$

Setting the summation of moment about b equal to zero yields

$$\delta_{fx} = 0.263 \text{ in.}$$

Moving to conjugate bar af, shown in Fig. 4(e), with the value of δ_{fx} known, θ_{ax} is readily determined to be 0.876×10^{-3}.

Returning to Fig. 4(f), with θ_{ax} known, the horizontal deflection components are easily found by summing up moments at the respective joints, to be

$$\delta_{fx} = 0.263 \text{ in.}$$
$$\delta_{bx} = 0.125 \text{ in.}$$

and

$$\delta_{dx} = 0.014 \text{ in.}$$
$$\delta_{cx} = 0.390 \text{ in.}$$

The value of δ_{ex} is computed from that of δ_{fx} and found to be 0.138 in.

The computation of the elastic weights W_{fx}, W_{bx}, and W_{dx} by Eq. 16 is omitted, since the procedure has been demonstrated in Example 1.

STATICALLY INDETERMINATE TRUSSES

The application of the bar chain method to the analysis of statically indeterminate trusses will be demonstrated by means of the two examples which follow.

Example 3.—To determine the redundant reaction H acting on the truss loaded, as shown in Fig. 5(a), consider first the conjugate bar chain shown in Fig. 5(b). It can be shown, in the manner previously demonstrated, that the elastic weights are

$$W_{ay} = (0.3996\ P - 1.3858\ H)\ K \quad \ldots\ldots\ldots\ldots \quad (21a)$$
$$W_{ey} = (3.4677\ P - 0.4619\ H)\ K \quad \ldots\ldots\ldots\ldots \quad (21b)$$

and

$$W_{by} = (0.5335\ P - 1.8477\ H)\ K \quad \ldots\ldots\ldots\ldots \quad (21c)$$
$$W_{fy} = (0.5335\ P - 4.1573\ H)\ K \quad \ldots\ldots\ldots\ldots \quad (21d)$$

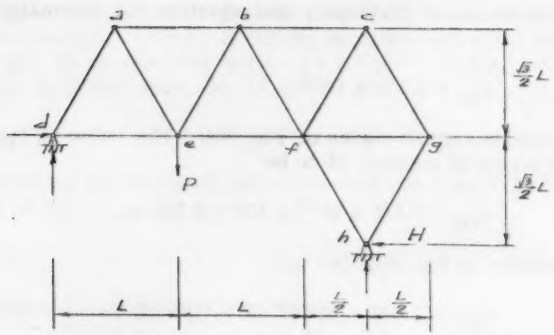

(a) Two-hinge truss. Cross-sectional areas of all members are equal to A.

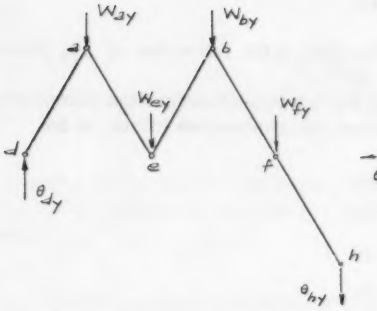

(b) Conjugate bar chain daebfh for vertical deflection components.

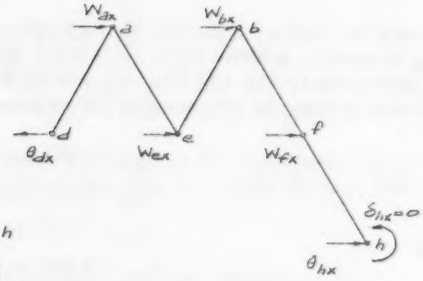

(c) Conjugate bar chain daebfh for horizontal deflection components.

FIG. 5.—EXAMPLE 3

in which K = 1/E A. The equilibrium conditions yield

$$\theta_{dy} = (2.7200\ P - 2.9563\ H)\ K \quad \ldots\ldots\ldots\ldots\ (22a)$$

and

$$\theta_{hy} = (-2.2140\ P + 4.8964\ H)\ K \quad \ldots\ldots\ldots\ldots\ (22b)$$

Consider next the conjugate bar chain shown in Fig. 5(c). The value of θ_{hx} can be determined from that of θ_{hy} just determined by Eq. 20 and is found to be

$$\theta_{hx} = (-1.6805\ P + 7.6678\ H)\ K \quad \ldots\ldots\ldots\ldots\ (23)$$

Since no deflection can take place at joint h, $\delta_{hx} = 0$, and equating the summation of moments about d to zero leads to

$$H = 0.2398\ P \quad \ldots\ldots\ldots\ldots\ (24)$$

which is the required solution.

Example 4.—To illustrate the construction of influence line by the bar chain method,[14] the influence line for the redundent horizontal reaction H on the truss shown in Fig. 5(a) will be discussed, assuming that defg is the loaded chord. Only vertical load will be considered; horizontal load can be treated in a similar manner.

By Mueller-Breslau principle, the ordinates of the influence line for H are given by

$$H_n = \delta_{ny}/\delta_{hx} \quad \ldots\ldots\ldots\ldots\ldots\ldots\ldots\ldots\ldots\ldots (25)$$

in which δ_{ny} denotes the vertical deflection component of the loaded joint due to any value of H applied on the truss, with the hinge support at joint h replaced by a horizontal roller support; and δ_{hx} is the corresponding horizontal deflection component of joint h.

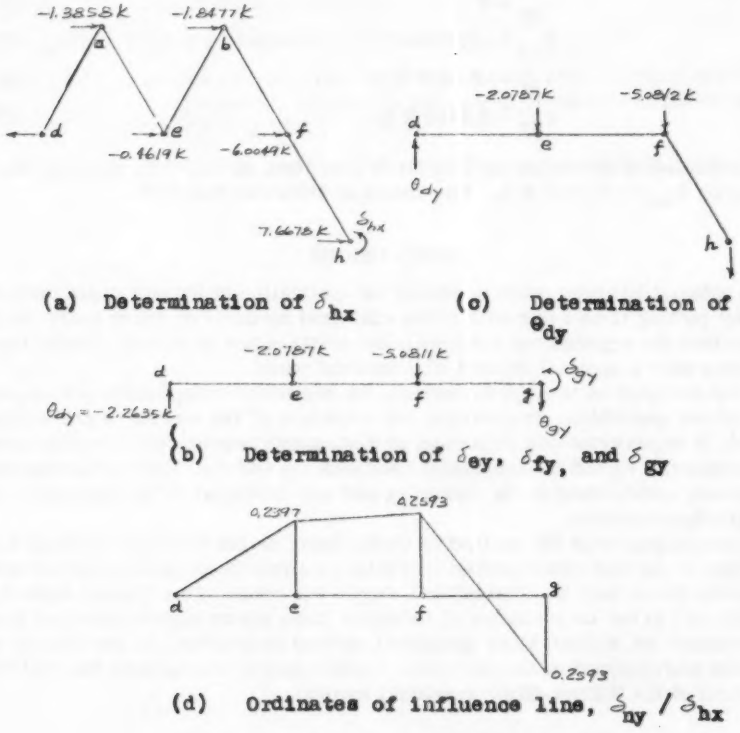

FIG. 6.—EXAMPLE 4, INFLUENCE LINE FOR H.

Consider first the conjugate frame daebfh for horizontal deflection components shown in Fig. 6(a). Due to H = 1, the values of the elastic weight, and the reaction indicated in the figure are obtained from Fig. 5(c), with P set equal

14 "Analysis of Statically Indeterminate Trussed Structures by Successive Approximations," by O. T. Voodhigula, Proceedings, ASCE, Vol. 67, 1941, p. 3.

to zero. The horizontal deflection component of joint h is, then, obtained by summing the moments about h and found to be

$$\delta_{hx} = -9.4407\ K\ L \quad \ldots\ldots\ldots\ldots\ldots\ldots\ldots\ldots (26)$$

To determine δ_{ny}, it is evident that the conjugate bar chain, shown in Fig. 6(b), which is the loaded chord, should be used. The elastic weights for joints e and f, due to H = 1 indicated in the figure, are computed in the usual way. Before proceeding to calculate δ_{ny}, it is necessary first to determine one of the three end reactions, say θ_{dy}, by means of another bar chain, say the one shown in Fig. 6(c). Thus, equating the summation of moments about h (Fig. 6(c)) to zero yields $\theta_{dy} = -2.2635\ K$. Transferring this value to Fig. 6(b), the values of δ_{ny} can now be calculated by summing the moments about joints d, e, f, and g, respectively. Thus,

$$\delta_{dy} = 0 \quad \ldots\ldots\ldots\ldots\ldots\ldots\ldots\ldots (27a)$$

$$\delta_{ey} = -2.2634\ K\ L \quad \ldots\ldots\ldots\ldots\ldots\ldots (27b)$$

and

$$\delta_{fy} = -2.4480\ K\ L \quad \ldots\ldots\ldots\ldots\ldots\ldots (27c)$$

$$\delta_{gy} = 2.4480\ K\ L \quad \ldots\ldots\ldots\ldots\ldots\ldots (27d)$$

The ordinates of the influence line for H are, then, obtained by dividing these values by $\delta_{hx} = -9.4407\ K\ L$. The result is shown in Fig. 6(d).

CONCLUSIONS

An attempt has been made to extend the application of the bar-chain method, thereby putting it on a par with other classical methods of truss analysis. It is seen that the expressions involved in the solution are relatively simple, thus, requiring only a nominal amount of numerical work.

In the analysis of truss deformation, the deflection components are usually the desired quantities. In contrast, the rotations of the members are seldom needed. It is nevertheless important to distinguish between the actual rotation of a member, $\delta\ \beta_1$ and its equivalent rotations, θ_x and θ_y. Their relationships are clearly established in the foregoing and are essential in the application of the bar-chain method.

In comparison with the method of Castigliano, or the unit-load method, one advantage of the bar-chain method lies in the fact that the deflection components of several joints may be obtained in a single bar chain. This feature makes it a useful tool in the construction of influence lines where higher accuracy than that obtained by Williot-Mohr graphical method is desired. In the manner of approach and application, the bar-chain method may be considered the analytic equivalent of the Williot-Mohr graphical method.

NOTATION

a, b, c = subscripts denoting joints of the truss;

e, e' = unit strains in members to the left and the right of a joint, respectively;

e_n, e'_n, e''_n = unit strains in members of a triangle (Fig. 1);

L, L' = lengths of members to the left and the right of a joint, respectively;

L_n, L'_n, L''_n = lengths of members of a triangle (Fig. 1);

L_0, L_1, L_2 = joints along lower chord of a truss;

U_0, U_1, U_2 = joints along upper chord of a truss;

W_{bx}, W_{by} = elastic weights on conjugate bar chains for horizontal and vertical deflection components, defined by Eqs. 16 and 13, respectively;

x, x' = horizontal projections of members to the left and the right of a joint, respectively;

y, y' = vertical projection of members to the left and the right of a joint, respectively;

α_b = internal angle (Fig. 1);

α_n, α'_n, α''_n = internal angles of a triangle (Fig.1);

β, β' = angles of inclination of members to the left and right of a joint, respectively, positive if measured clockwise from the horizontal (Fig. 2a);

δ_{ax}, δ_{ay} = horizontal and vertical deflection components of joint a, respectively; and

θ_b = external angle (Fig. 1).

Journal of the
STRUCTURAL DIVISION
Proceedings of the American Society of Civil Engineers

INFLUENCE OF PARTIAL BASE FIXITY ON FRAME STABILITY

By Theodore V. Galambos,[1] A. M. ASCE

SYNOPSIS

The buckling strength of a pinned-base rigid frame is considerably lower than that of an identical fixed-base frame. In current design practice in the United States, however, pinned column bases are specified for most structures because the construction of suitable foundations for fixed bases usually increases the over-all cost. It is shown that the rotational restraint offered by commonly used "pinned" column bases is sufficient to increase the buckling strength of these frames to almost that of identical fixed-base rigid frames.

INTRODUCTION

The buckling load of a pinned-base rigid frame is considerably below that of an identical fixed-base frame. This may be shown by any one of the many "exact" and approximate methods which are available for determining the buck-

Note.—Discussion open until October 1, 1960. To extend the closing date one month, a written request must be filed with the Executive Secretary, ASCE. This paper is part of the copyrighted Journal of the Structural Division, Proceedings of the American Society of Civil Engineers, Vol. 86, No. ST 5, May, 1960.

[1] Research Asst. Prof., Fritz Engrg. Lab., Lehigh Univ., Bethlehem, Pa.

ling strength of rigid frames. Many of these methods are available elsewhere.[2,3,4,5,6]

The single-story, single-bay rectangular rigid frame will be examined as an illustration. For simplicity it will be assumed that the axial force acting on each column is equal and that the frame is symmetric. The two frames which will be compared are shown in Figs. 1(a) and (b). Fig. 1(a) shows the pinned-base frame and Fig. 1(b) shows the fixed-base frame.

The frame shown in Figs. 1(a) and (b) may buckle in one of two modes:

1. It may fail by a sidesway buckling mode.
2. It may fail in a symmetric mode if sidesway is prevented at the top of the columns.

Of these two, the sidesway type buckling is the more critical. Therefore this mode of buckling will be considered here. The solid lines in Figs. 1(a) and (b) represent the stable, undeflected shape of the frame. The dashed lines show the unstable, sideswayed frame.

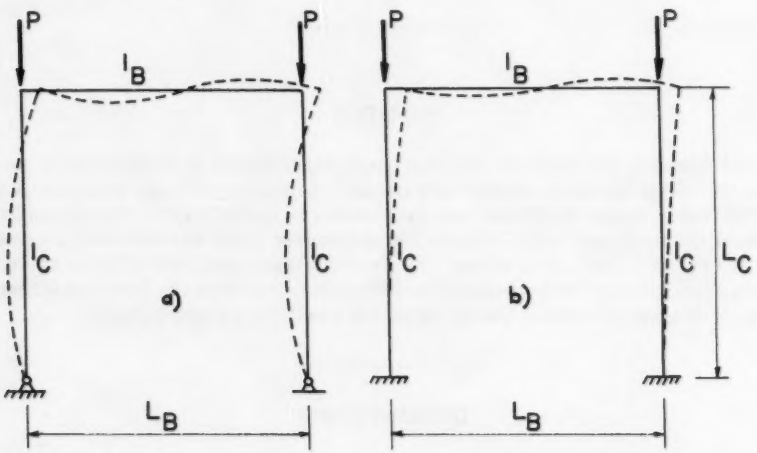

FIG. 1.—DEFLECTION CONFIGURATION OF PINNED BASE AND FIXED BASE RIGID FRAMES.

2 "Buckling Strength of Metal Structures," by F. Bleich, McGraw-Hill Book Co., New York, 1952, Chapters VI and VII.

3 "Theory of Elastic Stability," by S. Timoshenko, McGraw-Hill Book Co., New York, 1936, Chapter II.

4 "Rational Simplifications for the Buckling Length of Columns," by T. C. Kavanagh, Column Research Council, Proceedings of the Seventh Tech. Session, May, 1958.

5 "Guide to Design Criteria for Metal Compression Members," Column Research Council (to be published.)

6 "Din 4114 Knickung, Kippung, Beulung," "German Buckling Specification," English translation by T. V. Galambos and J. Jones, Column Research Council, June, 1957.

The problem of the pinned-base, single-story, single-bay rigid frame has been solved[7] as has the corresponding fixed-base frame.[8] The critical buckling load of either frame is

$$P_{cr} = \frac{\pi^2 E_t I_C}{(k L_C)^2} \quad \ldots\ldots\ldots\ldots\ldots\ldots \quad (1)$$

in which P_{cr} is the load causing frame buckling, E_t denotes the tangent modulus, I_C is the moment of inertia of the columns in the plane of bending, L_C represents the length of the columns, and k is a coefficient indicating the "effective" length of the column.

The critical buckling condition of the pinned-base frame is expressed by the following buckling equation:

$$\frac{\cot \phi}{\phi} - \frac{\gamma}{6} = 0 \quad \ldots\ldots\ldots\ldots\ldots\ldots \quad (2)$$

The corresponding equation for the fixed-base frame is

$$\phi \sin \phi \cos \phi \left[\frac{\cot \phi}{\phi} - \frac{\gamma}{6} \right] = 1 \quad \ldots\ldots\ldots\ldots \quad (3)$$

In Eqs. 2 and 3, γ is a non-dimensional ratio defined as

$$\gamma = \frac{I_C L_B \tau}{I_B L_C} \quad \ldots\ldots\ldots\ldots\ldots\ldots \quad (4)$$

in which I_B is the moment of inertia of the beam in the plane of bending, L_B denotes the length of the beam, and τ is the ratio of tangent modulus to modulus of elasticity, E_t/E. The term ϕ in Eqs. 2 and 3 is equal to

$$\phi = L_C \sqrt{\frac{P_{cr}}{E_t I_C}} \quad \ldots\ldots\ldots\ldots\ldots\ldots \quad (5)$$

The relationship between the coefficients k in Eq. 1 and ϕ in Eqs. 2 and 3 is established as follows: From Eq. 5,

$$P_{cr} = \frac{\phi^2 E_t I_C}{L_C^2} \quad \ldots\ldots\ldots\ldots\ldots\ldots \quad (6)$$

If this value of P_{cr} is equated to P_{cr} of Eq. 1, the relationship between k and ϕ is

$$k = \frac{\pi}{\phi} \quad \ldots\ldots\ldots\ldots\ldots\ldots \quad (7)$$

The curves relating the effective length factor k and the non-dimensional ratio γ, as computed by Eqs. 2 and 3, are given in Fig. 2 for the two column-base conditions. The coefficient k varies from k = 1.0 at $\gamma = 0$ to k = 2.0 at $\gamma = \infty$ for the fixed-base frame. The corresponding variation of k for the pinned-base frame is from k = 2.0 to $k = \infty$. It must be noted that k enters into the denominator of Eq. 1 as a squared term, and thus the reduction in strength due to a pinned-column base is quite considerable according to this theory. Taking for example the case where $\gamma = 1.0$, k = 1.16 for the fixed-base frame and k = 2.33 for the pinned-end condition. Substitution of these values of k into

[7] "Buckling Strength of Metal Structures," by F. Bleich, McGraw-Hill Book Co., New York, 1952, Section 73.

[8] Ibid., Section 74.

Eq. 1 shows that the fixed-base frame may carry 4.07 times as much load as the pinned-base frame. As γ increases, the difference tends to become larger. At $\gamma = 5.0$ the ratio of the two buckling strengths is 5.07.

STATEMENT OF THE PROBLEM

The foregoing discussion shows that by fixing the column bases, the buckling strength of a rigid frame can be increased by a factor of 4 or even 5. In European practice, use is made of this fact by usually specifying fixed-base structures, sometimes at no small expense to the builder. In American practice, on the other hand, the assumption of a pinned-base structure is the general rule.

It is, however, impossible to attain either a fully pinned end or a fully fixed-end condition in construction. The column bases are in a stage intermediate between the two extremes. The actual restraint depends on the details used in the construction of the bases.

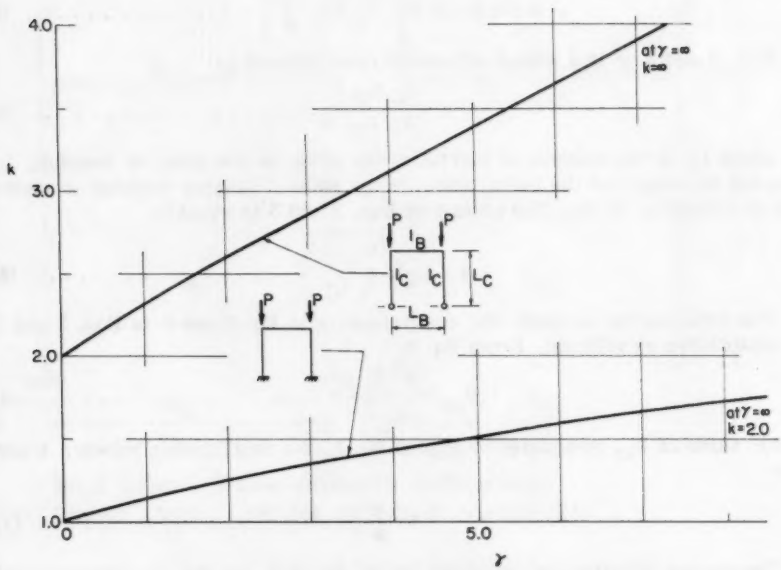

FIG. 2.—EFFECTIVE LENGTH FOR PINNED BASE AND FIXED BASE RIGID FRAMES.

The purpose of this paper is to investigate the extent of the influence of partial end restraint on the buckling strength of rigid frames. The relationships between base restraint and frame stability will be established to find out how the critical load varies as the restraint changes from full fixity to a fully pinned-end condition. The problem will be solved for two frames by the slope-deflection method described by F. Bleich.[9] These frames are:

1. Single-story, single-bay rigid frame.
2. Two-story, single-bay rigid frame.

[9] Ibid., Section 60.

Base restraint is simulated in the following analysis by inserting a restraining beam between the two column bases as shown in Fig. 3(a). This beam restrains the column ends in the same way as would be done by an actual base consisting of base plates, anchor bolts, the footing and the soil. Base restraints could also be represented by a set of springs which deform in proportion to the end rotation as shown in Fig. 3(b); $M = \beta\theta$, where M is the end moment, θ is the rotation, and β is the spring constant. In the subsequent derivations the frame in Fig. 3(a) will be analyzed; the approach for the system of springs (Fig. 3(b)) would be similar.

METHOD OF SOLUTION

Bleich has given[9] the moments at the ends of a member AB (Fig. 4) by the following equations:

$$M_A = \frac{E_t I}{L}\left[C\,\theta_A + S\,\theta_B - \rho\,(C + S)\right] \quad \ldots\ldots\ldots (8a)$$

and

$$M_B = \frac{E_t I}{L}\left[S\,\theta_A + C\,\theta_B - \rho\,(C + S)\right] \quad \ldots\ldots\ldots (8b)$$

in which θ_A and θ_B are end rotations of member AB, and ρ is the rotation of member AB with respect to the unloaded position. It is assumed here that the member has a uniform stiffness along its whole length. The coefficients C and S are defined as

$$C = \frac{c}{c^2 - s^2} \quad \ldots\ldots\ldots\ldots\ldots\ldots (9a)$$

and

$$S = \frac{s}{c^2 - s^2} \quad \ldots\ldots\ldots\ldots\ldots\ldots (9b)$$

in which

$$c = \frac{1}{\phi^2}(1 - \phi \cot \phi) \quad \ldots\ldots\ldots\ldots\ldots (10a)$$

and

$$s = \frac{1}{\phi^2}\left(\frac{1}{\sin \phi} - 1\right) \quad \ldots\ldots\ldots\ldots\ldots (10b)$$

Values of C and S corresponding to practical variations of ϕ are listed in Table 1. Table 1 also shows various other coefficients which will be defined later.

The sign convention of Eq. 8 is the following: Joint rotations θ and bar rotations ρ are positive when the rotation takes place in a clockwise sense. For example, all joint and bar rotations of the frame in Fig. 3(a) are clockwise and therefore positive.

A critical buckling equation is obtained by writing an expression for the moment at the ends of each member, using Eq. 8. Equilibrium is maintained at each joint by setting the sum of the moments at the joint equal to zero. Additional necessary equations are obtained from statical conditions. For the frame of Fig. 3(a) for example, an additional equation is obtained by summing

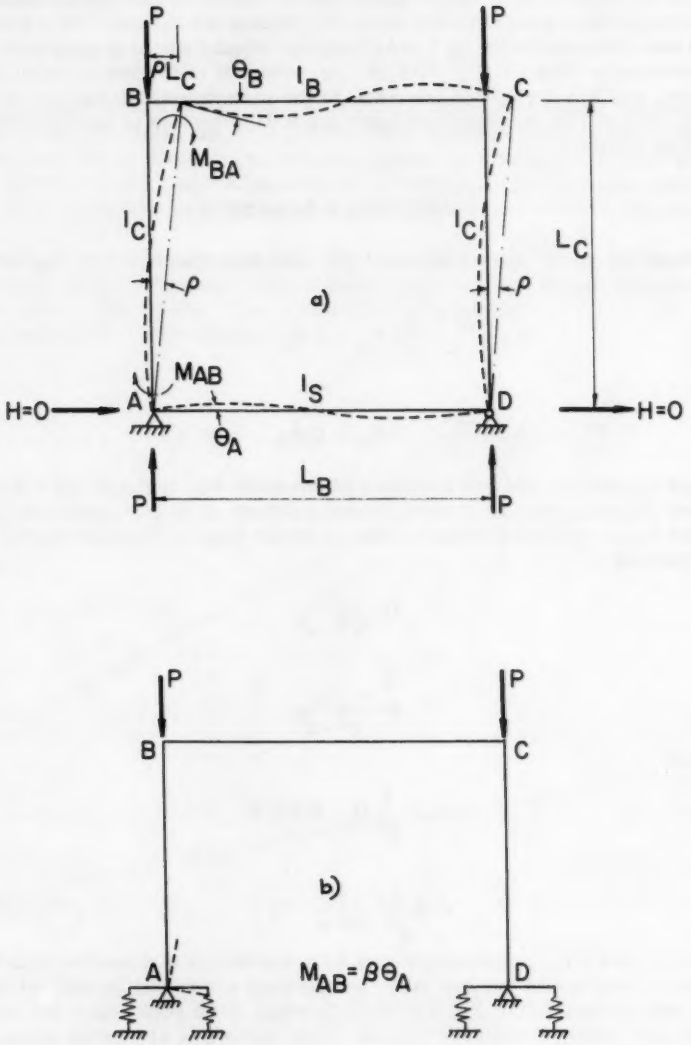

FIG. 3.—SINGLE-STORY SINGLE-BAY RECTANGULAR FRAME WITH BASE RESTRAINT.

the horizontal reactions and equating their sum to zero. As many independent equations are necessary as the number of unknown joint rotations θ and bar rotations ρ. Stability is satisfied when the determinant of the coefficients of the unknowns is equal to zero.

THE BUCKLING STRENGTH OF A SINGLE-STORY, SINGLE-BAY RIGID FRAME

The frame which is to be analyzed is shown in Fig. 3(a). Since the loading and the dimensions are symmetrical, only one half of the frame need be considered, because by symmetry $\theta_C = \theta_B$, $\theta_D = \theta_A$ and $\rho_{CD} = \rho_{AB}$. The unknown

TABLE 1

ϕ	k	S	C	K	Q	R
0		2.000	4.000	3.000	1.000	-1.000
0.1	31.416	2.000	3.999	3.002	0.997	-1.002
0.2	15.708	2.001	3.995	3.008	0.987	-1.007
0.3	10.472	2.003	3.988	3.018	0.970	-1.015
0.4	7.854	2.005	3.979	3.033	0.946	-1.028
0.6	5.236	2.012	3.952	3.075	0.877	-1.063
0.8	3.927	2.022	3.914	3.137	0.777	-1.115
1.0	3.142	2.034	3.865	3.225	0.640	-1.191
1.2	2.618	2.050	3.804	3.337	0.467	-1.287
1.4	2.244	2.070	3.732	3.491	0.241	-1.421
1.6	1.965	2.093	3.647	3.694	-0.047	-1.601
1.8	1.745	2.120	3.548	3.968	-0.420	-1.848
2.0	1.572	2.152	3.436	4.351	-0.915	-2.199
2.2	1.430	2.189	3.309	4.910	-1.601	-2.721
2.4	1.310	2.233	3.166	5.786	-2.620	-3.553
2.6	1.210	2.283	3.005	7.328	-4.323	-5.045
2.8	1.122	2.343	2.825	10.700	-7.875	-8.457
3.0	1.048	2.412	2.624	23.658	-21.034	-21.246

joint rotations then are θ_A, θ_B, and the unknown bar rotation is $\rho_{AB} = \rho$. For these three unknowns, three independent equations must be found. Joint and bar rotations are clockwise, therefore positive. The moments at the ends of bar AB are, according to Eq. 8, the following:

$$M_{AB} = \frac{E_t I_C}{L_C} \left[C_{AB}\theta_A + S_{AB}\theta_B - \rho \left(C_{AB} + S_{AB} \right) \right] \quad \ldots . \text{(11a)}$$

and

$$M_{BA} = \frac{E_t I_C}{L_C} \left[S_{AB}\theta_A + C_{AB}\theta_B - \rho \left(C_{AB} + S_{AB} \right) \right] \quad \ldots . \text{(11b)}$$

The direction of the moments in Eq. 11 is clockwise as shown in Fig. 4. Noting that $\rho_{AD} = \rho_{BC} = 0$, the bending moments of the end B of bar BC and the end A of bar AC are

$$M_{BC} = \frac{E_t I_B}{L_B} \left[C_{BC} \theta_B + S_{BC} \theta_B \right] \quad \ldots\ldots\ldots (12a)$$

and

$$M_{AD} = \frac{E_t I_S}{L_B} \left[C_{AD} \theta_A + S_{AD} \theta_A \right] \quad \ldots\ldots\ldots (12b)$$

There is no axial force present in bars AD and BC. Since therefore $\phi = 0$, the values of the coefficients C and S are obtained from Eq. 9 as

$$C_{AD} = C_{BC} = 2 \quad \ldots\ldots\ldots\ldots\ldots\ldots (13a)$$

and

$$S_{AD} = S_{BC} = 4 \quad \ldots\ldots\ldots\ldots\ldots\ldots (13b)$$

If these values of C and S are substituted into Eq. 12, and if the subscripts of C and S are dropped in Eq. 11, the equations for the four bending moments are

$$M_{AB} = \frac{E_t I_C}{L_C} \left[C \theta_A + S \theta_B - \rho (C + S) \right] \quad \ldots\ldots\ldots (14a)$$

$$M_{BA} = \frac{E_t I_C}{L_C} \left[S \theta_A + C \theta_B - \rho (C + S) \right] \quad \ldots\ldots\ldots (14b)$$

$$M_{BC} = \frac{6 E_t I_B \bar{\theta}_B}{L_B} \quad \ldots\ldots\ldots\ldots\ldots\ldots (14c)$$

and

$$M_{AD} = \frac{6 E_t I_S \bar{\theta}_A}{L_B} \quad \ldots\ldots\ldots\ldots\ldots\ldots (14d)$$

Next, the equations of equilibrium will be written at the two joints.
(1) Joint A:

$$M_{AB} + M_{AD} = 0 \quad \ldots\ldots\ldots\ldots\ldots\ldots (15)$$

Substituting M_{AB} and M_{AD} from Eq. 14

$$\frac{E_t I_C}{L_C} \left[C \theta_A + S \theta_B - \rho (C + S) \right] + \frac{6 E_t I_S}{L_B} \theta_A = 0 \quad \ldots\ldots (16)$$

In general E_t of the column will not equal E_t in the beam. Since no forces exist in the beam prior to buckling, all of the beam will remain elastic, and hence $E_t = E$ in this member. The equilibrium equation can now be rearranged as follows:

$$C \theta_A + S \theta_B - \rho (C + S) + \frac{6 I_S L_C \theta_A}{I_C L_B \tau} = 0 \quad \ldots\ldots\ldots (17)$$

If the abbreviation

$$\lambda = \frac{I_S L_C}{I_C L_B \tau} \quad \ldots\ldots\ldots\ldots\ldots\ldots (18)$$

is used, Eq. 17 can be written as:

$$\theta_A [C + 6\lambda] + \theta_B [S] - \rho [C+S] = 0 \quad \ldots\ldots (19)$$

(2) Joint B:

$$M_{BA} + M_{BC} = 0 \quad \ldots\ldots\ldots\ldots\ldots\ldots (20)$$

Performing the same operation as for joint A, the corresponding equilibrium equation will be

$$\theta_A [S] + \theta_B \left[C + \frac{6}{\gamma} \right] - \rho [C+S] = 0 \quad \ldots\ldots\ldots (21)$$

Eqs. 19 and 21 are two equations in the three unknowns θ_A, θ_B, and ρ. One additional expression is necessary for a solution. This additional equation is

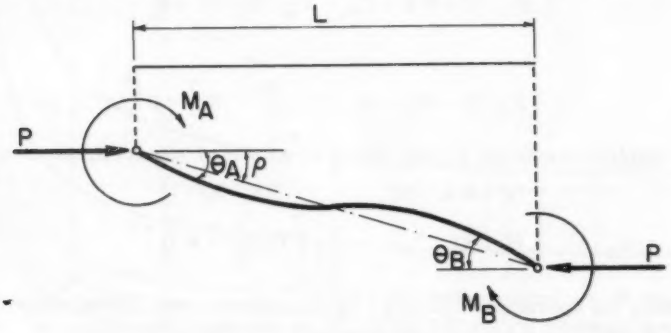

$$M_{AB} = \frac{E_t I}{L} \left[C\theta_A + S\theta_B - \rho (C+S) \right]$$

$$M_{BA} = \frac{E_t I}{L} \left[S\theta_A + C\theta_B - \rho (C+S) \right]$$

FIG. 4.—THE SLOPE DEFLECTION EQUATIONS.

obtained from the statical condition that the sum of the horizontal reactions at the bases must equal zero. Since the end moments of column AB are equal in sense to the end moments of column CD, the horizontal base reaction must act to the right for each column. But since the moments are also equal in magnitude, this can only be possible if the horizontal reaction of each column is zero.

The additional equation is derived by summing moments about point B (Fig. 3(a)).

$$M_{BA} + M_{AB} + P\,L_C\,\rho = 0 \quad \ldots\ldots\ldots\ldots\ldots (22)$$

If the values of M_{BA} and M_{AB} from Eq. 14 are substituted into Eq. 22, the following equation results:

$$\theta_A\,[C+S] + \theta_B\,[C+S] - 2\,\rho\,(C+S) + \frac{P\,L_C^2\,\rho}{E_t\,I_C} = 0 \quad \ldots\ldots (23)$$

Since $\frac{PL_C^2}{E_t\,I_C} = \phi^2$ (Eq. 5), the value of ρ is

$$\rho = \left[\frac{C+S}{2\,(C+S) - \phi^2}\right] \quad (\theta_A + \theta_B) \quad \ldots\ldots\ldots\ldots (24)$$

Substitution of ρ from Eq. 24 into Eq. 19 and 21 reduces the unknowns to θ_A and θ_B. With the abbreviation

$$K = \frac{(C+S)^2}{2\,(C+S) - \phi^2} \quad \ldots\ldots\ldots\ldots\ldots\ldots (25)$$

these equations reduce to the following:

$$\theta_A\,[C + 6\,\lambda - K] + \theta_B\,[S - K] = 0 \quad \ldots\ldots\ldots (26a)$$

and

$$\theta_A\,[S - K] + \theta_B\left[C + \frac{6}{\gamma} - K\right] = 0 \quad \ldots\ldots\ldots (26b)$$

The stability condition is that the determinant of the coefficients must be zero.

$$\begin{vmatrix} (C + 6\,\lambda - K) & (S - K) \\ (S - K) & \left(C + \frac{6}{\gamma} - K\right) \end{vmatrix} = 0 \quad \ldots\ldots\ldots (27)$$

Performing the operations indicated by this determinant, the equation for the buckling strength of a rectangular single-story, single-bay frame is

$$(Q + 6\,\lambda)\left(Q + \frac{6}{\gamma}\right) - R^2 = 0 \quad \ldots\ldots\ldots\ldots (28)$$

where

$$Q = C - K \quad \ldots\ldots\ldots\ldots\ldots\ldots (29a)$$

and

$$R = S - K \quad \ldots\ldots\ldots\ldots\ldots\ldots (29b)$$

It can be shown that Eq. 28 reduces to the buckling condition for the pinned-base frame (Eq. 2) when $\lambda = 0$ and the buckling condition for the fixed-base frame (Eq. 3) when $\lambda = \infty$.

The relationship between the effective length factor k and the varying degrees of base fixity expressed in terms of λ is shown in Fig. 5 for several constant values of the ratio γ. The left end of the curves in Fig. 5 corresponds to the values of k for a pinned-end frame ($\lambda = 0$), and the right end of the curves

approaches the k-values for a fixed-end frame ($\lambda \to \infty$) as an asymptote. The curves show that the effective length is rapidly reduced from its value for the case of a pinned-base frame as soon as a small amount of base restraint is present. For example, if this restraint is equal to the stiffness of the top beam ($I_S = I_B$, or $\lambda = 1.0$ when $L_C = L_B$) the values of k are almost equal to those for a fixed-base frame. This indicates that although the base is still relatively flexible, the small restraint offered by it produces almost the same effect as that of a fully rigid column base.

The effect of partial base fixity on the critical load is shown in Fig. 6. Here the base restraint coefficient λ is plotted versus the critical load P_{cr} (non-dimensionalized by the factor $\frac{L_C 2}{\pi^2 E_t I_C}$). It can again be observed that a small

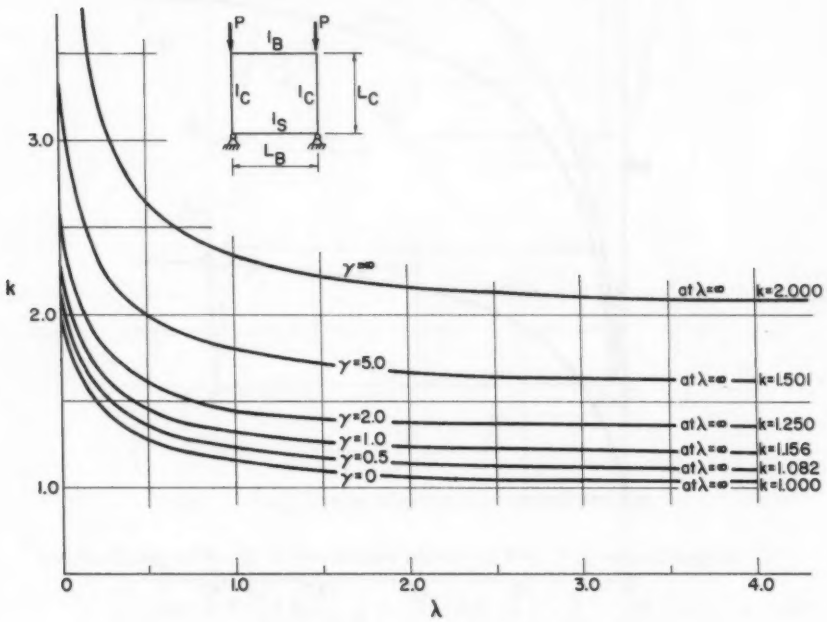

FIG. 5.—EFFECTIVE LENGTH OF COLUMNS IN A SINGLE-STORY SINGLE-BAY FRAME.

of restraint at the column ends can increase the critical load considerably.

In a rigid frame of usual proportions the critical load on the columns may be higher than that load which would cause partial yielding. In this case $E_t < E$ or $\tau < 1.0$. The value of k may be found approximately by assuming $\tau = 1.0$, calculating λ and γ and finding k from Eq. 28 or Fig. 5. The corresponding critical load is then computed from Eq. 1. If the stress due to P_{cr} is above the proportional limit of the material, E_t and thus τ can be obtained from a stub column stress-strain diagram.[10] A new value of λ, γ, and therefore k and P_{cr} can now be found for this value of τ. The value of the stress will be

10 "Basic Column Strength," by L. S. Beedle and L. Tall, Fritz Lab. Report 220A.34, Lehigh Univ., Bethlehem, Pa., 1959.

changed, and yet another τ can be computed. This process can be repeated until sufficient accuracy is obtained.

The additional work necessitated by the procedure outlined above will not be required, unless a very high degree of accuracy is desired. The value of λ (Eq. 18) will increase and the value of γ (Eq. 4) will decrease if τ is changed from 1.0 to its inelastic value of $\tau < 1.0$. It can be seen in Fig. 5 that if this occurs, k computed for $\tau < 1.0$ will always be smaller than k computed for $\tau = 1.0$. Thus the error will be on the safe side if τ is taken as 1.0. This error

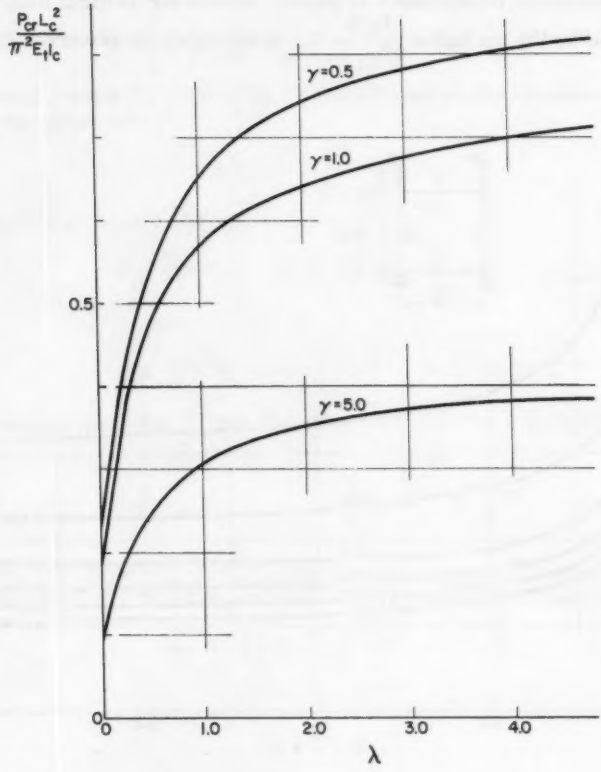

FIG. 6.—VARIATION OF CRITICAL LOAD WITH BASE RESTRAINT FOR A SINGLE-STORY SINGLE-BAY FRAME.

will in general not be large, since τ is usually not much less than 1.00 and fairly large changes in λ and γ will not change k appreciably if $\gamma \leq 2.0$ and $\lambda \geq 0.5$ (Fig. 5).

BUCKLING STRENGTH OF A TWO-STORY, SINGLE-BAY FRAME

In order to show that a situation similar to that described above exists for other frames, the buckling strength of another structure will be computed. This

is the two-story, single-bay, rectangular rigid frame shown in Fig. 7. The span of this frame is L_B, and the story heights are the same for each story (story height = L_C). The moment of inertia is equal to I_C for the columns and I_B for the beams. Base restraint is simulated by a beam which has a moment of inertia I_S.

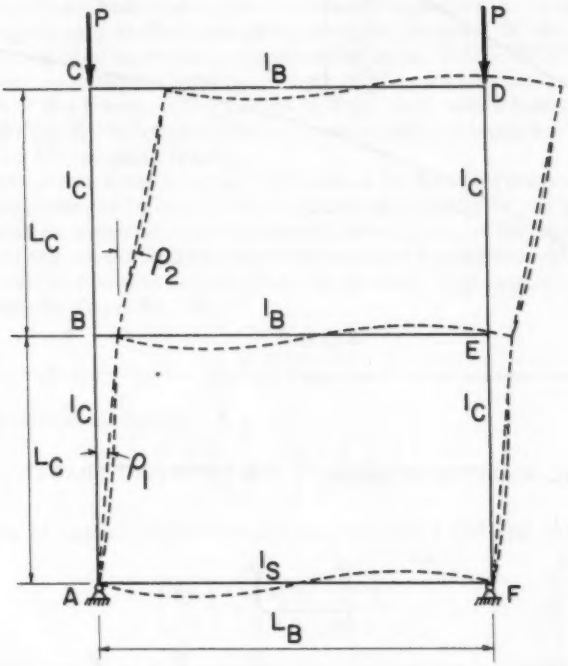

FIG. 7.—TWO-STORY SINGLE-BAY RIGID FRAME.

The buckling strength of the frame shown in Fig. 7 is expressed by

$$(Q + 6\lambda)\left(2Q + \frac{6}{\gamma}\right) - R^2\left(2Q + 6\lambda + \frac{6}{\gamma}\right) = 0 \quad \ldots\ldots\ldots (30)$$

The derivation of this equation is given in Appendix A. Eq. 30 reduces to

$$\frac{6}{\gamma} = \frac{R^2 - Q^2}{Q} \quad \ldots\ldots\ldots\ldots\ldots\ldots (31)$$

for a pinned-base frame ($\lambda = 0$) and to

$$\left(2Q + \frac{6}{\gamma}\right)\left(Q + \frac{6}{\gamma}\right) - R^2 = 0 \quad \ldots\ldots\ldots\ldots\ldots (32)$$

for a fixed-base frame ($\lambda = \infty$).

The plots of γ versus k for the pinned-base case and for the fixed-base case are shown in Fig. 8, and the relationship between k and λ for several constant

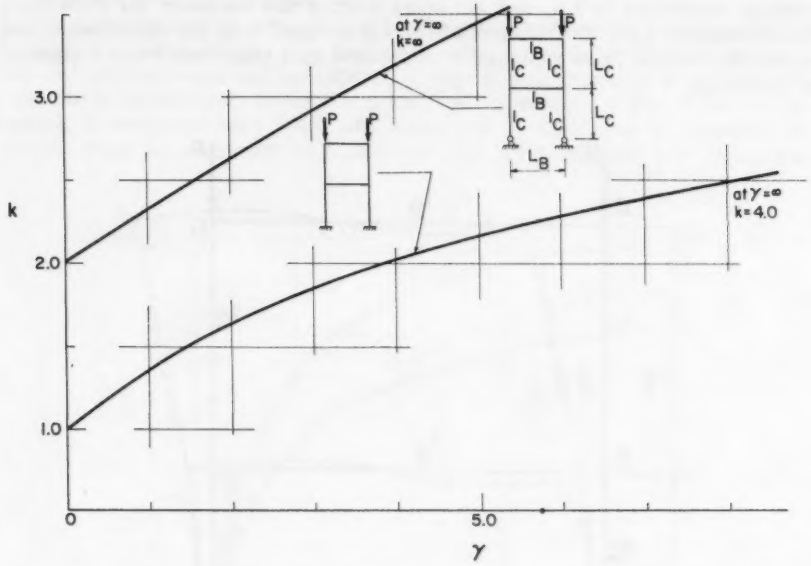

FIG. 8.—EFFECTIVE LENGTH FOR TWO-STORY FRAMES.

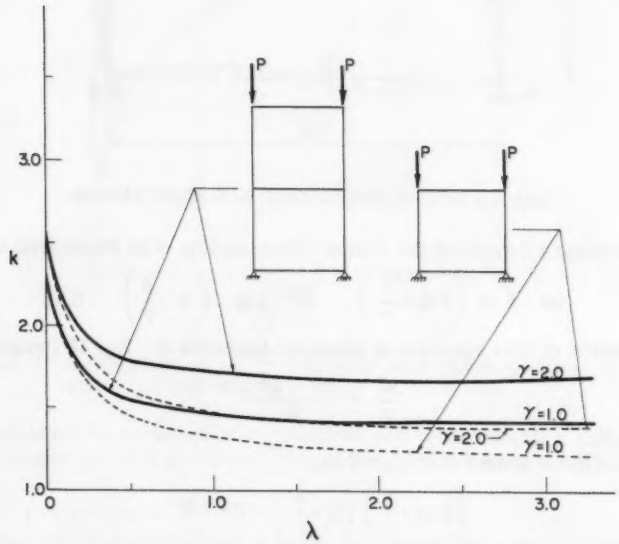

FIG. 9.—EFFECTIVE LENGTH OF COLUMNS IN ONE- AND TWO-STORY RIGID FRAMES.

values of γ is shown in Fig. 9. A rapid decrease of k (and thus an increase of P_{cr}) for a small amount of base fixity can again be observed. The curves for the single-story frame are also shown in Fig. 9 for comparison.

APPLICATIONS OF THE THEORY

In the preceding discussion equations were developed for the buckling strength of two symmetrically loaded symmetrical rigid frames. It was shown that a small amount of base restraint, as simulated by an elastic beam between the column bases, reduces the effective length of the columns and thus increases the strength of the frame. The curves in Figs. 5, 6, and 9 indicate that if the ratio $(I_S/L_B)(L_C/I_C)$ is greater than one, the buckling strength of the frame is nearly that of a fixed-base frame.

The problem which remains to be discussed is the determination of the restraint actually offered by column bases which were designed as "pinned." This must be known in order to evaluate the stiffness I_S/L_B of the base beam. The relationship between the column base restraint and the stiffness of the fictitious base beam can be obtained in the following manner: The moment at the end of the base beam is (from Eq. 14),

$$M = \frac{6\,E\,I_S\,\theta}{L_B} \quad \ldots\ldots\ldots\ldots\ldots\ldots (33)$$

If Eq. 33 is solved for I_S/L_B,

$$\left(\frac{I_S}{L_B}\right) = \left(\frac{M}{\theta}\right)\left(\frac{1}{6\,E}\right) \quad \ldots\ldots\ldots\ldots\ldots\ldots (34)$$

If the frame is manufactured from steel, ($E = 30 \times 10^6$ psi) the stiffness is equal to

$$\left(\frac{I_S}{L_B}\right) = \left(\frac{M}{\theta}\right)\left(\frac{1}{180 \times 10^6}\right) \quad \ldots\ldots\ldots\ldots\ldots\ldots (35)$$

In Eq. 35 the value of M/θ is unknown. This ratio is the initial slope of a curve showing the relationship between a moment and the corresponding rotation for a column base.

Column bases for so-called pinned-base structures consist, in general, of plates welded to the bottom of the columns. These plates are bolted by anchor bolts to the concrete of the footing. Rotation may take place between the column base and the footing, and the whole footing may rotate in the surrounding soil.

Before any conclusions can be drawn from the theory, it is necessary to know whether this ordinary pinned-base arrangement offers sufficient restraint to base rotation to decrease the effective column length towards that of a fixed-base frame.

There are few experimental and analytical studies available which show the moment-rotation characteristics of the footing in the surrounding soil. K. H. Roscoe and A. N. Schofield made measurements[11] of the rotation of eight column footings embedded in sandy soil. (This research was part of the full scale collapse tests of rigid north-light portal frames at Cambridge University.) The

[11] "The Stability of Short Pier Foundations in Sand," by K. H. Roscoe and A. N. Schofield, The British Welding Journal, Symposium on the Plastic Theory of Structures, Cambridge, England, September, 1956.

footings were designed to furnish full fixity to the column bases, and the experimental moment-rotation curves show that this was indeed the case for most of the columns.

An estimate of the stiffness of the foundation in the soil can be made by the following approximation: Before buckling the foundation is subjected to only a compressive force. At the inception of frame buckling an additional bending moment of indeterminate magnitude is present. Since M/θ, the ratio of this

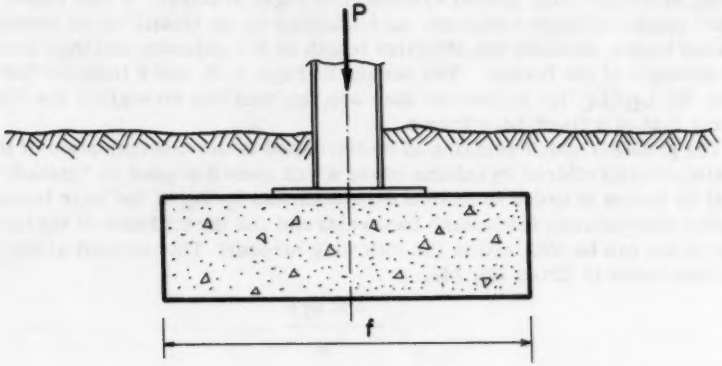

FOUNDATION BEFORE BUCKLING

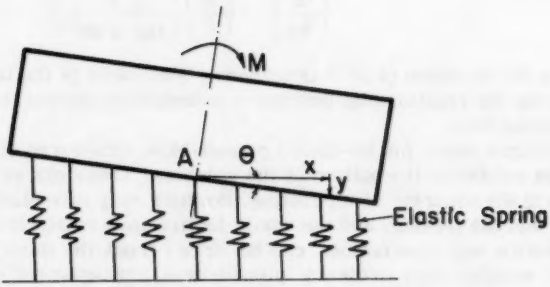

IDEALIZED SITUATION AT BUCKLING

FIG. 10.—SCHEMATIC REPRESENTATION OF RESTRAINT OFFERED BY FOUNDATIONS.

moment with respect to the corresponding rotation, is required only at the start of buckling, it can be assumed that the response of the soil to the moment is purely elastic. If it is assumed also that the foundation is rigid in comparison with the soil, the rotation can be represented by a set of elastic springs (Fig. 10). The reaction of the soil at any elementary area g dx (where

g is the width of the foundation) is K y dx (where K is the force, per linear inch, which is necessary to compress the soil 1 in., and y is the deflection). Taking moments about point A in Fig. 10, it is found that $M_x = x\ Ky\ dx$. Integrating over the length f of the foundation, noting that $y = \theta x$,

$$M = 2 \int_0^{f/2} \theta\ K x^2\ dx = \frac{K f^3 \theta}{12} \quad \ldots\ldots\ldots (36)$$

The modulus K can be correlated[12] with the "modulus of subgrade reaction," q, which is given in pounds per square inch per inch of deflection, by setting K = g q. The value of the base stiffness is then

$$\frac{M}{\theta} = \frac{g\ q\ f^3}{12} \quad \ldots\ldots\ldots\ldots\ldots\ldots (37)$$

Values of q must be determined by experiment or the designer can estimate them in accordance with his knowledge of the soil conditions. Magnitudes of q listed by J. H. Bateman[12] vary from 50 lb per cu in. to 400 lb per cu in.

Substitution of M/θ from Eq. 37 into Eq. 35 yields the following expression for the stiffness of the fictitious restraint beam due to the rotation of the foundation in the soil:

$$\frac{I_S}{L_B} = \frac{q\ g\ f^3}{2160 \times 10^6} \quad \ldots\ldots\ldots\ldots\ldots\ldots (38)$$

It must be realized that Eq. 38 is only an approximation. For a more accurate evaluation of the stiffness of foundations in soils further extensive analytical and experimental research is necessary. Eq. 38 gives only a conservative estimate for M/θ in case that no more precise information is available.

Analytical approximations have been developed for the case where the footing does not rotate in the soil.[13] Rotation takes place between the column ends and the footing due to the deformation of the base plate, the anchor bolts, and the concrete. Results of this investigation show that the slope of the moment rotation curve is

$$\frac{M}{\theta} = \frac{b\ d^2\ E_C}{12} \quad \ldots\ldots\ldots\ldots\ldots\ldots (39)$$

in which b is the width of the base plate, d denotes the length of the base plate, and E_C is the modulus of elasticity of the concrete. If Eq. 39 is substituted into Eq. 35, the stiffness of the ficticious restraining beam due to a moment between the column base and the foundation is

$$\frac{I_S}{L_B} = \frac{b\ d^2}{72\ h} \quad \ldots\ldots\ldots\ldots\ldots\ldots (40)$$

where n is the modular ratio $E_{steel}/E_{concrete}$.

Whichever of the two stiffnesses I_S/L_B (Eq. 38 or Eq. 40) yields the least stiffness would be used to determine the coefficient λ and thus the buckling strength of the frame.

To show the extent by which partial base fixity influences the buckling strength of a particular frame, an example is calculated in Appendix II.

---

12 "Introduction to Highway Engineering," by J. H. Bateman, John Wiley and Sons, New York, 1948.

13 "Moment Rotation Characteristics of Column Anchorages," by C. G. Salmon, L. Schlenker and B. G. Johnston, Proceedings, ASCE, Vol. 81, No. ST 3, April, 1955.

The critical load of a rectangular rigid frame of the type and loading shown in Fig. 1 is computed. First, the critical load is determined by assuming pinned bases; next the influence of partial base fixity is included in the calculation.

The following may be concluded from this example:

1. Even for as stocky a member as was used in this example (8WF31 column, 13 ft long, bent about the strong axis) it is seen that it is not worth while to compute the influence of $\tau \neq 1.0$, since the column strength is underestimated by only about 2% if $\tau = 1.0$ is used in the calculations.

2. The critical load, assuming pinned bases is 217 kips including the variation of τ). If the influence of base restraint is also considered (assuming a relatively poor soil, q = 150 lbs./in.^{3}) it is seen that P_{cr} = 281 kips. Thus the increase is about 30% of the critical load for pinned bases in this problem.

CONCLUSIONS

The following conclusions may be drawn about the effects of partial base restraint from this analysis:

1. Partial base fixity has a beneficial effect on the buckling strength of rigid frames.

2. The curves in Figs. 5 and 9 show that for single-bay, single and two story rectangular rigid frames, a small amount of base restraint reduces the effective length considerably from that of the pinned-base condition.

3. Further research on the moment-rotation characteristics of common column foundations is necessary before a more accurate estimate of the base restraint can be made. Available information indicates that presently used "pinned" column bases give enough restraint to increase the buckling strength of the frame considerably, especially if the footing is large.

4. The results of this investigation indicate that the restraint offered by the base details of one and two story frames analyzed as pin-based is in many cases adequate to prevent failure by frame instability. This fact is especially important for plastically designed structures, since the buckling strength computed on the basis of pinned-ends would otherwise often limit the full realization of the mechanism.

The method permits the calculation of the critical buckling load of any pinned-base frame, as long as an estimate of the base restraint can be made. For plastic design the method of analysis for determining an approximate conservative buckling load is the following: The plastic hinges of the incomplete mechanism are replaced by real hinges, and a stability analysis is made of this structure. If the critical loads of the structure for which all but the last hinge has formed is higher than or equal to the plastic collapse load, the frame will not fail by frame instability.

In Fig. 11 the curve for $\gamma = 1.0$ for a single story, single-bay frame is shown when a real hinge is placed at one of the knees. It is again seen that partial base fixity reduces the effective length rapidly, even if only a small amount of base restraint is present. Also shown in Fig. 11 is the equation representing the buckling strength, base restraint, and dimensional relationship for this structure.

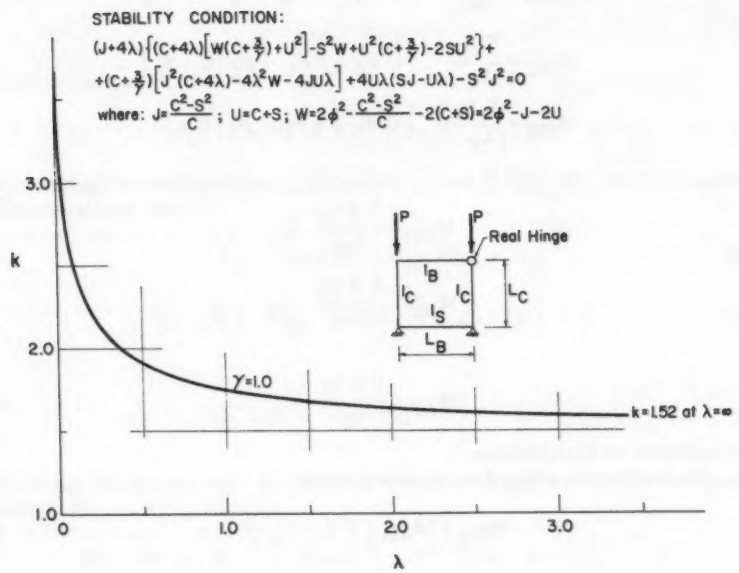

FIG. 11.—EFFECTIVE LENGTH OF COLUMNS IN A FRAME CONTAINING A HINGE.

ACKNOWLEDGMENTS

This study is part of the general investigation "Welded Continuous Frames and Their Components" being carried out at Fritz Engineering Laboratory, Lehigh University, under the direction of Lynn S. Beedle, F. ASCE. This investigation is sponsored jointly by the Welding Research Council and the United States Department of the Navy with funds furnished by the American Iron and Steel Institute, American Institute of Steel Construction, Office of Naval Research, Bureau of Ships, and Bureau of Yards and Docks.

William J. Eney, F. ASCE, is Director of Fritz Engineering Laboratory and Head of the Department of Civil Engineering.

The critical review by Jonathan Jones, F. ASCE, Le-Wu Lu, A. M. ASCE, Robert Ketter, A. M. ASCE, T. R. Higgins, and Bruno Thurlimann, M. ASCE, are gratefully acknowledged.

APPENDIX I

Derivation of the Critical Equation for a Two Story, One-Bay Frame.—The frame and its dimensions are shown in Fig. 7. Since the frame is symmetrical, only one half of the frame need be analyzed. All rotations are clockwise; thus the equations of the moments from Eq. 8 are:

$$M_{AB} = \frac{E\,I_C}{L_C}\left[C\,\theta_A + S\,\theta_B - \rho_1\,(C+S)\right] \quad \ldots\ldots\ldots (41a)$$

$$M_{BA} = \frac{E\,I_C}{L_C}\left[S\,\theta_A + C\,\theta_B - \rho_1 (C+S)\right] \quad \ldots\ldots\ldots (41b)$$

$$M_{BC} = \frac{E\,I_C}{L_C}\left[C\,\theta_B + S\,\theta_C - \rho_2 (C+S)\right] \quad \ldots\ldots\ldots (41c)$$

$$M_{CB} = \frac{E\,I_C}{L_C}\left[C\,\theta_C + S\,\theta_B - \rho_2 (C+S)\right] \quad \ldots\ldots\ldots (41d)$$

$$M_{CD} = \frac{6\,E\,I_B}{L_B}\,\theta_C \quad \ldots\ldots\ldots (41e)$$

$$M_{BE} = \frac{6\,E\,I_B}{L_B}\,\theta_B \quad \ldots\ldots\ldots (41f)$$

and

$$M_{AF} = \frac{6\,E\,I_S}{L_B}\,\theta_A \quad \ldots\ldots\ldots (41g)$$

Conditions of Equilibrium.–

1. No horizontal shear forces are present:

$$M_{BA} + M_{AB} + P\,L_C\,\rho_1 = 0 \quad \ldots\ldots\ldots (42a)$$

and

$$M_{BC} + M_{CB} + P\,L_C\,\rho_2 = 0 \quad \ldots\ldots\ldots (42b)$$

Substitution of the moments yields the following equation for ρ_1 and ρ_2:

$$\rho_1 = \frac{(C+S)\,(\theta_A + \theta_B)}{2(C+S) - \phi^2} \quad \ldots\ldots\ldots (43a)$$

and

$$\rho_2 = \frac{(C+S)\,(\theta_B + \theta_C)}{2(C+S) - \phi^2} \quad \ldots\ldots\ldots (43b)$$

2. Equilibrium at joint A:

$$M_{AB} + M_{AF} = 0 \quad \ldots\ldots\ldots (44)$$

If the values of the moments and ρ_1 and ρ_2 and the abbreviation K (Eq. 25) are substituted, the following equation results:

$$\theta_A\,[C - K + 6\lambda] + \theta_B\,[S - K] = 0 \quad \ldots\ldots\ldots (45)$$

3. Equilibrium at joint B:

$$M_{BA} + M_{BC} + M_{BE} = 0 \quad \ldots\ldots\ldots (46)$$

Substitution leads to:

$$\theta_A\,[S\text{-}K] + \theta_B\left[2\,C\text{-}2\,K + \frac{6}{\gamma}\right] + \theta_C\,[S\text{-}K] = 0 \quad \ldots\ldots (47)$$

4. Equilibrium at joint C:

$$M_{CB} + M_{CD} = 0 \quad \ldots\ldots\ldots\ldots\ldots\ldots (48)$$

Substitution leads to:

$$\theta_B \left[S - K\right] + \theta_C \left[C - K + \frac{6}{\gamma}\right] = 0 \quad \ldots\ldots\ldots (49)$$

Introducing the further simplifications of Q and R (Eq. 29), the three simultaneous equations are:

$$\theta_A \left[Q + 6\lambda\right] + \theta_B \left[R\right] = 0 \quad \ldots\ldots\ldots\ldots (50a)$$

$$\theta_A \left[R\right] + \theta_B \left[2Q + \frac{6}{\gamma}\right] + \theta_C \left[R\right] = 0 \quad \ldots\ldots\ldots (50b)$$

and

$$\theta_B \left[R\right] + \theta_C \left[Q + \frac{6}{\gamma}\right] = 0 \quad \ldots\ldots\ldots\ldots (50c)$$

Equating the determinant of the coefficients to zero, the following equation results as the buckling equation:

$$(Q + 6\lambda)\left(2Q + \frac{6}{\gamma}\right)\left(Q + \frac{6}{\gamma}\right) - R^2 \left(2Q + 6\lambda + \frac{6}{\gamma}\right) = 0 \quad \ldots\ldots (51)$$

APPENDIX II

It is desired to determine the critical load on an industrial frame of the type shown in Fig. 1. The top cross beam is a 10WF33 member, and the columns are 8WF31 members, arranged in such a manner that the web is in the plane of the frame. Weak-axis buckling out of the plane of the frame is assumed to be prevented by bracing. The span length is 20 ft 0 in. and the column height is 13 ft 0 in.

1. Assuming Pinned Column Bases

Column Size: 8WF31
$I_C = 109.7$ in.^{4}
$L_C = 156$ in.

Beam Size: 10WF33
$I_B = 170.9$ in.^{4}
$L_B = 240$ in.

Assume $\tau = 1.00$

$$\gamma = \frac{I_C}{L_C} = \frac{L_B}{I_B} = 0.987$$

From Fig. 2, k = 2.33

$$\frac{k\,L_C}{r_x} = \frac{2.33 \times 156}{3.47} = 105$$

The critical stress has been given[14] (as an approximate expression) as

14 "Basic Column Strength," by L. S. Beedle and L. Tall, Fritz Lab. Report 220A.34, Lehigh Univ., Bethlehem, Pa., 1959, Eq. 11.

$$\sigma_{cr} = 33.0 - \frac{8.80 \times \left(k\,L/r_x\right)^2}{10{,}000} = 23.4 \text{ ksi}$$

or

$$P_{cr} = \sigma_{cr} A = 214 \text{ kips}$$

An approximation for τ is obtained as follows:

$$\tau = \frac{E_t}{E} = \frac{\dfrac{\pi^2 E_t}{k\,L/r^2}}{\dfrac{\pi^2 E}{k\,L/r^2}} = \frac{\sigma_{cr}}{\sigma_E} \quad \ldots\ldots\ldots\ldots (52)$$

For this problem,

$$\sigma_E = \frac{\pi^2 E}{k\,L/r^2} = \frac{\pi^2 \times 30{,}000}{(105)^2} = 27.1 \text{ ksi}$$

and

$$\tau = \frac{\sigma_{cr}}{\sigma_E} = \frac{23.4}{27.1} = 0.864$$

Adjusting γ for $\tau < 1.00$:

$$(\gamma)_A = 0.987 \times 0.864 = 0.852$$

The corresponding value of k from Fig. 2 is 2.28. Calculating the new σ_{cr}, σ_E and another value of τ, it is found that the values of k and σ_{cr} after two cycles are equal to k = 2.27, σ_{cr} = 23.8 ksi, and P_{cr} = 217 kips.

2. Including the Influence of Base Restraint

Base plate size: 12 in. by 12 in.

Modular ratio E_S/E_C = n - 10

From Eq. 40, $I_S/L_B = \dfrac{b\,d^2}{72\,n} = \dfrac{(12)^3}{720} = 2.40$

Footing size: 6 ft 0 in. by 6 ft 0 in.

Assume q = 150 lb per cu in.

Then, from Eq. 38,

$$I_S\,L_B = \frac{q\,g\,f^3}{2160 \times 10^6} = \frac{150\,(72)^4}{2160 \times 10^6} = 1.86$$

Since this stiffness is smaller than the stiffness of the base-plate anchorage bolt detail (Eq. 38), it will be used in subsequent calculations:

$$\lambda = \frac{I_S}{L_B} \times \frac{L_C}{I_C} = \frac{1.86 \times 156}{109.7} = 2.67$$

if τ is assumed equal to 1.0 and $\gamma = 0.987$.

From Fig. 5, the corresponding value of k is 1.22, and σ_{cr} according to L. S. Beedle[14] is equal to 30.4 ksi, or $P_{cr} = 277$ kips. Proceeding as before to include the influence of $\tau < 1.0$, it is found that after two cycles k = 1.10, $\sigma_{cr} = 30.8$ ksi, and $P_{cr} = 282$ kips.

APPENDIX III.—NOMENCLATURE

- b = width of base plate;
- C = nondimensional coefficient, defined by Eq. 9;
- c = nondimensional coefficient defined by Eq. 10;
- d = length of base plate;
- E = modulus of elasticity;
- E_t = tangent modulus;
- E_C = modulus of elasticity of concrete;
- f = length of foundation;
- g = width of foundation;
- I_B = moment of inertia of beam;
- I_C = moment of inertia of column;
- I_S = moment of inertia of ficticious base restraint beam;
- K = spring constant of soil;
- K = nondimensional coefficient defined by Eq. 25;
- k = effective length coefficient;
- L_B = span length;
- L_C = length of column;
- M = bending moment;
- M_{AB} = moment at the end A of member AB;
- n = modular ratio;
- P = axial load in column;
- P_{cr} = critical load;
- Q = nondimensional coefficient defined by Eq. 29;
- q = modulus of subgrade reaction;
- R = nondimensional coefficient defined by Eq. 29;
- S = nondimensional coefficient defined by Eq. 9;
- s = nondimensional coefficient defined by Eq. 10;
- x = coordinate of distance;
- y = coordinate of deflection;

β = spring constant;

γ = nondimensional coefficient defined by Eq. 4;

λ = nondimensional coefficient defined by Eq. 18;

ϕ = nondimensional coefficient defined by Eq. 5;

θ = joint rotation;

ρ = bar rotation; and

τ = E_t/E.

Journal of the
STRUCTURAL DIVISION
Proceedings of the American Society of Civil Engineers

CONTENTS

DISCUSSION

Page

Review of Limit Design for Structural Concrete, by C. W. Yu and Eivind Hognestad. (December, 1958. Discussion: February, 1959, June, 1959, September, 1959. Discussion closed.)
by C. W. Yu and Eivind Hognestad (closure) 111

Bending Moments on Shell Boundaries, by H. H. Bleich and M. G. Salvadori. (October, 1959. Prior discussion: February, 1960. Discussion closed.)
by Zdeněk Sobotka 113

Ultimate Load Theory for Concrete Frame Analysis, by A. L. L. Baker. (November, 1959. Prior discussion: None. Discussion closed.)
by Bruno Barbarito and Guiliano Augusti 119

Fixed Point Method of Moment Design, by S. E. Huey. (November, 1959. Prior discussion: None. Discussion closed.)
by A. A. Eremin 125

Design of Prestressed Composite Steel Structures, by Rudolph Szilard. (November, 1959. Prior discussion: None. Discussion closed.)
by Sven H. Wichman 127

Lessons of Collapse of Vancouver 2nd Narrows Bridge, by A. Hrennikoff. (December, 1959. Prior discussion: None. Discussion closed.)
by Kuang-Han Chu 131

Cut-Off Points for Cover Plates, by Nat T. Kanarek. (December, 1959. Prior discussion: February, 1960. Discussion closed.)
by Nabi Taskinoglu 133

(Over)

Note.—This paper is a part of the copyrighted Journal of the Structural Division, Proceedings of the American Society of Civil Engineers, Vol. 86, No. ST 5, May, 1960.

Page

Analysis of Continuous Trusses by Carry-Over Moments, by Jan J. Tuma. (December, 1959. Prior discussion: None. Discussion closed.)
by Valeriu Petcu 135

Vierendeel Bents with Nonprismatic Members, by S. L. Lee and F. P. Wiesinger. (December, 1959. Prior discussion: None. Discussion closed.)
by Paul Rogers 139

Continuous Girder Bridge with Variable Moment of Inertia, by Sabri Sami. (January, 1960. Discussion: May, 1960. Discussion closes June 1, 1960.)
(Corrections) 145
by Keiichiro Hayashi 145
by Narbey Khachaturian 152

REVIEW OF LIMIT DESIGN FOR STRUCTURAL CONCRETE[a]

Closure by C. W. Yu and Eivind Hognestad

C. W. YU,[1] and EIVIND HOGNESTAD,[2] F. ASCE.—The authors wish to thank all the discussion contributors for the valuable additional information they have presented about limit design of structural concrete.

The three deflection curves produced by Mr. Ernst are most interesting. However, these curves by no means indicate that the deflection of structures designed by limit design need not be checked. Structural engineers often find that even sections worked out by the elastic theory have to be enlarged, not because of strength, but to satisfy deformation requirements.

The definition of a "plastic hinge," as proposed by Mr. Zaslavsky, is more detailed in nature than that of the authors', but cannot be applied in the general sense, since plastic hinges can also exist in structural members other than beams. The two examples quoted by Mr. Zaslavsky to demonstrate the strengthening of sections without lowering the load carrying capacity are very true. However, when a redundant structure of material having a comparatively low ultimate strain is considered, the situation would be different.

The authors fail to agree with Mr. Chan's view that it is unrealistic, in limit design, to seek an approximate elastic moment distribution. It must be remembered that deflection and crack control may often be even more important to satisfactory performance of a structure than ultimate strength. Furthermore, field and laboratory measurements indicate that deformation can be predicted fairly accurately by reasonable elastic assumptions, particularly since the deflection need not be known to an exact figure. An example, in this respect, is the case of the design of slabs by Johansen's yield line theory. The load factor or the l/d ratio will give little indication of the magnitude of deflection. The authors welcome the simplified compromise formula for l_p. It seems far more reasonable that the width of the support of a member is taken into account.

Mr. Mirza has made several points in the authors' paper more explicit. The expression he derived for θ may be more precise, but the difference between its results and those obtained by Eq. 4 is small.

The information given in Mr. Cowan's discussion contributes much to the paper. In answer to his question, in the authors' opinion it will not be economical to use spiral reinforcement in the compression zone of beams. The moment redistribution properites of over-reinforced and under-reinforced sec-

---

[a] December, 1958, by C. W. Yu and Eivind Hognestad.

[1] Dev. Engr., Structural Development Sect. Research and Development Div., Portland Cement Assn., Chicago, Ill.

[2] Mgr., Structural Development Sect., Research and Development Div., Portland Cement Assn., Chicago, Ill.

tions have been discussed in fair detail in the paper, and it does not seem warranted to extend such a discussion in this closure.

The authors consider Mr. Sawyer's discussion extremely valuable because of his explanation of the fundamental principles of limit design that formulated, very clearly, an approach to future development of the subject. The methods developed by Sawyer and Johnson in their paper are very powerful. The authors regret that this knowledge, and the recent papers by Ernst, became available only after the present paper had been completed.

Mr. Hajnal-Konyi has pointed out privately to the authors that in his paper[3] he has shown that moment redistribution in continuous beams only takes place when the load factor against shear failure is greater than that due to bending. He further demonstrated that moment redistribution can occur even when cold worked bars are used.

3 "Moment Redistribution in Continuous Beams Reinforced with Plain and Deformed Bars," by K. Hajnal-Konyi and H. E. Lewis, Symposium on the Strength of Concrete Structures, London, 1956.

BENDING MOMENTS ON SHELL BOUNDARIES[a]

Discussion by Zdeněk Sobotka

ZDENĚK SOBOTKA.[1]—The authors have made an extremely valuable contribution to the practical analysis of bending stresses in the boundary zones of the most important types of shells. Especially, the representation of the bending problem for the hyperbolic paraboloid by the displacement Eqs. 20 has a very great advantage before the solutions involving a stress function for the membrane stresses and displacements for some of the boundary conditions.

The aim of this discussion is to present a more general solution of the displacement equations and of the boundary-bending problem of shells.

Hyperbolic Paraboloid Supported on Four Straight Generatrices.—The displacements u, v, and w may be expressed by the double orthogonal series as follows

$$u = \sum_m \sum_n U_{mn} X_{u,m}(x) Y_{u,n}(y) \quad \ldots\ldots\ldots\ldots \quad (1a)$$

$$v = \sum_m \sum_n V_{mn} X_{v,m}(x) Y_{v,n}(y) \quad \ldots\ldots\ldots\ldots \quad (1b)$$

$$w = \sum_m \sum_n W_{mn} X_{w,m}(x) Y_{w,n}(y) \quad \ldots\ldots\ldots\ldots \quad (1c)$$

and the vertical component of the load is given in quite a similar way by

$$q_w = \sum_m \sum_n Q_{mn} X_{q,m}(x) Y_{q,n}(y) \quad \ldots\ldots\ldots\ldots \quad (2)$$

in which X_{um}, Y_{un}, X_{vm}, Y_{vn}, X_{wm}, Y_{wn} are the appropriately chosen functions satisfying the boundary conditions.

Introducing, similar to the authors Eq. 17, for the membrane energy, U_M, due to the strains $\Sigma_x = u_x$, $\Sigma_y = v_y$, $\gamma = u_x + v_x - \frac{2c}{ab} w$, the following expression

$$\begin{aligned} U_M &= \frac{h}{2} \iint \left(6_x \Sigma_x + 6_y \Sigma_y + \tau\gamma\right) dx\, dy \\ &= \frac{Eh}{2(1-\mu^2)} \iint \Sigma_x^2 + \Sigma_y^2 + 2\mu\, \Sigma_x \Sigma_y + \frac{1-\mu}{2} \gamma^2 \Big) dx\, dy \\ &= \frac{Eh}{2\ 1-\mu^2)} \iint \Big[u_x^2 + v_y^2 + 2\mu\, u_x v_y + \frac{1-\mu}{2} \left(u_y + v_x \right. \\ &\qquad - 2\alpha w\Big)^2 \quad dx\, dy, \quad \ldots\ldots\ldots\ldots\ldots \quad (3) \end{aligned}$$

---

[a] October, 1959, by H. H. Bleich and M. G. Salvadori.

[1] Docent of Theory of Elasticity and Strength of Materials, Prague, Czechoslovakia.

in which $\alpha = \frac{c}{ab}$. For the bending energy we may introduce the authors' Eq. 18 and for the potential energy of the load Eq. 19. Thus, we may obtain, for the displacements, the following variational equations.

$$\iint \left[u_{xx} + \mu v_{xy} + \frac{1-\mu}{2}\left(u_{yy} + v_{xy} - 2\alpha w_y\right) - \frac{\left(1-\mu^2\right)q_u}{Eh} \right] \delta u \, dx \, dy = 0 \quad \ldots \quad (4a)$$

$$\iint \left[v_{yy} + \mu u_{xy} + \frac{1-\mu}{2}\left(u_{xy} + v_{xx} - 2\alpha w_x\right) - \frac{\left(1-\mu^2\right)q_v}{Eh} \right] \delta v \, dx \, dy = 0 \quad \ldots \quad (4b)$$

$$\iint \left[\nabla_w^4 - \frac{12(1-\mu)\alpha}{h^2}\left(u_y + v_x - 2\alpha w\right) - \frac{12\left(1-\mu^2\right) q_w}{Eh^3} \right] \delta w \, dx \, dy = 0 \quad \ldots \quad (4c)$$

in which, according to the relationships of Eq. 1, the variations may be written in the form of

$$\delta u = X_{u1} \, Y_{u1} \, \delta U_{11} \quad \ldots \quad (5a)$$

$$\delta v = X_{v1} \, Y_{v1} \, \delta V_{11} \quad \ldots \quad (5b)$$

$$\delta w = X_{w1} \, Y_{w1} \, \delta W_{11} \quad \ldots \quad (5c)$$

Letting $q_u = q_v = 0$, and using, from the series given by Eqs. 1, the first terms only and substituting them with Eqs. 2 and 5 into Eqs. 6, we get after integration the following system of the three linear equations

$$U_{11} \, I_1 + V_{11} \, I_2 + W_{11} \, I_3 = 0 \quad \ldots \quad (6a)$$

$$U_{11} \, I_4 + V_{11} \, I_5 + W_{11} \, I_6 = 0 \quad \ldots \quad (6b)$$

$$U_{11} \, I_7 + V_{11} \, I_8 + W_{11} \, I_9 = Q_{11} \, I_{10} \quad \ldots \quad (6c)$$

for the three unknown coefficients U_{11}, V_{11}, W_{11}, in which

$$I_1 = \iint X_u \, Y_u \, X_u'' \, Y_u + \frac{1-\mu}{2} X_u \, Y_u'' \, dx \, dy, \quad \ldots \quad (7a)$$

$$I_2 = \frac{1+\mu}{2} \iint X_u \, Y_u \, X_v' \, Y_v' \, dx \, dy, \quad \ldots \quad (7b)$$

$$I_3 = -(1-\mu)\,\alpha \iint X_u \, Y_u \, X_w \, Y_w' \, dx \, dy, \quad \ldots \quad (7c)$$

$$I_4 = \frac{1+\mu}{2} \iint X_v \, Y_v \, X_u' \, Y_u' \, dx \, dy, \quad \ldots \quad (7d)$$

$$I_5 = \iint X_v \, Y_v \left(X_v \, Y_v'' + \frac{1-\mu}{2} X_v'' \, Y_v \right) dx \, dy, \quad \ldots \quad (7e)$$

$$I_6 = -(1-\mu)\,\alpha \iint X_v \, Y_v \, X_w' \, Y_w \, dx \, dy, \quad \ldots \quad (7f)$$

$$I_7 = -\frac{12(1-\mu)\alpha}{h^2} \iint X_w \, Y_w \, X_u \, Y_u' \, dx \, dy, \quad \ldots \quad (7g)$$

$$I_8 = -\frac{12(1-\mu)\alpha}{h^2} \iint X_w\, Y_w\, X_v'\, Y_v\, dx\, dy, \quad \ldots\ldots\ldots (7h)$$

$$I_9 = \iint X_w\, Y_w \left[X_w^{IV}\, Y_w + 2\, X_w''\, Y_w'' + X_w\, Y_w^{IV} + \frac{24\,(1-\mu)\,\alpha}{h^2}\, X_w\, Y_w \right] dx\, dy, \quad \ldots\ldots\ldots\ldots (7i)$$

$$I_{10} = \frac{12(1-\mu^2)}{Eh^3} \iint X_q\, Y_q\, X_w\, Y_w\, dx\, dy \quad \ldots\ldots\ldots\ldots (7j)$$

From Eqs. 6 the unknown coefficients may be computed as follows

$$U_{11} = \frac{(I_2\, I_6 - I_3\, I_5)\, I_{10}\, Q_{11}}{D}, \quad \ldots\ldots\ldots\ldots (8a)$$

$$V_{11} = \frac{(I_3\, I_4 - I_1\, I_6)\, I_{10}\, Q_{11}}{D}, \quad \ldots\ldots\ldots\ldots (8b)$$

$$W_{11} = \frac{(I_1\, I_5 - I_2\, I_4)\, I_{10}\, Q_{11}}{D}, \quad \ldots\ldots\ldots\ldots (8c)$$

in which

$$D = I_1\, I_5\, I_9 + I_2\, I_6\, I_7 + I_3\, I_4\, I_8 - I_3\, I_5\, I_7 - I_1\, I_6\, I_8 - I_2\, I_4\, I_9 \quad \ldots\ldots (9)$$

is the determinant of the system.

The preceding general solution may be applied for hyperbolic paraboloids supported on four straight generatrices with different boundary conditions.

In the case of the shell with built-in edges, the boundary conditions $u = v = 0$ are satisfied by the functions

$$u = U_{11} \sin\frac{\pi x}{a} \sin\frac{\pi y}{b}, \quad \ldots\ldots\ldots\ldots (10)$$

$$v = V_{11} \sin\frac{\pi x}{a} \sin\frac{\pi y}{b}, \quad \ldots\ldots\ldots\ldots (11)$$

whereas for the vertical displacement, the function

$$w = W_{11} \left[\cos\frac{\pi x}{2a} \cos\frac{\pi y}{2b} - k\left(a^2 - x^2\right)\left(b^2 - y^2\right) \right], \quad \ldots\ldots (12)$$

in which

$$k = \frac{\pi}{3a^2\, b^2\, \sqrt{2}}, \quad \ldots\ldots\ldots\ldots (13)$$

satisfies the condition $w = 0$ along all boundaries, the condition $\frac{\partial w}{\partial x} = 0$ in the points with the coordinates $x = \pm a$, $y = \pm \frac{b}{2}$ and the condition $\frac{\partial w}{\partial y} = 0$ in the four other points with the coordinates $x = \pm \frac{a}{2}$, $y = \pm b$.

The uniform load may be expressed approximately by

$$q = Q_{11} \cos \frac{\pi x}{2a} \cos \frac{\pi y}{2b}, \quad \ldots\ldots\ldots\ldots\ldots (14)$$

in which the value of Q_{11} will be determined by the usual manner used for computing the coefficients of Fourier series as follows:

$$Q_{11} = \frac{4 \int_o^a \int_o^b q \cos \frac{\pi x}{2a} \cos \frac{\pi y}{2b} \, dx \, dy}{4 \int_o^a \int_o^b \cos^2 \frac{\pi x}{2a} \cos^2 \frac{\pi y}{2b} \, dy \, dy} = \frac{16 \, q}{\pi^2} \quad \ldots\ldots\ldots (15)$$

Eqs. 7(a) to (c) give for $X_u = X_v = \sin \frac{\pi x}{a}$, $Y_u = Y_v = \sin \frac{\pi y}{b}$, $X_w \, Y_w = \cos \frac{\pi x}{2a} \cos \frac{\pi y}{2b} - k\left(a^2 - x^2\right)\left(y^2 - b^2\right)$, $X_q = \cos \frac{\pi x}{2a}$, and $Y_q = \cos \frac{\pi y}{2b}$ the following values:

$$I_1 = -\frac{\pi^2 \, b}{a} - \frac{(1 - \mu) \, \pi^2 \, a}{2b}, \quad \ldots\ldots\ldots\ldots\ldots\ldots (16)$$

$$I_2 = I_4 = \frac{1 - \mu}{2} \pi^2, \quad \ldots\ldots\ldots\ldots\ldots\ldots\ldots\ldots (17)$$

$$I_3 = \frac{32 \, (1 - \mu) \, \alpha \, a}{9\pi} - \frac{8 \, (1 - \mu) \, \alpha \, k \, a^3 \, b^2}{\pi^4}\left(\pi^2 + 4\right), \quad \ldots\ldots (18)$$

$$I_5 = -\frac{\pi^2 \, a}{b} - \frac{(1 - \mu) \, \pi^2 \, b}{2a}, \quad \ldots\ldots\ldots\ldots\ldots\ldots (19)$$

$$I_6 = \frac{32 \, (1 - \mu) \, \alpha \, b}{9\pi} - \frac{8 \, (1 - \mu) \, \alpha \, k \, a^2 \, b^3}{\pi^4}\left(\pi^2 + 4\right), \quad \ldots\ldots (20)$$

and so forth.

Substituting the preceding values into the Eqs. 8(a-c) to 10, 11, and 12, we get the displacements u, v, and w.

Then, the bending moments of the shallow shell are given by the formulas that are quite analogous to those which are valid for the plates as follows

$$M_x = \frac{Eh^3}{12\left(1 - \mu^2\right)}\left(\frac{\gamma^2 w}{\gamma x^2} + \mu \frac{\gamma^2 w}{\gamma y^2}\right)$$

$$= \frac{Eh^3 \, W_{11}}{12\left(1 - \mu^2\right)}\left\{\frac{\pi \sqrt{2}}{3 \, a^2 \, b^2}\left[b^2 - y^2 + \mu\left(a^2 - x^2\right)\right]\right.$$

$$\left. - \frac{\pi^2}{4}\left(\frac{1}{a^2} + \frac{\mu}{b^2}\right) \cos \frac{\pi x}{2a} \cos \frac{\pi y}{2b}\right\}, \quad \ldots\ldots\ldots\ldots (21)$$

and,

$$M_y = \frac{Eh^3}{12\left(1 - \mu^2\right)} \left(\frac{\gamma^2 w}{\gamma y^2} + \mu \frac{\gamma^2 w}{\gamma x^2} \right)$$

$$= \frac{Eh^3 W_{11}}{12\left(1 - \mu^2\right)} \left\{ \frac{\pi \sqrt{2}}{3 a^2 b^2} \left[a^2 - x^2 + \mu\left(b^2 - y^2\right) \right] \right.$$

$$\left. - \frac{\pi^2}{4} \left(\frac{1}{b^2} + \frac{\mu}{a^2} \right) \cos \frac{\pi x}{2a} \cos \frac{\pi y}{2b} \right\} \quad \ldots\ldots\ldots\ldots\ldots\ldots (22)$$

ULTIMATE LOAD THEORY FOR CONCRETE FRAME ANALYSIS[a]

Discussion by Bruno Barbarito and Guiliano Augusti

BRUNO BARBARITO,[1] and GIULIANO AUGUSTI.[2]—The aims of the writers are (a) to indicate some interesting test results, recently obtained in the laboratory of the Strength of Materials Institute at the University of Naples, and (b) to compare the applicability, to concrete structures, of Baker's ultimate load theory and of the (n+1) plastic hinge theory, used throughout the world in limit analysis of steel structures.

In several tests[3,4] the limit behavior of the reinforced concrete members shown in Fig. 1 was determined, under eccentric thrust or simple flexion. Two groups of tests (referred to in the following as Series No. 1 and No. 2) were carried out on members reinforced as indicated in Fig. 1, the third group (referred to as Series No. 3) on members without reinforcement. Strengths of the used materials, in pounds per square feet, are in Table 1.

The assumed ultimate stress distribution for reinforced section is indicated[5] in Fig. 2(a). The yield profiles M-N (moment-load) were computed setting $\sigma_{oc} = c_u$ and $\sigma_{os} = t_y$, and are indicated with solid lines in Fig. 3(a) and 3(b).

In Figs. 3(a) and 3(b) are also plotted the experimental points, each of which is the average of four tests. For eccentric thrust a plot is made of each value of $e = M/N$. In this case the rupture and the primary failure of concrete (both by crushing or by cracking) practically coincided. In simply flexion tests ($N = 0$) wide cracks of concrete began in the points marked by a circle, but collapse occurred for rupture of tensile reinforcement only at points indicated with a square. (These latter points agree with stress distribution of Fig. 2(a), setting $\sigma_{oc} = c_u$ and $\sigma_{os} = t_R$.)

It may be seen from Figs. 3(a) and (3b) that theoretical and experimental profiles M-N are in very good agreement. To assume that Fig. 2(a) indicates the ultimate stress distribution was satisfactorily confirmed. It is also seen that cracks will occur outside the computed profiles due to large reinforcement deformations beyond yield point.

For members without reinforcement, the ultimate stress distributions shown in Fig. 2(b) was assumed (large eccentricities) and Fig. 2(c) (little

---

[a] November, 1959, by A. L. L. Baker.

[1] Dr. Engr., Asst. of Strength of Materials.

[2] Dr. Engr., Asst. of Bridge Constructions, Univ. of Naples, Naples, Italy.

[3] "La rottura delle sezioni presso inflesse in cemento armato," by A. Raithel and B. Barbarito, Giorn. Genio Civ., N. 6, 1959.

[4] "La rottura delle sezioni pressoinflesse in conglomerato non armato," by B. Barbarito, Giorn. Genio Civ. Publication pending.

[5] Sul calcolo a rottura delle strutture in conglomerato armato. "L'industria italiana del cemento," by V. Franciosi, No. 4, 1954.

eccentricities). The value of σ_{of} (flexion tensile strength) and σ'_{oc} (prism strength) were directly obtained by testing members, identical to the other ones, in simple compression and flexion. The profile M-N of Fig. 3(c), computed according to Figs. 2(b) and 2(c), appears to be the most agreeable to the experimental points (Fig. 3c).

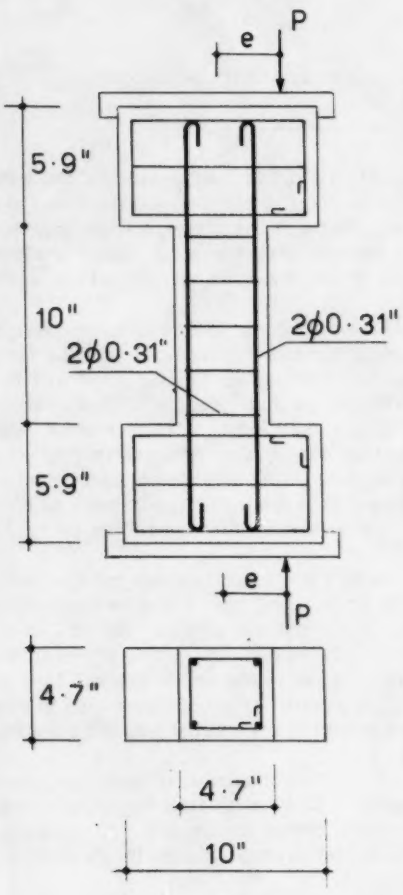

FIG. 1.—REINFORCED CONCRETE MEMBER

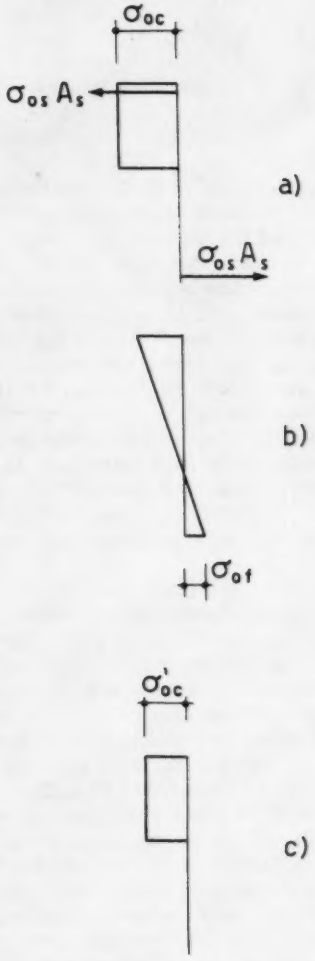

FIG. 2.—STRESS DISTRIBUTION

In the reinforced members the concrete actual strength was equal to the cubic strength c_u, while in non-reinforced members it was only 2,850 psi, or a value of 65 c_u.

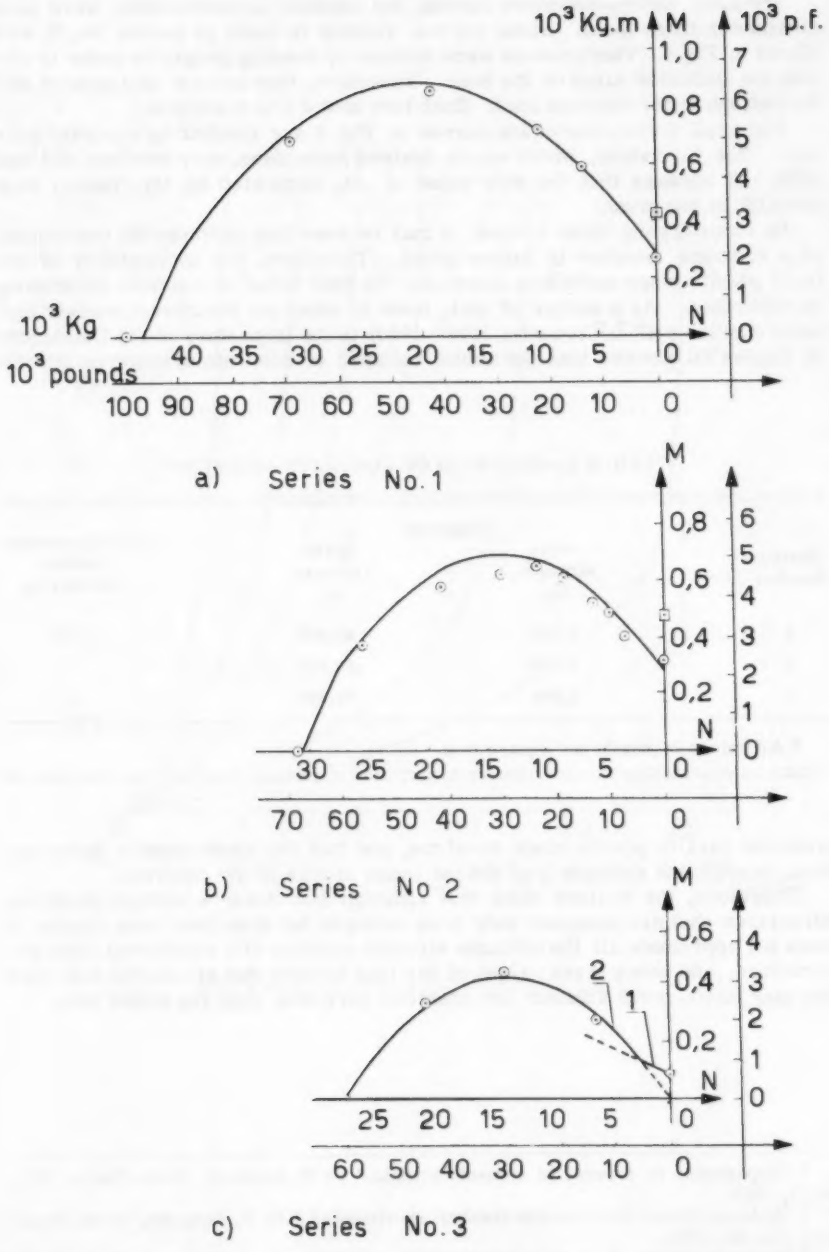

FIG. 3.—YIELD PROFILES

The axial force—curvature curves, for constant eccentricities, were also obtained in these tests. Some curves, related to tests of series No. 2, are shown in Fig. 4. (These curves were derived by reading gauges in order to obtain the indicated value of the load. Therefore, they are not inclusive of deformations under constant load. Each test lasted 3 to 4 minutes.)

The axial force—curvature curves in Fig. 4 are limited by concrete failure. The Σ_u values, which can be derived from them, vary between .004 and .008. It appears that the safe value of .01, suggested by Mr. Baker, may actually be too great.

By investigating these curves, it may be seen that permissible curvatures of a concrete member is rather great. Therefore, the applicability of the (n+1) plastic hinge method to determine the load factor of concrete structures is confirmed. As a matter of fact, tests of concrete structural models that were carried out[6,7,8] recently (1954-1959) in the laboratory of the University of Naples all showed that the actual collapse of concrete structures occurs

TABLE 1.—STRENGTH OF CONCRETE MEMBERS[a]

Series Number	Concrete cubic strength, C_u	yield stress, t_y	Reinforcement rupture stress, t_R
1	4,000	45,500	4400
2	2,700	45,500	—
3	4,400	62,500	—

[a] All valves in pounds per square inch.

when the (n+1)th plastic hinge develops, and that the elasti-plastic deformations beneath the collapse load did not cause cracks of the concrete.

Therefore, the writers think that although Mr. Baker's method produces structures that are safe, not only from collapse but also from wide cracks, it does not appreciate all the ultimate strength sources of a reinforced concrete structure, and hence gives values of the load factors that are on the safe side but may be too much smaller, for practical purposes, than the actual ones.

6 "Esperienze su travetti in cemento armato," by T. Renzulli, Giorn. Genio Civ., No. 2, 1957.

7 "In tema di calcolo a rottura: risultati sperimentali," by V. Sorgente, Giorn. Genio Civ., No. 12, 1957.

8 "Prova a rottura di un arco incastrato in conglomerato armato," by T. Renzulli, Giorn. Genio Civ., No. 10, 1959.

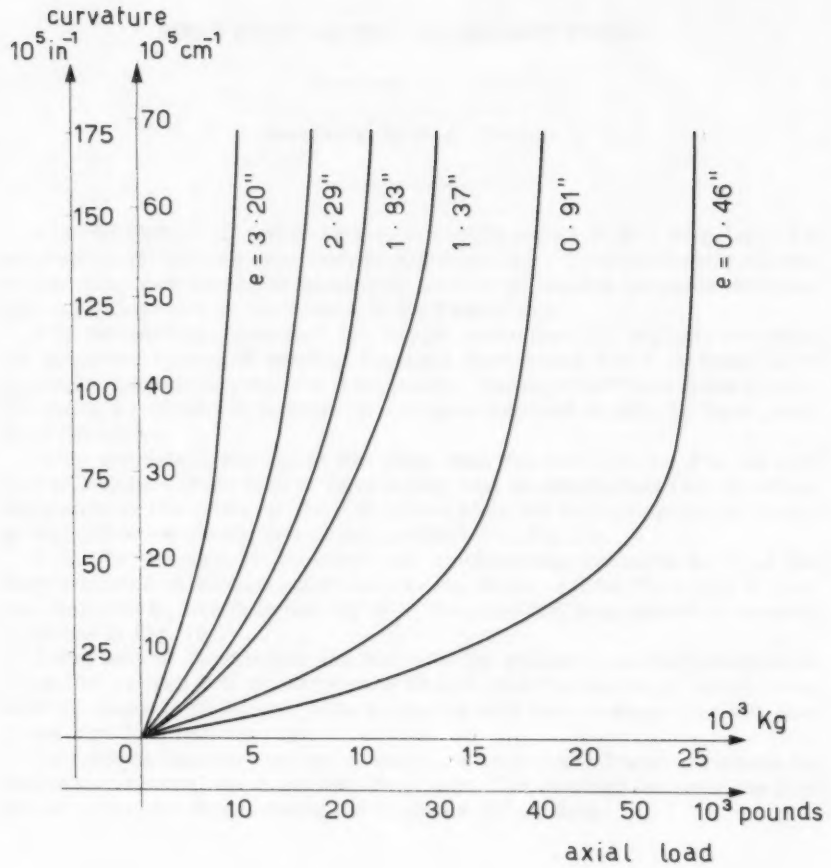

FIG. 4.—AXIAL FORCE-CURVATURE CURVES

FIXED POINT METHOD OF MOMENT DESIGN[a]

Discussion by A. A. Eremin

A. A. EREMIN,[1] M. ASCE.—It was correctly stated by Mr. Huey that "The academic solutions are often tedious and difficult." To avoid lengthy computations Mr. Huey developed simplified method of bending moments distribution in rigid frames by application of the fixed points.

It is interesting to note that Mr. Ritter, more than 100 yrs ago, developed the graphical method of bending moments distribution which is based on the graphical construction with the fixed points. Lately, (1960) numerous graphical and semi-graphical methods of moments distribution with the fixed points were developed.

In the restrained-end beams Mr. Huey used two fixed points. For the rigid frame members three sets of fixed points may be established that the writer designated in the order of their distances from the midspan point by central points, inflection points, and elastic points,[2,3] in Fig. 10.

With the purpose of checking and emphasizing, the advantages of Mr. Huey's method of moments distribution, the writer solved the author's illustrating problem, shown in his Fig. 8 by the graphical distribution of moments as shown in Fig. 10.

Three sets of fixed points are tied with the graphic construction known as three line polygon. It is interesting to note that the maximum error in the bending moments in Fig. 10, when compared with those computed by Mr. Huey in his Fig. 8, is less than 3%.

This shows that the concept of fixed points in rigid frame members has important practical value and Mr. Huey should be credited for using the fixed points in his new simple method of moments distribution.

---

[a] November, 1959, by S. E. Huey.

[1] Assoc. Bridge Engr., Bridge Dept., Calif. State Highway Div.

[2] "Simplified Graphical Distribution of Bending Moments," by A. A. Eremin, 1948, publication by the author.

[3] Discussion of "Arches and Bents," Transactions, ASCE, 1950, p. 630.

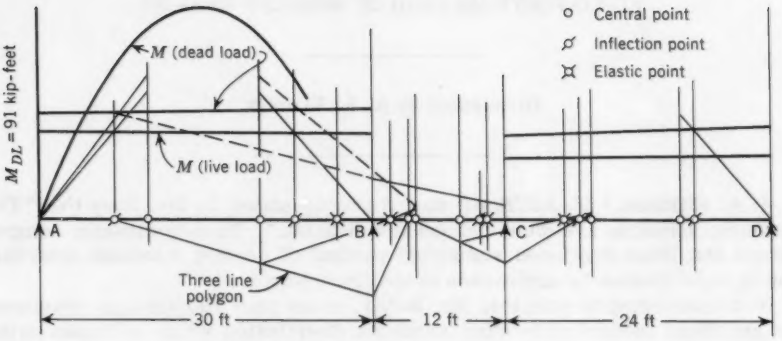
Central point
Inflection point
Elastic point
M (dead load)
M (live load)
M_{DL} = 91 kip-feet
A
B
C
D
Three line polygon
30 ft
12 ft
24 ft

FIG. 10

DESIGN OF PRESTRESSED COMPOSITE STEEL STRUCTURES[a]

Discussion by Sven H. Wichman

SVEN H. WICHMAN,[1] M. ASCE.—Mr. Szilard has presented a very interesting and comprehensive paper on prestressed composite structures. Such structures combine the advantages as well as complexities inherent in both prestressed and composite construction. But complexities and controversial points can be considered as well as assets, since they stimulate discussion and research with the result that even data unfavorable to the complex original idea will be useful for the perfection of simpler systems.

In this discussion, comments are limited to only three of the many complex problems associated with prestressed composite structures.

Creep of Concrete.—A collection and thorough evaluation of scattered creep data is long due, but a problem as complex as creep would be difficult to handle in a paper dealing with prestressed composite structures. At least six variables in creep phenomenon can be listed: 1) water - cement ratio, 2) cement - aggregate ratio, 3) type, gradation and distribution of aggregate, 4) amount and type of curing, 5) age when permanent loading started, and 6) climatic conditions of locality, such as, average relative humidity, characteristics of cyclic variations of relative humidity, and average temperature.

Development of creep theory as a function of relative humidity is noteworthy, and it would be complete if it can be proven that the other variable can be neglected. Due to the absence of such information, it seems that the advantages of prestressed composite construction would become more obvious when presented on the basis of current American Assoc. of State Highway Officials, AASHO specification requirements.

Thermal Stresses.—Thermal stresses in composite structures can be traced back to three distinctly different origins, although the effects and mode of calculation are essentially similar.

The expansion coefficient of steel is well established, but the available concrete expansion coefficients vary to such an extent as to make any refined calculations almost meaningless. Practically the only way to determine the coefficient, while the structure is in the design stage, is to investigate the aggregate likely to be used for the concrete, or to specify one particular aggregate since, of the numerous variables, the expansion coefficient of aggregate affects the final coefficient most.

A compilation of rock expansion coefficient data would be very helpful in this respect. Rock classification in such data should be based on mineral content or possibly specific gravity, rather than on popular designations. Equations for computing differential expansion stresses have been developed[2] by R. David.

---

[a] November, 1959, by Rudolph Szilard.

[1] Structural Engr., Brookhaven Natl. Lab., Upton, L.I., N.Y.

[2] Discussion of "Application of AASHO Specifications to Bridge Design," by Robert David, Proceedings, ASCE, Vol. 84, No. ST 1, January, 1958, pp. 84-92.

Typically, a concrete bridge slab is directly exposed to the rays of the sun, while steel girders are in the shade. This condition has been treated by Mr. Szilard for the purpose of finding the loss of prestress. Further development of the formulas into readily applicable form would be helpful to the designers.

Differential strains due to unequal time rates of heat absorption and heat dissipation (or due to unequal diffusivity coefficients) are caused by rapid atmospheric temperature changes. Temperature drops of 35°F within five min and rises of 40°F in less than ten min have been recorded.[3]

If the rate of temperature change is a function of time, the heat transfer condition is termed "unsteady state." This state involves a complicated combination of heat conductivity, specific heat and physical properties of the material and its surroundings, and as such does not lend itself to accurate and simple analytical solutions.

For the purpose of comparison, it is sufficient to compare thermal diffusivity coefficients of steel and concrete. This coefficient is defined as thermal conductivity, divided by the product of density and specific heat. Its value for steel is about twenty-five times greater than that of concrete, which very roughly means that heat will penetrate a unit thickness of steel twenty-five times faster than a unit thickness of concrete.

There is hardly any question that structural steel members can quickly react to the oddest temperature changes Nature can supply. As for concrete, there definitely is a time lag present, and, consequently, stresses are induced in between steel and concrete. Only experimental proof can establish the correct quantitative basis of such stresses. Consideration of these stresses may be termed as undue refinement, but not before definite evidence is available that there is no connection between brittle failures and rapid temperature changes. As long as definite data is not available, it may be entirely reasonable to add some 20°F to the normal AASHO design temperature variations ranges of 120°F to 150°F.

Flexibility.—As pointed out by the author, it is not advisable to strive for too shallow prestressed girders of the proposed type. This, of course, is due to the fact that a prestressed girder can carry more load than a conventional girder of the same cross section, prestressing forces being arranged so that the resulting stresses are opposite to those caused by applied loads. As loads increase, so do deflections. Dead load deflections are reduced by upward deflection caused by prestressing, which is just another form of camber. Live load deflections, however, are hardly affected by the prestressing mechanism, since the cross sectional area and distribution of mass still control stiffness of the girder.

A small increase in the depth of girders is not objectionable in river crossings and in many grade separation structures. However, for the Interstate Highway System, the headroom requirements are on the upturn, and may soon be 16 ft instead of the present 14 ft. For bridges in this category, even a few inches of reduced girder depth can make the necessary cost increases more tolerable.

Furthermore, it is likely that the AASHO limiting live load deflection-span ratio of 1/800 will be reduced to 1/1000 for composite bridges. A recommendation on this effect has been made[4] by the Committee on Deflection Limita-

---

3 "Climatic Atlas of the United States," by Stephan S. Visher, 1954, pp. 153-154.

4 "Deflection Limitation on Bridges," by Committee on Deflection Limitation, of Bridges of the Structural Div., Proceedings, ASCE, Vol. 84, No. ST 3, May, 1958.

tion of Bridges of the Structural Division, (American Society of Civil Engineers). This recommendation is based on findings that composite bridges actually deflect relatively close to the computed values, whereas bridges designed without composite action actually exhibit a considerable degree of such action.

The prospects of increased bridge clearance and more stringent composite girder deflection requirements indicate that there is a need for bridge girders that can carry more loads, are shallower and yet not excessively flexible, and are available within present cost ranges.

It is hard to meet the combined headroom—flexibility—economy requirements with girders prestressed by cables. The super-high strength strands, probably the most expensive structural carbon steels available, are a total loss as far as stiffness of a small bridge is concerned.

A larger, solid steel prestressing element, rigidly connected to the bottom flange of the girder, will substantially increase the sectional properties of the composite girder. Of the various shapes, round, square and flat, only the flat prestressing element is readily adaptable to composite structures. And of various fastening methods, welding apparently produces the most complete integration of the girder and the plate.

Proper material of the plate emerges from several conditions. First, weldability has to be well proven, and secondly, allowable strength must be higher than that of the girder, but for economy the excess should be limited to the amount of stress induced by prestressing, that in turn is limited by lateral stability of the girder during fabrication and transportation. High strength low alloy steels (ASTM A242) of low carbon content meet these requirements. A composite girder, prestressed with such a plate, can be dimensioned so that balanced design requirements are rather closely met.

It is practicable to prestress and weld such a beam only in the shop. Thus the concrete slab is not prestressed and does not have to be of higher strength. There may be a conflict of nomenclature since such a girder more properly may be called a "prestressed steel girder in composite action with concrete slab."

Prestress can be applied by mechanical or thermal means. Thermal prestressing appears to be simpler and faster. It is necessary to heat the plate to temperatures not more than 100°F above the girder temperature. Heat does not necessarily have to be applied uniformly. The procedure requires some well planned coordination, but it can be developed into a routine operation, costing hardly more than the welding of conventional cover plates, especially when numerous nearly equal units are involved.

In closing, the writer wishes to stress that the foregoing comments are in no way intended to detract from the originality of Mr. Szilard's conception of prestressed composite structural system. It is hoped that the thoughts expressed herein will encourage new discussions and lead to the improvement of this potentially useful method.

LESSONS OF COLLAPSE OF VANCOUVER 2ND NARROWS BRIDGE[a]

Discussion by Kuang-Han Chu

KUANG-HAN CHU,[1] F. ASCE.—Mr. Hrennikoff has made a valuable contribution in his study of the causes of the collapse of the Vancouver Narrows Bridge, Vancouver, B.C. The writer, however, can not agree with the author in the use of American Assoc. of State Highway Officials formula for pin end columns, $f = 15000 - \frac{1}{3}\left(\frac{l}{r}\right)^2$ in evaluating the buckling strength of the web of 36 in. WF section. The above formula was based on the Final Report of ASCE Committee of Steel Column Research.[2]

In the derivation of this formula, a reduced length of 85% of the full length was assumed. Therefore, for an ideally simply supported column, the formula should be $f = 15000 - \frac{1}{3}\left(\frac{l}{0.85r}\right)^2$. Applying this to the example shown in the paper, with $l/r = 85.5$, the allowable stress with 33% increase should be 15.5 ksi instead of 16.8 ksi. This value of 15.5 ksi corresponds to factors of safety of 1.14 and 1.17, respectively, with respect to the test values of 17.73 ksi and 18.23 ksi. These factors of safety are for erection stresses. For normal loading, they correspond to factors of safety of 1.52 and 1.56, respectively. These values, although about 15% lower than the specified value of 1.76 (referring to steel with minimum yield of 33,000 psi), seem to be adequate.

---

[a] December, 1959, by A. Hrennikoff.
[1] Assoc. Prof., Civ. Engrg., Dept., Ill. Inst. of Tech., Chicago, Ill.
[2] Transactions, Vol. 98, 1933, pp. 1457-58.

CUT-OFF POINTS FOR COVER PLATES[a]

Discussion by Nabi Taskinoglu

NABI TASKINOGLU,[1] A.M. ASCE.—The author's method of finding cover plate lengths is easy and practical but applicable only for simple beam spans.

By making (Parabolic Interpolation) a very accurate result can be obtained and continuous beam spans can be included in this method. The example given in the paper will be taken and this method will be shown numerically.

Plate length will be estimated as:

$$.666 \times 67.08 = 44.72 \text{ ft}$$

This point is 11.18 feet from the support. Dead load and live load moments can be calculated in a short time. These moments are:

$$M^{S}_{DL} = 287 \text{ ft-kips}$$

$$M^{C}_{DL} = 57.8 \text{ ft-kips}$$

$$M_{LL} = 522 \text{ ft-kips}$$

Fiber stresses will be found by using the same section properties. Total of these stresses are found as:

$$fsi = 17.067 \text{ kips/sq. in.}$$

which is more than permissible stress and plate length should be longer. Now curve "C" can be assumed a parabola passing from this point. By using the same notation as X = distance from centerline of span to theoretical cut-off point, this relation can be written:

$$\left(\frac{X}{\frac{44.72}{2}}\right)^2 = \left(\frac{29.5 - 13.5}{29.5 - 17.067}\right)^2$$

From this equation, X can be found as:

$$X = 25.35 \text{ ft}$$

and length of cover plate is determined as:

---

[a] December, 1959, by Nat T. Kanarek.

[1] Structural Engr., Ellerbe and Co., St. Paul, Minn.

$$2 \times 25.35 = 50.7 \text{ ft}$$

This shows that calculated length of cover plate is accurate enough and can easily be generalized for continuous beam spans.

The procedure in continuous beam spans is slightly different. After finding the maximum total-stress location, two points (one at each side of maximum stress point and approximately 20% of span length distance to each point) should be chosen and maximum stresses should be calculated without cover plate section properties.

Then by the same assumption, it can be said that a skew parabola is the envelope of maximum total stresses without cover plates where these three points are on this curve.

By using skew parabola properties, we can find a quadratic equation for each point. Solution of these equations can be accepted as final solution without further tedious calculations.

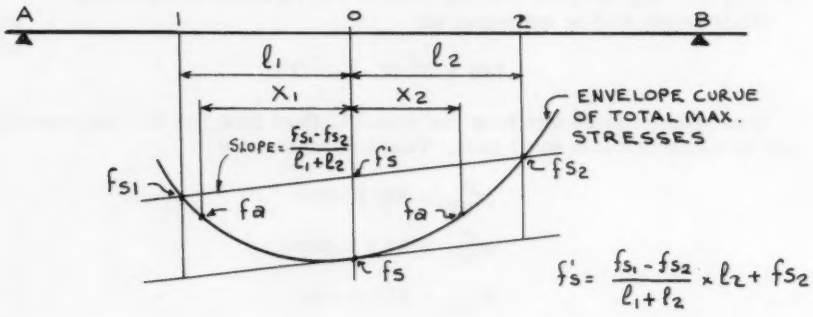

FIG. 1

In Fig. 1 A-B is a span of a continuous beam. From this figure, after finding stresses at points (0), (1) and (2), equations can be written as

$$f_2 = f_s + \frac{f_{s_1} - f_{s_2}}{l_1 + l_2} X_1 - \left(\frac{X_1}{l_1}\right)^2 \left(f_s - f'_s\right) \ldots\ldots\ldots \quad (1)$$

$$f_2 = f_s = \frac{f_{s_1} - f_{s_2}}{l_1 + l_2} X_2 - \left(\frac{X_2}{l_2}\right)^2 \left(f_s - f'_s\right) \ldots\ldots\ldots \quad (2)$$

in which f_s is the maximum total stress of the span without cover plate, f_{s_1} indicates the total stress at point 1, and f_{s_2} is the total stress at point 2, and f_s refers to the allowable fiber stress. x_1 and x_2, that are the distances to be found to theoretical cut-off point 0, can then be found.

By using influence line tables, stresses at points 1 and 2 can be found in a short time and, without further trial, cut-off points can be determined.

ANALYSIS OF CONTINUOUS TRUSSES BY CARRY-OVER MOMENTS[a]

Discussion by Valeriu Petcu

VALERIU PETCU.[1]—In his interesting paper, Mr. Tuma uses the method of successive approximations. He neglects, however, the convergence of the system of equations. It appears there is a need to examine this problem.

Wittmeyer's criterion of convergence,[2] applied in the case studied, furnishes the inequality

$$| r_{ij} | + | r_{kj} | < 1 \quad \ldots\ldots\ldots\ldots\ldots\ldots \quad (1)$$

To verify whether or not the condition of Eq. 1 is fulfilled, we shall refer to the example of Fig. 10 and Table 1 of the paper.

From the columns 5, 6 and 7, of Table 1, it is seen that if all the top and bottom members are of infinite stiffness, the remainder of the bars being elastic, the maximum value of the carry-over factors results.

$$r_{12} = r_{21} = +.500$$

whereas; if the top bars, 3 and 4, are elastic, all others being of infinite stiffness, the minimum value of the carry-over factors is obtained.

$$r_{12} = r_{21} = -.500$$

From these results it is seen that carry-over factors vary between

$$-.500 < r < +.500$$

That is, the system of equations in the paper verifies the condition of convergence (Eq. 1). Contrary to continuous beams, whose carry-over factors are always negative, continuous trusses may have either positive or negative carry-over factors, according to the ratio between the stiffness of top and bottom members and the stiffness of web members. This peculiarity allows one to conclude that cases exist in which $r = 0$. This indicates that cases may arise when the unknowns of the equations in the system can reduce to only two, or even a single unknown instead of three.

In the example to which reference is made, if one considers the section of top and bottom members to be 5.6 times that of the web members, then

---

[a] December, 1959, by Jan J. Tuma.

[1] Research Engr., Structural Analysis Dept., Bldg. Research Inst., Bucharest, Rumania.

[2] "Über die Lösung von linearen Gleichungssystemen durch Iteration," by H. Wittmeyer, Zeitschrift für Angewandte Mathematik und Mechanik, No. 5, 1936.

$r_{12} = r_{21} = 0$, and the system will consist of two equations, each having only one unknown.

Since, for current cases, the top and bottom members have larger sections than the web members, without attaining such ratios as to eliminate the carry-over factors, the carry-over factors generally have negative values and the system of equations is very rapidly convergent.

As is known, the method of successive approximations generally does not allow one to obtain a solution with free terms appearing literally. Solving the system of equations requires free terms to be expressed numerically. It is for this reason that each loading case must be separately investigated, or influence lines can be traced for the support moments. Both cases imply a great amount of computations. However, for the largest number of cases, continuous trusses have uniform spans and support conditions, with eventual exceptions at the end spans.

The system of equations corresponding to these conditions can be written as

$$\left.\begin{aligned}
\gamma' X_1 + X_2 + K_1 &= 0 \\
X_1 + \gamma X_2 + X_3 + K_2 &= 0 \\
X_2 + \gamma X_3 + X_4 + K_3 &= 0 \\
\cdots\cdots\cdots\cdots\cdots\cdots & \\
X_{n-2} + \gamma X_{n-1} + X_n + K_{n-1} &= 0 \\
X_{n-1} + \gamma'' X_n + K_n &= 0
\end{aligned}\right\} \quad \cdots\cdots\cdots\cdots (2)$$

in which X_i is the unknown and K_i indicates the free terms.

In a previous paper[3] the writer has proven the solution of this system to be

$$X_j = \frac{A''_{n-j} \sum_{i=1}^{j-1} (-1)^{j-i} A_{i-1} K_i + A'_{j-1} \sum_{i=j}^{n} (-1)^{i-j} A''_{n-i} K_i}{\overline{D}_n} \quad \cdots\cdots (3)$$

in which

$$A'_n = D_n + \delta' . D_{n-1} \quad \cdots\cdots\cdots\cdots\cdots\cdots (4a)$$

$$A''_n = D_n + \delta'' . D_{n-1} \quad \cdots\cdots\cdots\cdots\cdots\cdots (4b)$$

$$D_n = \gamma D_{n-1} - D_{n-2} \quad \cdots\cdots\cdots\cdots\cdots\cdots (4c)$$

$$\overline{D}_n = A'_n + \delta'' . A'_{n-1} = A''_n + \delta' . A''_{n-1} \quad \cdots\cdots\cdots\cdots (4d)$$

$$\delta' = \gamma' - \gamma \quad \cdots\cdots\cdots\cdots\cdots\cdots (4e)$$

$$\delta'' = \gamma'' - \gamma \quad \cdots\cdots\cdots\cdots\cdots\cdots (4f)$$

---

3 "On the Solution of the Elastic Equilibrium Equations with Matrices of Jacobi Type," (in Rumanian) by Valeriu Petcu, Studii si Cercetări de Mecanică Aplicată, Bucharest, X, No. 3, 1959, pp. 855-865.

It is to be noted that all numerical coefficients in the general Eq. 3 may be obtained by simple recurrent formulas. Thus, for the given conditions, the solution of the system of equations considered can be written as a function of the literal value of the free terms, thus avoiding the aforementioned disadvantage of the method of successive approximations.

To illustrate the above statements reference will be made to the author's example number 2.

The following notations are made:

$$M_2 = X_1 \; ; \; M_3 = X_2 \; ; \; M_4 = X_3 \; ; \; M_5 = X_4$$

$$\frac{1}{\tau_{12}} = \frac{1}{\tau_{23}} = \frac{1}{\tau_{32}} = \frac{1}{\tau_{34}} = \frac{1}{\tau_{43}} = \frac{1}{\tau_{54}} = \gamma = \gamma' = 5.5$$

$$\frac{1}{\tau_{45}} = \gamma'' = 2.75$$

$$-5.5\, m_2 + M_1 = K_1 \; ; \; -5.5\, m_3 = K_2$$

$$-5.5\, m_4 = K_3 \; ; \; -2.75\, m_3 = K_4$$

From them results,

$$\delta' = 0 \; ; \; \delta'' = -2.75 \; ; \; A'_n = D_n$$

D_0	D_1	D_2	D_3	D_4
1	5.5	29.3	156	829
A''_0	A''_1	A''_2	A''_3	A''_4
1	2.75	14.2	75.3	421

$$\overline{D}_n = A''_n = 421$$

The solution of the system is then

$$X_1 = M_2 = -.188\, K_1 + .035\, K_2 - .007\, K_3 + .003\, K_4$$

$$X_2 = M_3 = +.035\, K_1 - .195\, K_2 + .038\, K_3 - .014\, K_4$$

$$X_3 = M_4 = -.007\, K_1 + .038\, K_2 - .202\, K_3 + .074\, K_4$$

$$X_4 = M_5 = +.003\, K_1 - .014\, K_2 + .074\, K_3 - .390\, K_4$$

Eq. 3 can successfully be used to determine the influence lines of the support moments.

VIERENDEEL BENTS WITH NONPRISMATIC MEMBERS[a]

Discussion by Paul Rogers

PAUL ROGERS,[1] F. ASCE.—Messrs. Lee and Wiesinger should be commended for their excellent treatise on this interesting problem. Their extension of the moment-distribution method to the Vierendeel bents emphasizes the creative genius of the late Hardy Cross, the originator of moment distribution.

The writer will confine his discussion to the practical aspects of Vierendeel bents. While a great deal has been written about such bents, only a few have actually been used in this country. In fact, excepting Belgium, Vierendeel bents are rather infrequently employed. The reluctance of designers to the use of Vierendeel bents may be attributed, but not limited, to some of the causes that are to be discussed.

In addition to the considerable bending moments obtained through analysis, there exist substantial axial forces. After all, Vierendeel bents are trusses with the diagonals removed. The presence of such axial forces is conspicuously omitted by practically all authors. Despite this, members designed for moments and axial forces might turn out to be uneconomical.

Even with conventional trusses, secondary stresses often cause complications, even though web-members are usually relatively flexible beyond the gusset plates. Such secondary stresses become of utmost importance for Vierendeel bents and girders, due to increased rigidity and moment resistance of members. As an example, a Vierendeel truss of 100 ft span, with one end on pins and the other on rollers, may have such deformations, due to the relative shortening of the top chord and lengthening of the bottom chord, that some of the verticals might be several inches out of plumb under full loading conditions. This requires secondary stress analyses, analogous to settlement of support, and re-distribution of fixed-end moments. It is questionable whether such extensive numerical computations are warranted.

The most likely application of Vierendeel bents is in architectural engineering, where diagonals are undesirable, and where the excessive extra costs are sometimes tolerated. The writer had occasion to employ the Vierendeel truss principle for the exterior bent of a power plant structure (Fig. 1).

The interior bay was taken up by a heavy suspended boiler, and, thus, the exterior bay had to resist the wind forces by a Vierendeel action. The writer was convinced (and still is) that an approximate solution is entirely adequate and he proceeded as follows:

Applying the wind force as a uniformly distributed load on a continuous beam, he obtained bending moments, shears and reactions (Fig. 2). Using the

---

[a] December, 1959, by S. L. Lee and F. P. Wiesinger.

[1] Cons. Engr., Chicago, Ill.

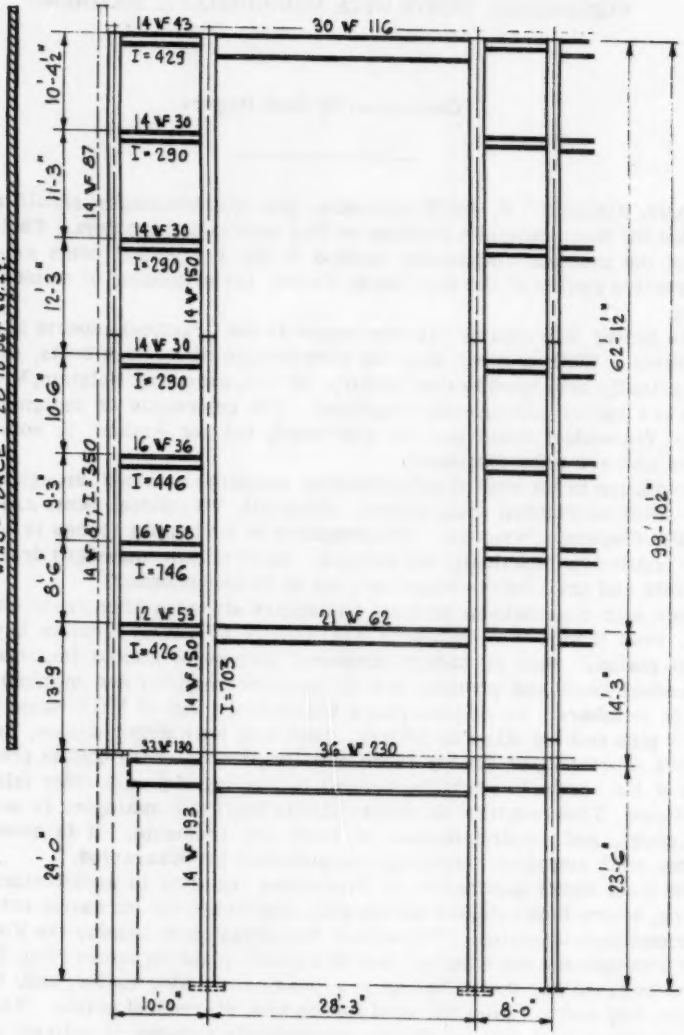

FIG. 1.—LONGITUDINAL SECTION THRU BOILER-BAY

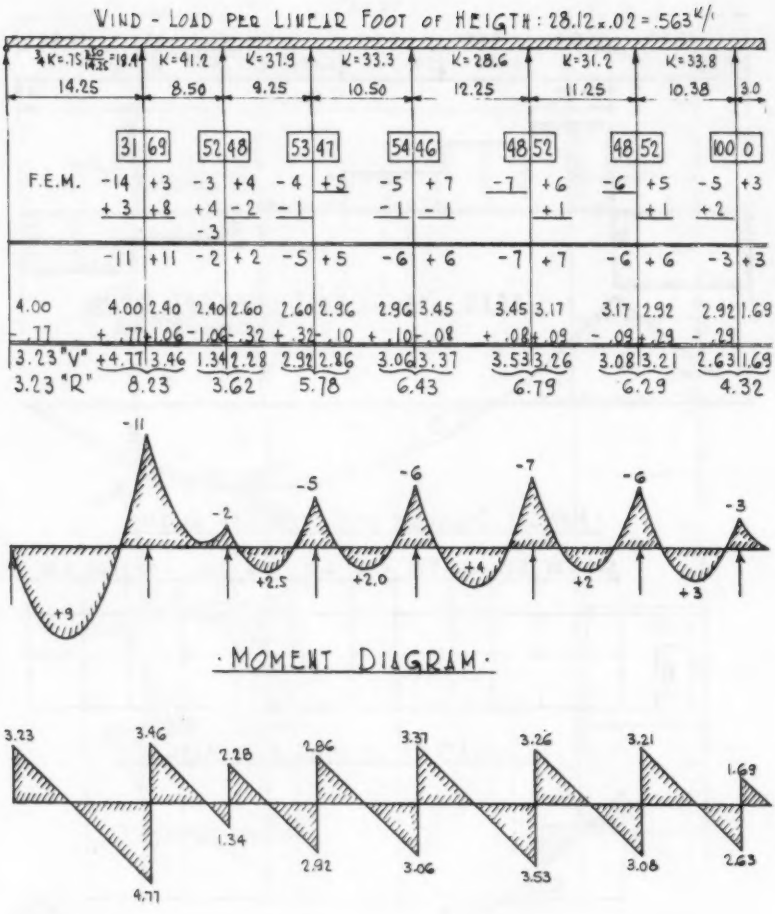

FIG. 2.—SHEAR-DIAGRAM

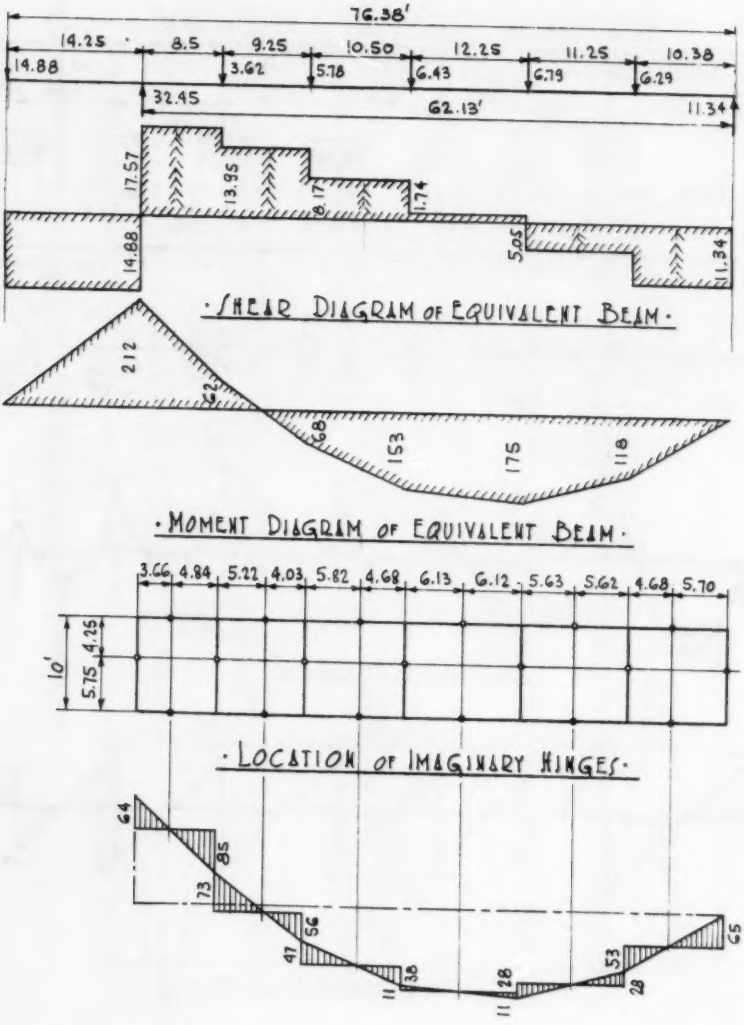

FIG. 3.—TOTAL MOMENTS ON GIRDER

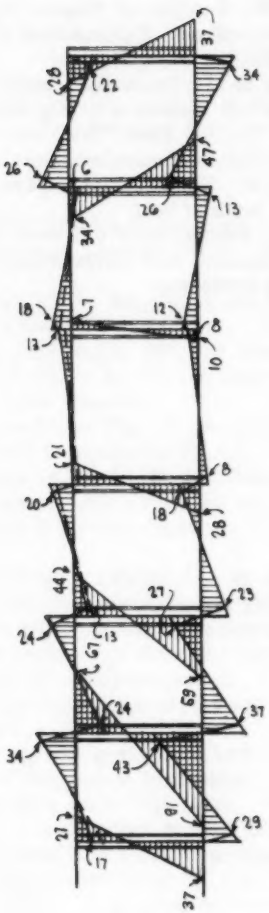

FIG. 4(a).—FINAL MOMENTS IN FOOT-KIPS.

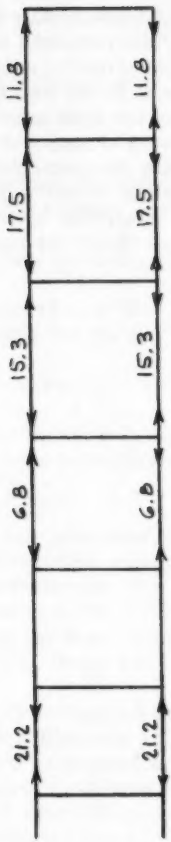

FIG. 4(b).—DIRECT STRESS IN KIPS.

reactions as concentrated loads, a general moment diagram is obtained for an equivalent girder. Then, starting from the conjecture that there are points of inflection in all members of a Vierendeel bent where the values of moments are zero, the absolute moments (sum of top and bottom chords) are obtained by projecting the locations of the imaginary hinges upon the moment diagram (Fig. 3). The writer's assumption as to the location of hinges (in ratio of squares of stiffnesses) may be subject to objections. Relocation of the hinges would not substantially alter the values of the moments.

The final moments for all the members of the Vierendeel bents are obtained by properly assigning (through statics) moments to top and bottom chords and to the web members (Fig. 4). The top chord (exterior column), also, has the wind moments added and then the maximum moments are taken at the faces of supports for selection of sizes. The axial forces are obtained by dividing the moments from Fig. 3 by the depth of bent.

While the writer's practical solution is substantially different from the authors' analytical method, it is readily admitted that fundamental analysis and research are the core of all engineering problems.

CONTINUOUS GIRDER BRIDGE WITH VARIABLE MOMENT OF INERTIA[a]

Corrections
Discussion by Keiichiro Hayashi, Narbey Khachaturian

CORRECTIONS.—In the January Journal of the Structural Division, on page 29, the distance between the concentrated load P and the support B should be ψ_n S.

On page 32, in Eq. 19c, a bracket should appear after the term C_4 and at the end of the equation.

On page 34, in Eq. 22b, the term 4/16 should be changed to n/16.

On page 34, in Eq. 22c, a bracket should appear after the term C_4 and at the end of the equation.

On page 34, in Fig. 17, the distance between the concentrated load P and the support B should be ψ_n S.

On page 38, in Eq. 26, a bracket should appear after the term 1/16.

On page 39, in the equation for D_{10}, the first set of the parentheses should encompass the entire fraction.

KEIICHIRO HAYASHI,[4] A.M. ASCE.—The author has presented an interesting study on the continuous girder bridge with the variable moment of inertia. As an electronic computer is available to many engineers, they can do a rigorous analysis of this kind very easily. In this respect, the writer thinks this paper is timely and useful. The writer has studied the same problem with the stiffness matrix analysis and found that it is equally useful and has some advantage.

Consider the continuous bridge on which the load P is applied as in Fig. 18(a). If hinges are introduced at all the supports, the structure will deform with this load as in Fig. 18(b). The joint rotations are expressed as the matrix $|\theta|$. On the other hand, if the redundant moments are considered as outside moments and these moments only are applied at every hinge, the same structure will deform as in Fig. 18(c). The joint rotations are shown by the matrix $|\theta'|$. According to the stiffness matrix analysis, the product of the post-multiplication of the flexibility matrix $|F|$ by the (redundant) moment matrix $|m|$ is the joint rotation matrix $|\theta'|$. That is

$$|F| \cdot |m| = |\theta'| \quad \ldots\ldots\ldots\ldots\ldots\ldots (36)$$

From the continuity requirement, these rotations have to be the same as the rotations due to the load on the hinged structure. Thus,

---

[a] January, 1960, by Sabri Sami.
[4] Engr., Bechtel Assocs., New York, N.Y.

$$| F | \cdot | m | = | \theta | \quad \ldots\ldots\ldots\ldots\ldots\ldots (37)$$

It is interesting to notice that the above relation is true only at the inner joints. It is also known from the beginning that the moments at the two hinged ends are zero. Also by the reciprocal theorem, $| \theta |$ is the same as the loads multiplied by the deflections at the points of loading due to the unit-end moments. The name of the loading matrix is given here to $| \theta |$.

The following are the flexibility matrix $| F |$ for the basic members, and the loading matrix $| \theta |$ for the different types of loading. The unnecessary elements are not shown.

1) Flexibility matrix is

$$\begin{vmatrix} F_{ll} & F_{lr} \\ F_{rl} & F_{rr} \end{vmatrix} \quad \ldots\ldots\ldots\ldots\ldots\ldots (38)$$

in which for the inner member (Fig. 19)

$$F_{ll} = F_{rr} = \frac{n\,s}{32\,E\,I_o(m_1-1)}\left[3 - \left(\frac{2}{m_1}\right)^2 + \frac{(3\,m_1 - 2)\tan^{-1}\sqrt{m_1 - 1}}{\sqrt{m_1 - 1}}\right] \ldots (39)$$

$$F_{lr} = F_{rl} = \frac{n\,s}{32\,E\,I_o(m_1-1)}\left[3 - \frac{2}{m_1} + \frac{(3\,m_1 - 4)\tan^{-1}\sqrt{m_1 - 1}}{\sqrt{m_1 - 1}}\right] \ldots . (40)$$

For the left end member (Fig. 20a) $F_{ll} = F_{lr} = F_{rl}$ are to be disregarded since they are related with the hinged end and will not appear in the fixed matrix.

$$F_{rr} = \frac{n\,s}{32\,E\,I_o\,(m_1-1}\left\{\frac{4(m_1 - 1)}{m_2^3\left(\frac{m_1 - m_2}{m_2}\right)n}\left[\frac{m_2}{m_1} - 2\,\frac{m_2}{m_1}\right)^2 + \frac{\tan^{-1}\sqrt{\frac{m_1 - m_2}{m_2}}}{\sqrt{\frac{m_1 - m_2}{m_2}}}\right]\right\} \quad \ldots\ldots\ldots\ldots\ldots\ldots\ldots\ldots (41)$$

and for the right end member (Fig. 20b) $F_{rr} = F_{lr} - F_{rl}$ are again disregarded.

$$F_{ll} = \frac{n\,s}{32\,E\,I_o\,(m_1-1)}\left\{\frac{4\,(m_1 - 1)}{m_2^3\left(\frac{m_1 - m_2}{m_2}\right)n}\left[\frac{m_2}{m_1} - 2\left(\frac{m_2}{m_1}\right)^2 + \frac{\tan^{-1}\sqrt{\frac{m_1 - m_2}{m_2}}}{\sqrt{\frac{m_1 - m_2}{m_2}}}\right]\right\} \quad \ldots\ldots\ldots\ldots\ldots\ldots\ldots\ldots (42)$$

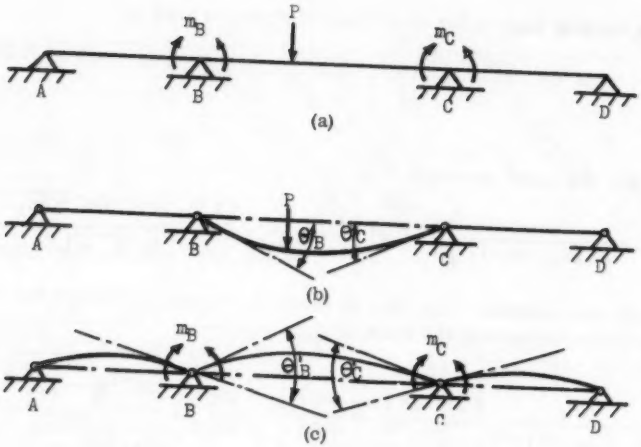

FIG. 18

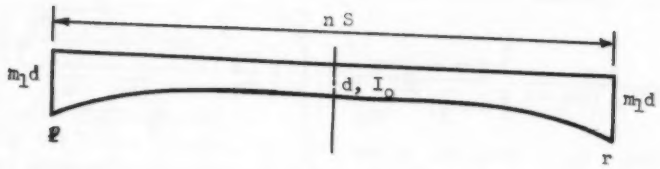

FIG. 19

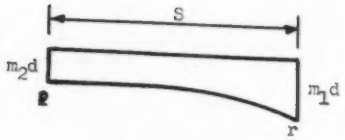

FIG. 20

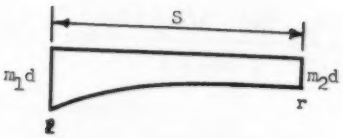

FIG. 20b

2) The loading matrix for uniformly distributed load is

$$\left| \begin{matrix} \theta_l \\ \theta_r \end{matrix} \right| \quad \ldots\ldots\ldots\ldots\ldots\ldots\ldots\ldots (43)$$

in which for the inner member (Fig. 21)

$$\theta_l = \theta_r = \frac{n\,s}{32\,E\,I_o\,m_1 - 1)} \left\{ w\,n^2\,s^2 \left[\frac{3}{4} - \frac{1}{2\,m_1} + \frac{(3\,m_1 - 4)\tan^{-1}\sqrt{m_1 - 1}}{4\sqrt{m_1 - 1}} \right] \right\} \quad (44)$$

for the left end member (Fig. 22a) θ_l must be disregarded since the continuity condition does not hold at the ends, and

$$\theta_r = \frac{n\,s}{32\,E\,I_o\,(m_1 - 1)} \left\{ \frac{2\,w\,s^2\,(m_1 - 1)}{n\,m_2^3 \left(\frac{m_1 - m_2}{m_2} \right)} \left[-\left(\frac{m_2}{m_1} \right) + \frac{\tan^{-1} \sqrt{\frac{m_1 - m_2}{m_2}}}{\sqrt{\frac{m_1 - m_2}{m_2}}} \right] \right\} \quad (45)$$

and for the right end member (Fig. 22b)

$$\theta_l = \frac{n\,s}{32\,E\,I_o\,(m_1 - 1)} \left\{ \frac{2\,w\,s^2\,(m_1 - 1)}{n\,m_2^3 \left(\frac{m_1 - m_2}{m_2} \right)} \left[-\left(\frac{m_2}{m_1} \right) + \frac{\tan^{-1} \sqrt{\frac{m_1 - m_2}{m_2}}}{\sqrt{\frac{m_1 - m_2}{m_2}}} \right] \right\} \quad (46)$$

and θ_r is disregarded. The loading matrix for concentrated load is as shown in Eq. 43 in which, for the inner member (Fig. 23),

$$\theta_l = \frac{n\,s}{32\,E\,I_o\,(m_1 - 1)} \left\{ pns \left[(1 - \psi) \left(\frac{1}{(m_1 - 1)(1 - 2\psi)^2 + 1} - \frac{1}{m_1} \right) \right.\right.$$
$$+ \frac{1 - 3(m_1 - 1)(1 - 2\psi)}{2\sqrt{m_1 - 1}} \tan^{-1} \sqrt{m_1 - 1}\,(1 - 2\psi)$$
$$\left.\left. - \frac{(1 - 2\psi) - 3(m_1 - 1)}{2\sqrt{m_1 - 1}} \tan^{-1} \sqrt{m_1 - 1} \right] \right\} \quad \ldots\ldots\ldots\ldots\ldots (47)$$

$$\theta_r = \frac{n\,s}{32\,E\,I_o\,(m_1 - 1)} \left\{ pns \left[\psi \left(\frac{1}{(m_1 - 1)(1 - 2\psi)^2 + 1} - \frac{1}{m_1} \right) \right.\right.$$
$$- \frac{1 + 3(m_1 - 1)(1 - 2\psi)}{2\sqrt{m_1 - 1}} \tan^{-1} \sqrt{m_1 - 1}\,(1 - 2\psi)$$
$$\left.\left. + \frac{(1 - 2\psi) + 3\,m_1 - 1)}{2\sqrt{m_1 - 1}} \tan^{-1} \sqrt{m_1 - 1} \right] \right\} \quad \ldots\ldots\ldots\ldots\ldots (48)$$

for the left end member (Fig. 24a) θ_l is disregarded.

$$\theta_r = \frac{n\,s}{32\,E\,I_o\,(m_1-1)}\left\{\frac{4\,ps\,(m_1-1)}{n\,m_2^3\left(\frac{m_1-m_2}{m_2}\right)}\left[\psi\left(\frac{1}{\left(\frac{m_1-m_2}{m_2}\right)\psi^2+1}-\frac{m_2}{m_1}\right)\right.\right.$$
$$\left.\left.+\frac{1}{\sqrt{\frac{m_1-m_2}{m_2}}}\tan^{-1}\sqrt{\frac{m_1-m_2}{m_2}}\,\psi-\frac{\psi}{\sqrt{\frac{m_1-m_2}{m_2}}}\tan^{-1}\sqrt{\frac{m_1-m_2}{m_2}}\right]\right\} \quad \ldots (49)$$

for the right end member (Fig. 24b)

$$\theta_l = \frac{n\,s}{32\,E\,I_o\,(m_1-1)}\left\{\frac{4\,ps\,(m_1-1)}{n\,m_2^3\left(\frac{m_1-m_2}{m_2}\right)}\left[(1-\psi)\left(\frac{1}{\left(\frac{m_1-m_2}{m_2}\right)(1-\psi)^2+1}\right)\right.\right.$$
$$-\frac{m_2}{m_1}\Big)+\frac{1}{\sqrt{\frac{m_1-m_2}{m_2}}}\tan^{-1}\sqrt{\frac{m_1-m_2}{m_2}}\,(1-\psi)$$
$$\left.\left.-\frac{(1-\psi)}{\sqrt{\frac{m_1-m_2}{m_2}}}\tan^{-1}\sqrt{\frac{m_1-m_2}{m_2}}\right]\right\} \quad \ldots\ldots\ldots\ldots\ldots\ldots (50)$$

and θ_r is to be disregarded.

Using the above results, the problem of the three span bridge in the author's paper will be solved. In calculating the elements of the matrices, the common factor of $\frac{n\,s}{32\,E\,I_o\,(m_1-1)}$ is omitted.

1) Flexibility matrix are obtained as follows:

For span A-B,

$$f_{AA} = f_{AB} = f_{BA} \quad \text{are disregarded, and}$$
$$f_{BB} = \left\{\frac{4 \times 2}{2 \times 1.4} \times \left[\frac{1}{3} - 2\times\left(\frac{1}{3}\right)^2 + \frac{0.9553}{1.4142}\right]\right\} = 2.2474$$

For span B-C,

$$f_{BB} = f_{CC} = \left[3 - \left(\frac{2}{3}\right)^2 + \frac{7 \times 0.9553}{1.4142}\right] = 7.2841$$

$$f_{BC} = f_{CB} = \left[3 - \frac{2}{3} + \frac{5 \times 0.9553}{1.4142}\right] = 5.7108$$

For span C-D

$$f_{CC} = 2.2474$$

with $f_{DD} = f_{CD} = f_{DC}$ disregarded.

FIG. 21

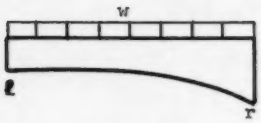

FIG. 22a

FIG. 22b

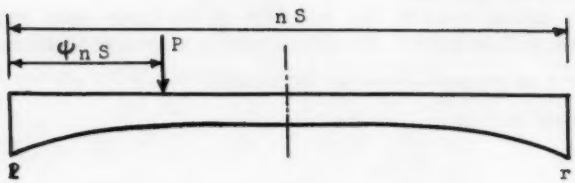

FIG. 23

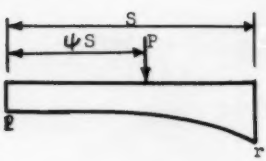

FIG. 24a

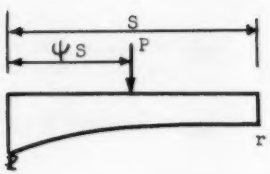

FIG. 24b

2) Loading matrix are obtained as follows:

For the uniform load w in pounds per foot, on the middle span B-C only is,

$$\theta_B = \theta_C = 1.4^2 \times ws^2 \times \left[\frac{3}{4} - \frac{1}{6} + \frac{5 \times 0.9553}{4 \times 1.4142}\right] = 2.7983\ ws^2$$

with θ_A and θ_D disregarded since the continuity condition does not hold at the ends.

For the uniform load w on the span A-B only is,

$$\theta_B = \frac{2 \times 2 \times ws^2}{1.4 \times 2}\left[-\frac{1}{3} + \frac{0.9553}{1.4142}\right] = 0.4889\ ws^2$$

$$\theta_C = 0$$

with θ_A and θ_D disregarded.

for the uniform load w, on all the span is

$$\theta_B = \theta_C = 2.7983\ ws^2 + 0.4889\ ws^2 = 3.2872\ ws^2$$

with θ_A and θ_D again disregarded.

Thus, the matrices for three conditions combined are

$$\begin{vmatrix} & & & \\ -2.2474 & +7.2841 & 5.7108 & \\ & 5.7108 & 7.2841 & +2.2474 \\ & & & \end{vmatrix} \times \begin{matrix} (a) & (b) & (c) \\ - & - & - \\ m_B & m'_B & m''_B \\ m_C & m'_C & m''_C \\ - & - & - \end{matrix}$$

$$= \begin{matrix} (a) & (b) & (c) \\ - & - & - \\ 2.7983\,w\,s^2 & 0.4889\,w\,s^2 & 3.2872\,w\,s^2 \\ 2.7983\,w\,s^2 & 0 & 3.2872\,w\,s^2 \\ - & - & - \end{matrix}$$

Due to the fact that the continuity condition does not hold at two ends and the end moments are zero, the first and the last rows of all three matrices and the first and the last columns of the flexibility matrix have to be disregarded. Hence, the matrices to be solved are those shown. Solving the above matrices, the moments are

$$\begin{matrix} (a) & (b) & (c) \\ m_B & m'_B & m''_B \\ m_C & m'_C & m''_C \end{matrix} = \begin{matrix} (a) & (b) & (c) \\ 0.1836\,w\,s^2 & 0.08015\,w\,s^2 & 0.2157\,w\,s^2 \\ 0.1836\,w\,s^2 & -0.048\,w\,s^2 & 0.2157\,w\,s^2 \end{matrix}$$

The writer thinks that the author's and the writer's methods are based on the same principle and, therefore, the author's D-factors and the writer's matrices have the identical elements.

Although the author has covered a wide range of the practical applications, they are still limited. The matrix analysis, on the other hand, can be easily adapted to the bridge with any number of spans and with any combination of loading. Once the programming of the electronic computer application with this matrix analysis is prepared for a general case, it will be much more compact and easily used.

NARBEY KHACHATURIAN,[5] M. ASCE.—The author has presented an interesting application of the principle of virtual work to the analysis of continuous structures. This method originated from a study on the slab rigid-frame bridges that was developed by the writer in connection with his doctoral dissertation.[6] Unfortunately the results of this study, in the form presented by the author, are of only academic interest and are applicable in a very limited way.

The analysis shown by the author is valid only for beams of rectangular cross section. Therefore, the results cannot be applied to "girder bridges," as the author has indicated in the title of his paper. Steel and prestressed concrete girder bridges are generally of box or I-section and reinforced concrete girder bridges are of T-sections. In fact, the only type of structure to which the results apply directly is the reinforced concrete slab bridge. The reinforced concrete slab bridge has a limited application since it is economical only when the span lengths are short.

Furthermore, the derivations are made on the basis of a particular law of variation for the intrados. The author does not state whether or not his results are applicable to continuous beams with straight or parabolic haunches, or if applicable, approximately how much is the maximum error in each case. There is no indication in the paper that the method may be conveniently applicable to non-rectangular sections.

---

[a] January, 1960 by Sabri Sami.

[5] Assoc. Prof. of Civ. Engrg., Univ. of Illinois, Urbana, Ill.

[6] "A Study of Proportions of Rigid Frame Bridges," by Narbey Khachaturian, Ph.D. thesis, Dept. of Civ. Engrg., Univ. of Illinois, 1952, pp. 9-32.

PROCEEDINGS PAPERS

The technical papers published in the past year are identified by number below. Technical-division sponsorship is indicated by an abbreviation at the end of each Paper Number, the symbols referring to: Air Transport (AT), City Planning (CP), Construction (CO), Engineering Mechanics (EM), Highway (HW), Hydraulics (HY), Irrigation and Drainage (IR), Pipeline (PL), Power (PO), Sanitary Engineering (SA), Soil Mechanics and Foundations (SM), Structural (ST), Surveying and Mapping (SU), and Waterways and Harbors (WW), divisions. Papers sponsored by the Department of Conditions of Practice are identified by the symbols (PP). For titles and order coupons, refer to the appropriate issue of "Civil Engineering." Beginning with Volume 82 (January 1956) papers were published in Journals of the various Technical Divisions. To locate papers in the Journals, the symbols after the paper number are followed by a numeral designating the issue of a particular Journal in which the paper appeared. For example, Paper 2270 is identified as 2270(ST9) which indicates that the paper is contained in the ninth issue of the Journal of the Structural Division during 1959.

VOLUME 85 (1959)

MAY: 2014(AT2), 2015(AT2), 2016(AT2), 2017(HY5), 2018(HY5), 2019(HY5), 2020(HY5), 2021(HY5), 2022(HY5), 2023(PL2), 2024(PL2), 2025(PL2), 2026(PP1), 2027(PP1), 2028(PP1), 2029(PP1), 2030(SA3), 2031(SA3), 2032(SA3), 2033(SA3), 2034(ST5), 2035(ST5), 2036(ST5), 2037(ST5), 2038(PL2), 2039(PL2), 2040(AT2)[c], 2041(PL2)[c], 2042(PP1)[c], 2043(ST5)[c], 2044(SA3)[c], 2045(HY5)[c], 2046(PP1), 2047(PP1).

JUNE: 2048(CP1), 2049(CP1), 2050(CP1), 2051(CP1), 2052(CP1), 2053(CP1), 2054(CP1), 2055(CP1), 2056(HY6), 2057(HY6), 2058(HY6), 2059(IR2), 2060(IR2), 2061(PO3), 2062(SM3), 2063(SM3), 2064(SM3), 2065(ST6), 2066(WW2), 2067(WW2), 2068(WW2), 2069(WW2), 2070(WW2), 2071(WW2), 2072(CP1)[c], 2073(IR2)[c], 2074(PO3)[c], 2075(ST6)[c], 2076(HY6)[c], 2077(SM3)[c], 2078(WW2)[c].

JULY: 2079(HY7), 2080(HY7), 2081(HY7), 2082(HY7), 2083(HY7), 2084(HY7), 2085(HY7), 2086(SA4), 2087(SA4), 2088(SA4), 2089(SA4), 2090(SA4), 2091(EM3), 2092(EM3), 2093(EM3), 2094(EM3), 2095(EM3), 2096(EM3), 2097(HY7)[c], 2098(SA4)[c], 2099(EM3)[c], 2100(AT3), 2101(AT3), 2102(AT3), 2103(AT3), 2104(AT3), 2105(AT3), 2106(AT3), 2107(AT3), 2108(AT3), 2109(AT3), 2110(AT3), 2111(AT3), 2112(AT3), 2113(AT3), 2114(AT3), 2115(AT3), 2116(AT3), 2117(AT3), 2118(AT3), 2119(AT3), 2120(AT3), 2121(AT3), 2122(AT3), 2123(AT3), 2124(AT3), 2125(AT3).

AUGUST: 2126(HY8), 2127(HY8), 2128(HY8), 2129(HY8), 2130(PO4), 2131(PO4), 2132(PO4), 2133(PO4), 2134(SM4), 2135(SM4), 2136(SM4), 2137(SM4), 2138(HY8)[c], 2139(PO4)[c] 2140(SM4)[c].

SEPTEMBER: 2141(CO2), 2142(CO2), 2143(CO2), 2144(HW3), 2145(HW3), 2146(HW3), 2147(HY9), 2148(HY9), 2149(HY9), 2150(HY9), 2151(IR3), 2152(ST7)[c], 2153(IR3), 2154(IR3), 2155(IR3), 2156(IR3), 2157(IR3), 2158(IR3), 2159(IR3), 2160(IR3), 2161(SA5), 2162(SA5), 2163(ST7), 2164(ST7), 2165(SU1), 2166(SU1), 2167(WW3), 2168(WW3), 2169(WW3), 2170(WW3), 2171(WW3), 2172(WW3), 2173(WW3), 2174(WW3), 2175(WW3), 2176(WW3), 2177(WW3), 2178(CO2)[c], 2179(IR3)[c], 2180(HW3)[c], 2181(SA5)[c], 2182(HY9)[c], 2183(SU1)[c], 2184(WW3)[c], 2185(PP2)[c], 2186(ST7)[c], 2187(PP2), 2188(PP2).

OCTOBER: 2189(AT4), 2190(AT4), 2191(AT4), 2192(AT4), 2193(AT4), 2194(EM4), 2195(EM4), 2196(EM4), 2197(EM4), 2198(EM4), 2199(EM4), 2200(HY10), 2201(HY10), 2202(HY10), 2203(PL3), 2204(PL3), 2205(PL3), 2206(PO5), 2207(PO5), 2208(PO5), 2209(PO5), 2210(SM5), 2211(SM5), 2212(SM5), 2213(SM5), 2214(SM5), 2215(SM5), 2216(SM5), 2217(SM5), 2218(ST8), 2219(ST8), 2220(EM4), 2221(ST8), 2222(ST8), 2223(ST8), 2224(HY10), 2225(HY10), 2226(PO5), 2227(PO5), 2228(PO5), 2229(ST8), 2230(EM4), 2231(EM4), 2232(AT4)[c], 2233(PL3)[c], 2234(EM4)[c], 2235(HY10)[c], 2236(SM5)[c], 2237(ST8)[c], 2238(PO5)[c], 2239(ST8), 2240(PL3).

NOVEMBER: 2241(HY11), 2242(HY11), 2243(HY11), 2244(HY11), 2245(HY11), 2246(SA6), 2247(SA6), 2248(SA6), 2249(SA6), 2250(SA6), 2251(SA6), 2252(SA6), 2253(SA6), 2254(SA6), 2255(SA6), 2256(ST9), 2257(ST9), 2258(ST9), 2259(ST9), 2260(HY11), 2261(ST9)[c], 2262(ST9), 2263(HY11), 2264(ST9), 2265(HY11), 2266(SA6), 2267(SA6), 2268(SA6), 2269(HY11)[c], 2270(ST9).

DECEMBER: 2271(HY12)[c], 2272(CP2), 2273(HW4), 2274(HW4), 2275(HW4), 2276(HW4), 2277(HW4), 2278(HW4), 2279(HW4), 2280(HW4), 2281(IR4), 2282(IR4), 2283(IR4), 2284(IR4), 2285(PO6), 2286(PO6), 2287(PO6), 2288(PO6), 2289(PO6), 2290(PO6), 2291(PO6), 2292(SM6), 2293(SM6), 2294(SM6), 2295(SM6), 2296(SM6), 2297(WW4), 2298(WW4), 2299(WW4), 2300(WW4), 2301(WW4), 2302(WW4), 2303(WW4), 2304(HW4), 2305(ST10), 2306(CP2), 2307(CP2), 2308(ST10), 2309(CP2), 2310(HY12), 2311(HY12), 2312(PO6), 2313(PO6), 2314(ST10), 2315(HY12), 2316(HY12), 2317(HY12), 2318(WW4), 2319(SM6), 2320(SM6), 2321(ST10), 2322(ST10), 2323(HW4)[c], 2324(CP2)[c], 2325(SM6)[c], 2326(WW4)[c], 2327(IR4)[c], 2328(PO6)[c], 2329(ST10)[c], 2330(CP2).

VOLUME 86 (1960)

JANUARY: 2331(EM1), 2332(EM1), 2333(EM1), 2334(EM1), 2335(HY1), 2336(HY1), 2337(EM1), 2338(EM1), 2339(HY1), 2340(HY1), 2341(SA1), 2342(EM1), 2343(SA1), 2344(ST1), 2345(ST1), 2346(ST1), 2347(ST1), 2348(EM1)[c], 2349(HY1)[c], 2350(ST1), 2351(ST1), 2352(SA1)[c], 2353(ST1)[c], 2354(ST1).

FEBRUARY: 2355(CO1), 2356(CO1), 2357(CO1), 2358(CO1), 2359(CO1), 2360(CO1), 2361(PO1), 2362(HY2), 2363(ST2), 2364(HY2), 2365(SU1), 2366(HY2), 2367(SU1), 2368(SM1), 2369(HY2), 2370(SU1), 2371(HY2), 2372(PO1), 2373(SM1), 2374(HY2), 2375(PO1), 2376(HY2), 2377(CO1)[c], 2378(SU1), 2379(SU1), 2380(SU1), 2381(HY2)[c], 2382(ST2), 2383(SU1), 2384(ST2), 2385(SU1)[c], 2386(SU1), 2387(SU1), 2388(SU1), 2389(SM1), 2390(ST2)[c], 2391(SM1)[c], 2392(PO1)[c].

MARCH: 2393(IR1), 2394(IR1), 2395(IR1), 2396(IR1), 2397(IR1), 2398(IR1), 2399(IR1), 2400(IR1), 2401(IR1), 2402(IR1), 2403(IR1), 2404(IR1), 2405(IR1), 2406(IR1), 2407(SA2), 2408(SA2), 2409(HY3), 2410(ST3), 2411(SA2), 2412(HW1), 2413(WW1), 2414(WW1), 2415(HY3), 2416(HW1), 2417(HW3), 2418(HW1)[c], 2419(WW1)[c], 2420(WW1), 2421(WW1), 2422(WW1), 2423(WW1), 2424(SA2), 2425(SA2)[c], 2426(HY3)[c], 2427(ST3)[c].

APRIL: 2428(ST4), 2429(HY4), 2430(PO2), 2431(SM2), 2432(PO2), 2433(ST4), 2434(EM2), 2435(PO2), 2436(ST4), 2437(ST4), 2438(HY4), 2439(EM2), 2440(EM2), 2441(ST4), 2442(SM2), 2443(HY4), 2444(ST4), 2445(EM2), 2446(ST4), 2447(EM2), 2448(SM2), 2449(HY4), 2450(ST4), 2451(HY4), 2452(HY4), 2453(EM2), 2454(EM2), 2455(EM2)[c], 2456(HY4)[c], 2457(PO2)[c], 2458(ST4)[c], 2459(SM2)[c].

MAY: 2460(AT1), 2461(ST5), 2462(AT1), 2463(AT1), 2464(CP1), 2465(CP1), 2466(AT1), 2467(AT1), 2468(SA3), 2469(HY5), 2470(ST5), 2471(SA3), 2472(SA3), 2473(ST5), 2474(SA3), 2475(ST5), 2476(SA3), 2477(ST5), 2478(HY5), 2479(SA3), 2480(ST5), 2481(SA3), 2482(CO2), 2483(CO2), 2484(HY5), 2485(HY5), 2486(AT1)[c], 2487(CP1)[c], 2488(CO2)[c], 2489(HY5)[c], 2490(SA3)[c], 2491(ST5)[c], 2492(CP1), 2493(CO2).

c. Discussion of several papers, grouped by divisions.

AMERICAN SOCIETY OF CIVIL ENGINEERS

OFFICERS FOR 1960

PRESIDENT

FRANK A. MARSTON

VICE-PRESIDENTS

Term expires October, 1960:
PAUL L. HOLLAND
LLOYD D. KNAPP

Term expires October, 1961:
CHARLES B. MOLINEAUX
LAWRENCE A. ELSENER

DIRECTORS

Term expires October, 1960:
PHILIP C. RUTLEDGE
WESTON S. EVANS
TILTON E. SHELBURNE
CRAIG P. HAZELET
DONALD H. MATTERN
JOHN E. RINNE

Term expires October, 1961:
THOMAS J. FRATAR
EARL F. O'BRIEN
DANIEL B. VENTRES
CHARLES W. BRITZIUS
WAYNE G. O'HARRA
FRED H. RHODES, JR.
N. T. VEATCH

Term expires October, 1962:
ELMER K. TIMBY
SAMUEL S. BAXTER
THOMAS M. NILES
TRENT R. DAMES
WOODROW W. BAKER
BERNHARD DORNBLATT

PAST PRESIDENTS

Members of the Board

LOUIS R. HOWSON
FRANCIS S. FRIEL

EXECUTIVE SECRETARY

WILLIAM H. WISELY

TREASURER

E. LAWRENCE CHANDLER

ASSISTANT TREASURER

ENOCH R. NEEDLES

PROCEEDINGS OF THE SOCIETY

HAROLD T. LARSEN
Manager of Technical Publications

PAUL A. PARISI
Editor of Technical Publications

MARVIN L. SCHECHTER
Associate Editor of Technical Publications

IRVIN J. SCHWARTZ
Assistant Editor of Technical Publications

COMMITTEE ON PUBLICATIONS

PHILIP C. RUTLEDGE, *Chairman*

THOMAS M. NILES, *Vice-Chairman*

TILTON E. SHELBURNE
WESTON S. EVANS
WAYNE G. O'HARRA
BERNHARD DORNBLATT

ST 5

PART 2

MAY 1960 — 15 NO. ST 5
VOLUME 86 PART 2

Your attention is invited

NEWS OF THE STRUCTURAL DIVISION OF ASCE

JOURNAL OF THE STRUCTURAL DIVISION
PROCEEDINGS OF THE AMERICAN SOCIETY OF CIVIL ENGINEERS

DIVISION ACTIVITIES

STRUCTURAL DIVISION

Proceedings of the American Society of Civil Engineers

NEWS

May, 1960

Contents

ASCE Convention, Reno . . . . . Pg. 1
Executive Committee . . . . . Pg. 2
Committee on Buildings . . . . . Pg. 3
Committee on Wood . . . . . Pg. 4
Commentary on Plastic Design . . . . . Pg. 5
West Coast Conference on Applied Mechanics . . . . . Pg. 6
Fall Meetings . . . . . Pg. 6
Structural Division Journal . . . . . Pg. 7

ASCE CONVENTION, RENO, JUNE 19-24, 1960

The Structural Division Program for the Reno ASCE Convention will have as its theme the subject "Loads and Stresses." Stewart Mitchell is the Structural Division Program Sessions Chairman as well as the General Program Chairman for the whole Convention. He and his associates have prepared an excellent program which deserves our support.

There will be four half-day sessions on Monday and Tuesday, June 20 and 21. The tentative arrangement is three papers on Monday AM on the strength of bolted joints by Professor W. H. Munse, Professor L. S. Beedle and Mr. T. R. Higgins. On Monday PM there will be papers on high strength steel for bridges by L. C. Hollister, tests of a steel plate girder by D. D. Vasarhelyi, and high strength deformed bars by Mr. Eivind Hognestad. Tuesday AM will be devoted to reinforced concrete with papers on shear and diagonal tension by Professor Boris Bressler, strength of long columns by John Kozak, and loads and stresses in ultimate load design by Professor Phil M. Ferguson. Tuesday afternoon there will be a joint meeting with the Structural Engineers

Note.—No. 1960-15 is part of the copyrighted Journal of the Structural Division, Proceedings of the American Society of Civil Engineers, Vol. 86, No. ST 5, May, 1960.
Copyright 1960 by the American Society of Civil Engineers.

Association of California. It will be a panel session on the newly revised earthquake code.

The complete program for the Convention is published in CIVIL ENGINEERING.

EXECUTIVE COMMITTEE

The Executive Committee of the Structural Division held a three-day meeting during the recent ASCE Convention at New Orleans. There was 100% attendance at this meeting. Present were Robert D. Dewell, Chairman, Em Emerson J. Ruble, Nathan J. Whitman, Jr., George S. Vincent, Charles T. G. Looney, Secretary, and Elmer K. Timby, Contact Member for the Board of Direction.

The Committee discussed the necessity of meeting with the Administrative Committees of the Division at least once a year. It was pointed out that the Division had fifty Task Committees actively engaged in the conduct of research work and that it was impossible to conduct efficiently all of the business of the Division through the mails. It was considered most desirable that at each ASCE Convention, certain Administrative Committees individually hold meetings and then meet with the Executive Committee to review the activities of their various Task Committees and the future plans of the Administrative Committee. Tentative plans call for requesting approval for the Committee on Metals and the Committee on Nuclear Structures and Materials to meet at the Reno Convention.

Considerable discussion developed over the proposal to form a Nuclear Coordinating Committee in the Society. The purpose of this Committee would be to explore the possibility of forming a separate Nuclear Technical Division. The Executive Committee decided to endorse the formation of this Committee with the proviso that its function be limited to providing information on the pros and cons of the formation of a new division.

The Executive Committee studied the general problem of supporting the various Research Councils. It was decided to request the Society to supply funds to support the Research Councils.

The Administrative Committee on Buildings met with the Executive Committee. Chairman Dewell, who is the Contact Member of the Committee on Buildings, emphasized the importance of the organization of this Committee to the ASCE. The purpose of each Task Committee was carefully reviewed. An article describing the organization and aims of the Committee on Buildings appears in this issue of the NEWSLETTER.

It was noted that Elmer K. Timby has been appointed Official Representative of the ASCE at the Stockholm, Sweden Congress of the International Association for Bridge and Structural Engineering. Frank Baron has been appointed Official Representative of the Structural Division at the same Congress. It is expected that Frank Baron will report on this Congress at the Boston ASCE Convention.

The Executive Committee also discussed the budget, travel reimbursements, publications and received reports on the activities of the various Technical Committees. Considerable time was spent in going over the programs for the Reno and Boston Structural Division Programs.

COMMITTEE ON BUILDINGS

The Administrative Group for the Committee on Buildings met in New Orleans at our last convention to organize the various Task Committees. Within the framework of the purposes for which the Committees were originally established, namely, (a) to make recommendations which will lead to the improvement of relations between the engineer and others who participate in design and construction in the building field; (b) to review and correlate the technical problems in the building field for the purpose of recommending action and study by this Committee or by codes with other Committees of the Society; (c) to encourage dissemination of available knowledge in the building field, each Task Committee is soliciting members in three catagories. These classes of committee membership are; (a) the control group which will administer the affairs of the Committee, (b) the actual committee members, and (c) the affiliate members who although are not official members would receive the correspondence and have the privilege of taking part in committee deliberations and actions. From time to time, it may be necessary to shift the membership classifications among the various groups on the basis of interest and availability.

All members wishing to serve on any of the various Task Committees are asked to write to the individual chairman listed below, expressing the applicant's willingness to serve, his special field of interest, education, and the type of membership in which he would be most interested.

TASK COMMITTEE ON STRUCTURAL DESIGN METHODS

The Task Committee on Structural Design Methods is considering the broad general aspects and the philosophy of design of structures in the building field. A number of projects have been suggested for study by this Committee, one of which is the evaluation of the electronic computation for building design.

Anyone interested in being appointed to membership on this Committee, kindly write to Milo S. Ketchum, 730 Klamath Street, Denver 4, Colorado.

TASK COMMITTEE ON THE STUDY OF BUILDING CODES AND SPECIFICATIONS

The Task Committee on the Study of Building Codes and Specifications will be studying the existing codes from the broad approach of policy and functional considerations, rather than from the technical and problem solving attitudes, and will review such areas of need as a constructive critic. Special problems of a technical nature will be referred to appropriate committees or new sub-committees organized for this purpose. All engineers wishing to serve on this Task Committee, kindly write to Charles W. Yoder, 3505 West Center Street, Milwaukee 10, Wisconsin.

TASK COMMITTEE ON INTER-PROFESSIONAL ACTIVITIES

The immediate function of the Task Committee on Inter-Professional Activities is to define the relationship of the structural engineer in the broad field of civil engineering, and to establish the proper inter-professional understanding among all engineers directly related to building design.

Anyone interested in becoming a member of this Committee, kindly write to Professor A. L. Miller, University of Washington, Seattle, Washington.

THE TASK COMMITTEE ON LATERAL FORCES

The Task Committee on Lateral Forces under the Chairmanship of R. W. Binder is now studying the problem of "drift" of buildings as caused by both wind and seismic loads and would invite data and opinions from various interested engineers.

Mail all comments to R. W. Binder, Bethlehem Pacific Coast Steel, P. O. Box 258, Torrance, California.

For the Reno Convention in June, the Committee is cooperating with the Program Committee in organizing a panel on the various aspects of seismic design for buildings.

COMMITTEE ON WOOD

The Administrative Committee of the Committee on Wood met at the Forest Products Laboratory on January 20, 1960. In attendance were T. K. May, Chairman, F. J. Hanrahan, R. E. Eby and A. D. Freas. In addition, John G. Shope of the National Lumber Manufacturers' Association attended as did R. D. Dewell and Emerson Ruble, members of the Executive Committee of the Structural Division.

For the past few years the principal task of the Committee on Wood has been the revision of ASCE Manual 17, "Timber Piles and Construction Timbers". After considerable discussion, it was decided to drop this project and also to recommend that Manual 17 be eliminated from the ASCE list of publications. It was pointed out that most of the material in Manual 17 was now obsolete. Much of the new material that would have been incorporated in the manual is available in a number of other places. Some of the material has been published in the Structural Division Journal and it is anticipated that some of the chapters that are nearly completed will also be published in future issues of the Journal.

Attention was then focused on the desirable organization and future functions of the Committee. It was decided to disband all Task Committees and it was agreed that the following new Task Committees should be organized:

Task Committee on Technical Presentation—Chairman-John G. Shope
The scope of this committee is to encourage and facilitate publication of technical papers and reports and to develop technical sessions on wood.

Task Committee on Technical Literature—Chairman-Wayne C. Lewis
The scope of this committee is to compile, maintain, and publish periodically a classified bibliography of selected technical literature.

Task Committee on Wood Research—Chairman-Lee W. Crandall
The scope of this committee is to maintain a list of recommended research projects and to lend its aid in the evaluation and stimulation of proposed research. This list of research projects will be available to colleges and research institutions.

COMMENTARY ON PLASTIC DESIGN IN STEEL

The final progress report on the Commentary on Plastic Design in Steel is appearing in the April 1960 issue of the Engineering Mechanics Division Journal. It continues the work of a Joint Committee of Welding Research Council and the American Society of Civil Engineers. The purpose is to provide the background of theory and test upon which recommendations may be based for design by the plastic method.

The Joint Committee has approved the publication of this Commentary with a strong recommendation that it be read carefully by all structural engineers. It is based on a series of preliminary reports prepared for the WRC and the ASCE by a research group at Fritz Engineering Laboratory, Department of Civil Engineering, Lehigh University.

Although much of the experimental and theoretical work reported was performed at Lehigh University, the WRC-ASCE Joint Committee has broadened this Commentary by including the results of research at other institutions both here and abroad.

The complete Commentary will eventually be published by ASCE as a final joint report of the WRC and ASCE. The complete table of contents of the Commentary with the dates of publication in the Engineering Mechanics Division Journal appears below:

1. INTRODUCTION (July 1959)	1.1 Structural Design 1.2 Plasticity and Design—Some Advantages and Limitations
2. BASIC PRINCIPLES (July 1959)	2.1 Behavior of Material and Structural Elements 2.2 Plastic Theory
3. ANALYSIS AND DESIGN (July 1959)	3.1 Assumptions 3.2 Statical Method of Analysis 3.3 Mechanism Method of Analysis 3.4 Other Methods
4. GENERAL PROVISIONS (July 1959)	4.1 Introduction 4.2 Types of Construction 4.3 Material 4.4 Structural Ductility 4.5 Yield Stress Level 4.6 Plastic Moment 4.7 Loads 4.8 Load Factors
5. VERIFICATION OF PLASTIC THEORY (July 1959)	5.1 Basic Concepts 5.2 Continuous Beams 5.3 Frames
6. ADDITIONAL DESIGN CONSIDERATIONS (October 1959)	6.1 Shear Force 6.2 Local Buckling 6.3 Lateral Buckling 6.4 Variable Repeated Loading
7. COMPRESSION MEMBERS (January 1960)	7.1 Introduction 7.2 Reduction of the Plastic Moment Due to Axial Thrust

7.3 Moment-Carrying Capacity of Columns
7.4 Rotation Capacity
7.5 The Influence of Lateral—Torsional Buckling
7.6 Frame Stability

8. CONNECTIONS (April 1960)
8.1 Straight Corner Connections
8.2 Haunched Corner Connections
8.3 Tapered Haunched Connections
8.4 Curved Haunched Connections
8.5 Beam-to-Column Connections
8.6 Details with Regard to Welding
8.7 Details with Regard to Bolting

9. DEFLECTIONS (April 1960)
9.1 Introduction
9.2 Deflections in the Elastic Range
9.3 Deflections in the Plastic Range
9.4 Deflection at Ultimate Load
9.5 Step-by-Step Calculations
9.6 Approximate Deflection at Working Load
9.7 Rotation Requirements

WEST COAST CONFERENCE ON APPLIED MECHANICS

The 1960 West Coast Conference on Applied Mechanics will be held at California Institute of Technology, Pasadena, June 27-29. This conference is co-sponsored annually by the West Coast Committee of ASCE and the West Coast Committee of the Engineering Mechanics Division of ASCE.

The purpose of the conference is to promote the presentation and discussion of original research in the field of applied mechanics, including linear and non-linear mechanics, dynamics, vibrations, plates and shells, elasticity, plasticity, viso-elasticity, and properties of materials.

Last year's conference at Stanford was an outstanding success with 39 research papers presented and general lectures by Professors R. M. Rosenberg, Eli Sternberg and P. G. Hodge. Over 200 specialists in Applied Mechanics from England, Germany, and Canada, as well as the United States attended. With the exception of a few papers submitted directly to the conference and accepted for presentation, papers sponsored by ASME are selected from papers accepted for publication in JAM and those by ASCE from papers submitted to the EMD Journal of the ASCE.

Professor James M. Gere, Stanford, is chairman and Professor B. J. Hartz, University of Washington, is secretary of the ASCE West Coast Committee for 1960

FALL MEETINGS

The Second National Conference on Electronic Computation will be held at the Pittsburgh Hilton Hotel on September 8 and 9, 1960. Four main themes are planned: Design Applications, Structural Analysis, Mathematical Methods and Professional Problems. In addition, at least six major manufacturers of data-processing equipment will exhibit their machines.

The National Fall Meeting of the American Welding Society will be held at the Hotel Penn Sheraton, Pittsburgh, from September 26 to 29, 1960. The pro-

gram for this meeting includes sessions devoted to the theme Welded Structures. These sessions are co-sponsored by the Structural Division of the ASCE, the American Welding Society and the Column Research Council.

The Annual Fall Meeting of the ASCE will be held at Boston from October 9 to 14, 1960. The theme of the Structural Division Program will be Basic Research.

Further details of these three meetings will appear in future issues of the NEWSLETTER.

STRUCTURAL DIVISION JOURNAL

The next issue of the Structural Division Newsletter will be published in August. Material for this issue must reach the editor before the end of June. Committee Chairmen are requested to send to the editor news items and minutes of any task committee meetings.

Gerard F. Fox, Newsletter Editor
Howard, Needles, Tammen & Bergendoff
99 Church Street
New York 7, New York